

PROBABILISTIC SAFETY ANALYSIS  
OF EARTH RETAINING STRUCTURES  
DURING EARTHQUAKES

by

D.A. Grivas and C. Souflis

Report No. CE-82-9

Department of Civil Engineering  
Rensselaer Polytechnic Institute  
Troy, New York

Sponsored by the Earthquake Hazard Mitigation Program  
of the National Science Foundation under Grant No.  
PFR-7905500

July 1982

Any opinions, findings, conclusions  
or recommendations expressed in this  
publication are those of the author(s)  
and do not necessarily reflect the views  
of the National Science Foundation.



<b>REPORT DOCUMENTATION PAGE</b>	<b>1. REPORT NO.</b> NSF/CEE-82030	<b>2.</b>	<b>3. Recipient's Accession No.</b> PFR 26259 3									
<b>4. Title and Subtitle</b> Probabilistic Safety Analysis of Earth Retaining Structures During Earthquakes		<b>5. Report Date</b> July 1982										
<b>7. Author(s)</b> D.A. Grivas, C. Souflis		<b>6.</b>										
<b>9. Performing Organization Name and Address</b> Rensselaer Polytechnic Institute Department of Civil Engineering Troy, NY 12181		<b>8. Performing Organization Rept. No.</b>										
<b>12. Sponsoring Organization Name and Address</b> Directorate for Engineering (ENG) National Science Foundation 1800 G Street, N.W. Washington, DC 20550		<b>10. Project/Task/Work Unit No.</b>										
<b>15. Supplementary Notes</b> Submitted by: Communications Program (OPRM) National Science Foundation Washington, DC 20550		<b>11. Contract(C) or Grant(G) No.</b> (C) (G) PFR7905500										
<b>16. Abstract (Limit: 200 words)</b> A procedure is presented for determining the probability of failure of earth retaining structures under static or seismic conditions. Four possible modes of failure (overturning, base sliding, bearing capacity, and overall sliding) are examined and their combined effect is evaluated with the aid of combinatorial analysis. The probability of failure is shown to be a more adequate measure of safety than the customary factor of safety. As earth retaining structures may fail in four distinct modes, a system analysis can provide a single estimate for the possibility of failure. A Bayesian formulation of the safety of retaining walls is found to provide an improved measure for the predicted probability of failure under seismic loading. The presented Bayesian analysis can account for the damage incurred to a retaining wall during an earthquake to provide an improved estimate for its probability of failure during future seismic events.		<b>13. Type of Report &amp; Period Covered</b>  <b>14.</b>										
<b>17. Document Analysis a. Descriptors</b> <table border="0" style="width:100%"> <tr> <td style="width:33%">Earthquakes</td> <td style="width:33%">Dynamic structural analysis</td> <td style="width:33%">Retaining walls</td> </tr> <tr> <td>Damage</td> <td>Earthquake resistant structures</td> <td>Bayes theorem</td> </tr> <tr> <td>Loads (forces)</td> <td>Static loads</td> <td>Bridge abutments</td> </tr> </table> <p><b>b. Identifiers/Open-Ended Terms</b> Ground motion</p> <p><b>c. COSATI Field/Group</b></p>				Earthquakes	Dynamic structural analysis	Retaining walls	Damage	Earthquake resistant structures	Bayes theorem	Loads (forces)	Static loads	Bridge abutments
Earthquakes	Dynamic structural analysis	Retaining walls										
Damage	Earthquake resistant structures	Bayes theorem										
Loads (forces)	Static loads	Bridge abutments										
<b>18. Availability Statement</b>  NTIS		<b>19. Security Class (This Report)</b>	<b>21. No. of Pages</b>									
		<b>20. Security Class (This Page)</b>	<b>22. Price</b>									



TABLE OF CONTENTS

	PAGE
PREFACE. . . . .	v
LIST OF TABLES . . . . .	vi
LIST OF FIGURES. . . . .	vii
LIST OF SYMBOLS. . . . .	ix
ABSTRACT . . . . .	xii
CHAPTER 1 INTRODUCTION. . . . .	1
1.1 Scope of the Present Study. . . . .	3
CHAPTER 2 FIELD OBSERVATIONS ON SEISMIC DAMAGE OF EARTH RETAINING STRUCTURES. . . . .	9
2.1 Gravity Retaining Walls. . . . .	9
2.2 Force-Governed Retaining Walls . . . . .	10
2.3 Bridge Abutments . . . . .	11
2.4 Wingwalls of Bridge Abutments. . . . .	14
2.5 Quay Walls of Gravity Type . . . . .	15
2.6 Quay Walls of Anchored Bulkhead Type . . . . .	17
2.7 Factors Contributing to Damage of Earth Retaining Structures . . . . .	18
CHAPTER 3 MODELS FOR DAMAGE ASSESSMENT AND PREDICTION: A LITERATURE REVIEW . . . . .	21
CHAPTER 4 FAILURE CRITERIA AND PROBABILITY OF FAILURE . . . . .	29
4.1 Modes of Failure and Failure Criteria . . . . .	29
4.2 Expressions of Capacity and Demand . . . . .	34
4.2.1 Overturning . . . . .	34
4.2.2 Base Sliding. . . . .	36
4.2.3 Bearing Capacity. . . . .	37
4.2.4 Overall Sliding . . . . .	40
4.3 Determination of the Probability of Failure. . . . .	42
4.3.1 Static Conditions . . . . .	42
4.3.2 Seismic Conditions. . . . .	43
4.3.3 Total Probability of Failure. . . . .	45

	PAGE
CHAPTER 5 SEISMIC SAFETY PREDICTION . . . . .	50
5.1 Wall Performance under Static Conditions. . . . .	50
5.2 Posterior Distribution of Soil Strength Parameters. . . . .	51
5.3 Posterior Probability of Failure. . . . .	53
5.4 Seismic Capacity of a Retaining Wall. . . . .	53
5.5 Prediction of Wall Performance after the Occurrence of an Earthquake . . . . .	54
CHAPTER 6 CASE STUDY. . . . .	58
6.1 Description of the Facility . . . . .	58
6.2 Ground Motion Parameters . . . . .	64
6.3 Behavior of the Wingwall before the Seismic Activity. . . . .	64
6.3.1 Description of Failure . . . . .	64
6.3.2 Cause of Failure . . . . .	66
6.3.3 Representative Cross-Section and Material Parameters . . . . .	70
6.3.4 Static Force System along the Wall . . . . .	74
6.4 Behavior of the Wingwall during the Seismic Activity. . . . .	78
6.4.1 Observed Wall Movement and Design Specifications. . . . .	78
6.4.2 Back-Calculation of Wall Movement . . . . .	78
6.4.3 Seismic Force System along the Wall . . . . .	82
6.5 Failure Analysis . . . . .	85
6.5.1 Statistical Values of Safety Margin . . . . .	85
6.5.2 Determination of Probability of Failure . . . . .	87
6.6 Results . . . . .	88
6.6.1 Static Conditions. . . . .	89
6.6.2 Seismic Conditions . . . . .	89
CHAPTER 7 REFERENCES . . . . .	102
CHAPTER 8 DISCUSSION . . . . .	110
CHAPTER 9 SUMMARY AND CONCLUSIONS. . . . .	113
APPENDIX A POSTERIOR PROBABILITY OF FAILURE FOR THE CASE OF COHESIONLESS SOILS . . . . .	117
APPENDIX B COMPUTER PROGRAMS . . . . .	120

## PREFACE

This is the final report on the research project entitled "Reliability of Soil Retaining Structures during Earthquakes". This study is sponsored by the Earthquake Hazard Mitigation Program of the National Science Foundation under Grant No. PFR-7905500, and is directed jointly by Dr. Dimitri A. Grivas, Associate Professor of Civil Engineering, Rensselaer Polytechnic Institute, and Dr. Milton E. Harr, Professor of Civil Engineering, Purdue University. Drs. Ralph B. Peck and Neville C. Donovan serve as advisors to the project of which Dr. Michael Gaus is the Earthquake Hazard Mitigation Program Manager.

The authors are thankful to the National Science Foundation for sponsoring this research. Special thanks are also extended to Mrs. Betty Alix and Mrs. Jo Ann Grega for their typing of this report.

## LIST OF TABLES

		PAGE
TABLE 1.1	MODEL TEST RESULTS OF RIGID WALLS UNDER EARTHQUAKE-LIKE LOADS . . . . .	4
TABLE 6.1	CHARACTERISTICS OF THE SEISMIC ACTIVITY . . . . .	65
TABLE 6.2	DETERMINATION OF CENTER OF GRAVITY FOR THE REPRESENTATIVE SECTION OF THE WALL . . . . .	72
TABLE 6.3	STATISTICAL VALUES OF MATERIAL PROPERTIES. . . . .	75
TABLE 6.4	DESIGN SEISMIC COEFFICIENTS SUGGESTED BY THE GREEK ASEISMIC CODE . . . . .	80
TABLE 6.5	TOTAL HORIZONTAL PERMANENT DISPLACEMENT OF THE WALL . . . . .	83
TABLE 6.6	DETERMINATION OF PROBABILITY OF FAILURE: STATIC CONDITIONS . . . . .	90
TABLE 6.7	DETERMINATION OF PROBABILITY OF FAILURE: SEISMIC CONDITIONS ( $\alpha_h = 0.02g$ , $\alpha_v = 0$ ) . . . . .	91
TABLE 6.8	DETERMINATION OF PROBABILITY OF FAILURE: SEISMIC CONDITIONS ( $\alpha_h = 0.04g$ , $\alpha_v = 0$ ) . . . . .	92
TABLE 6.9	DETERMINATION OF PROBABILITY OF FAILURE: SEISMIC CONDITIONS ( $\alpha_h = 0.06g$ , $\alpha_v = 0$ ) . . . . .	93
TABLE 6.10	DETERMINATION OF PROBABILITY OF FAILURE: SEISMIC CONDITIONS ( $\alpha_h = 0.08g$ , $\alpha_v = 0$ ) . . . . .	94
TABLE 6.11	PRIOR AND POSTERIOR PROBABILITIES OF FAILURE. . . . .	97
TABLE 6.12	STATISTICAL VALUES OF THE SEISMIC CAPACITY . . . . .	100
TABLE 6.13	PREDICTED PROBABILITY OF FAILURE ON THE BASIS OF THE SEISMIC CAPACITY OF THE WALL. . . . .	101
TABLE B-1	NAME AND DESCRIPTION OF PROGRAM VARIABLES. . . . .	127
TABLE B-2	DATA INPUT AND DISPLAY OUTPUT . . . . .	131
TABLE B-3	DATA INPUT AND DISPLAY OUTPUT . . . . .	137



## LIST OF FIGURES

			PAGE
FIGURE	4.1	THE POSSIBLE MODES OF FAILURE OF GRAVITY RETAINING WALLS . . . . .	30
FIGURE	4.2	DEFINITION OF FAILURE FUNCTION UNDER STATIC CONDITIONS $G_0$ . . . . .	33
FIGURE	4.3	SEISMIC LOADING ON RETAINING WALL FOR OVER-TURNING AND BASE SLIDING . . . . .	35
FIGURE	4.4	SEISMIC LOADING ON RETAINING WALL AND ITS FOUNDATION . . . . .	39
FIGURE	4.5	SEISMIC LOADING ON RETAINING WALL FOR OVERALL SLIDING . . . . .	41
FIGURE	4.6	DEFINITION OF FAILURE FUNCTION UNDER STATIC CONDITIONS . . . . .	44
FIGURE	4.7	DEFINITION OF FAILURE FUNCTION UNDER SEISMIC CONDITIONS . . . . .	46
FIGURE	4.8	DEFINITION OF FAILURE UNDER SEISMIC CONDITIONS . . . . .	47
FIGURE	4.9	EQUIVALENT SYSTEM REPRESENTATION OF A RETAINING WALL . . . . .	48
FIGURE	6.1	PLAN VIEW OF THE WINGWALL AND ADJACENT STRUCTURES..	59
FIGURE	6.2	FRONT VIEW OF THE WINGWALL USED IN CASE STUDY AND ADJACENT FACILITIES . . . . .	60
FIGURE	6.3	CROSS-SECTION OF TORRENT DRAINING FACILITY AT LOCATION A-A . . . . .	61
FIGURE	6.4	CROSS-SECTION OF WINGWALL AT LOCATION B-B . . . . .	62
FIGURE	6.5	CROSS-SECTION OF WINGWALL AT LOCATION C-C . . . . .	63
FIGURE	6.6	PLAN VIEW OF THE WINGWALL ILLUSTRATING THE POSITION OF THE CRACK AND THE DISTRIBUTION OF THE SETTLEMENT OF THE BACKFILL . . . . .	67

LIST OF FIGURES (contd)

	PAGE
FIGURE 6.7 CROSS-SECTION OF WINGWALL AT LOCATION D-D BEFORE THE EARTHQUAKE . . . . .	68
FIGURE 6.8 REPRESENTATIVE SECTION OF WINGWALL USED IN STABILITY ANALYSIS . . . . .	71
FIGURE 6.9 FRONT VIEW OF THE WINGWALL SHOWING THE LOCATION OF THE REPRESENTATIVE CROSS-SECTION. . . . .	73
FIGURE 6.10 CROSS-SECTION OF THE WINGWALL AT LOCATION D-D AND THE REALIZED MOVEMENT DUE TO THE EARTHQUAKE . . . . .	79
FIGURE 6.11 SLICES USED IN THE OVERALL STABILITY ANALYSIS OF THE WINGWALL . . . . .	95
FIGURE 6.12 THE STANDARDIZED NORMAL VARIATE $u$ AND ITS CUMULATIVE DENSITY FUNCTION $\Phi(u)$ . . . . .	98
FIGURE 6.13 DETERMINATION OF THE RELATIONSHIP BETWEEN $u$ AND $\alpha_h$ WITH THE AID OF LINEAR REGRESSION ANALYSIS . . . . .	99

## LIST OF SYMBOLS

### English Characters

a	Inclination of load on wall base with respect to the vertical direction
B	Width of base of retaining wall
$b_i$	Regional parameters appearing in expression for seismic hazard
C	Capacity (resistance against failure)
c	Cohesion of backfill material
$c_f$	Cohesion of foundation material
$c_r$	Width of the crest of the wall
D	Demand (force or moment that tends to cause failure)
$D_f$	Foundation depth
$D_r$	Damage Ratio
$d_p$	Permanent horizontal displacement of retaining wall (outwards)
e	Eccentricity of load along the wall base
FS	Factor of safety
F( )	Cumulative distribution of the quantity in parenthesis
f( )	Probability density function of the quantity in parenthesis
$G_o$	Conditions of retaining wall under static loading (geometry, material, and loading)
H	Height of retaining wall
$H_b$	Height of the backfill behind a retaining wall

English Characters (continued)

H	Failure function
i	Backfill inclination with respect to the horizontal
K	Normalizing constant
$k_h$	Maximum horizontal seismic acceleration of a retaining wall (design value)
$k_v$	Maximum vertical seismic acceleration of a retaining wall (design value)
L	Distance between the site and the earthquake source
$L_w$	Length of the wall footing
M	Earthquake magnitude (in Richter scale)
$P_A$	Total active force
$P_{AH}$	Horizontal component of total active force
$P_{AV}$	Vertical component of total active force
$P[ ]$	Probability of the event in brackets
$P_f$	Probability of failure
$p(z)$	Lateral earth pressure at depth z
R	Seismic capacity
r	Reliability ( $=1 - P_f$ )
SM	Safety margin
$S_x$	Standard deviation of variate x
T	Predominant period of an earthquake
V	Maximum horizontal seismic velocity
$V_x$	Variance of variate x
$W_w$	Weight of retaining wall

English Characters (continued)

$\bar{x}$	Mean value of random variable $x$
$z$	Depth

Greek Characters

$\alpha_h$	Maximum horizontal component of seismic accera- tion
$\alpha_v$	Maximum vertical component of seismic acceleration
$\alpha'_h$	Horizontal acceleration due to an earthquake
$\alpha'_v$	Vertical acceleration due to an earthquake
$\gamma$	Unit weight of the backfill material
$\gamma_b$	Unit weight of the retaining wall
$\gamma_f$	Unit weight of the foundation material
$\delta$	Angle of friction between retaining wall and backfill material
$\delta_f$	Angle of friction between retaining wall base and foundation material
$\lambda_A$	Lateral active earth pressure coefficient
$\mu_x$	Median of quantity $x$
$\xi(c, \phi)$	Joint distribution of $c$ (=cohesion) and $\phi$ (=angle of friction)
$\xi'(c, \phi)$	Posterior joint distribution of $c$ (=cohesion) and $\phi$ (=angle of friction)
$\phi$	Angle of friction of the backfill material
$\phi_f$	Angle of internal friction of the foundation material
$\psi$	Mobilized shear strength of backfill material
$\psi_d$	Coefficient to account for different design schemes
$\omega$	Circular frequency

## ABSTRACT

A simplified procedure for the determination of the probability of failure of earth retaining structures under static and seismic conditions is presented. Four possible modes of failure are examined (overturning, base sliding, bearing capacity, and overall sliding) and their combined effect is evaluated with the aid of combinatorial analysis. Limit equilibrium is expressed as a function of the soil strength parameters (random variables) that are present in the development of the capacity (resistance) of the structure along a particular failure mode. The seismic load is introduced in terms of the maximum horizontal ground acceleration (random variable) determined through a seismic hazard analysis at the site of the facility.

A Bayesian formulation of the problem makes it possible to account for observations on the safety of the wall in order to provide an improved measure for the predicted probability of failure under seismic loading. This formulation permits (a) the derivation of an expression for the seismic capacity of the wall, defined as the maximum horizontal acceleration that can be experienced by the wall without failure, and (b) the consideration of the damage incurred to a retaining wall during an earthquake in safety predictions for future seismic events.

The developed procedure is applied to an actual case study involving the safety of a wingwall. The required information has been

obtained during detailed investigations on sites affected by the February and March, 1981, earthquakes in Greece. For the first time ever, the actual magnitude of the movement experienced by a retaining wall during a seismic event is available and compared with theoretical predictions.

Among the conclusions drawn from this study are: (a) the probability of failure is a more adequate measure of safety than the customary factor of safety; (b) a Bayesian formulation of the safety of retaining walls provides an improved measure for the probability of failure under seismic loading; and (c) when safety prediction is made before construction (at the design stage), the probability of failure is always greater than that predicted under static conditions. When safety prediction is made after the successful construction of a retaining wall, the new predicted probability of failure under seismic loading (posterior) is always smaller than that predicted before construction (prior).





## CHAPTER 1

### INTRODUCTION

As earth retaining walls are among the most frequently encountered geotechnical structures, the ability to predict their safety under static or seismic conditions is of paramount importance in geotechnical practice. The reliability of such a prediction depends, among other factors, on the accuracy with which one can describe the force system on a retaining wall. The latter is the result of the interaction that takes place between the wall, on one hand, and the backfill and foundation materials, on the other. It is therefore not surprising that a considerable amount of research activity has concentrated on efforts aiming at a better understanding of the manner with which wall and soil interact during loading.

Coulomb is recognized as the first to provide an analytical solution to the problem. His pioneering study, conducted at a time (1770's) when even trigonometric functions were not yet in use, was based on a sliding wedge analysis and provided the limit value for the total force on a (frictionless) wall at failure. Approximately eighty years later, Rankine studied the state of stress within cohesionless materials and the forces they exert on retaining structures. His analysis was based on the observation that small deformations of the soil are sufficient to bring about full frictional resistance and thus produce "active" or "passive" state, depending on the direction of the soil movement.

The seismic effect on the force system on a wall was investigated for the first time by Okabe (1926) and Mononobe (1929) who provided a method for its description that is commonly referred to as the Mononobe-Okabe procedure. This is basically the Coulomb sliding wedge approach in which two additional forces are included: the horizontal and vertical components of the seismic inertia of the backfill material. A simplified version of the Mononobe-Okabe procedure was presented by Seed (Seed and Whitman, 1970), while Prakash and Basavanna (1969) attempted to improve upon the method through an analysis that would satisfy the additional condition of equilibrium of moments acting on the sliding wedge.

A simple analytical procedure for the determination of the pressure distribution along retaining walls by considering the wall movement was proposed by Dubrova (1963). Although developed for static conditions, the Dubrova method was later extended to provide the pressure distributions that result from the occurrences of earthquakes (Saran and Prakash, 1977). Additional theoretical studies on the seismic safety of earth retaining structures were conducted, the difference among these being mainly due to differences in the assumptions made about the seismic response of the backfill material. Thus, they may be distinguished into elastic, elastic-plastic, or completely-plastic approaches in which the earthquake effects are introduced in a quasi-static or dynamic manner. The results obtained from these studies have indicated that important factors for the seismic safety of earth retaining struc-

tures include the strength properties of the backfill and foundation materials, the structural design of the wall, and earthquake characteristics (Nazarian and Hadjian, 1979).

Finally, improved instrumentation and testing ability, including tests on wall models using shaking tables under simulated earthquake loads, have contributed significantly towards understanding the wall-soil interaction and the resulting force system. In Table 1.1 is given a list of model tests conducted with the aid of shaking tables together with a brief summary of the conditions and the results obtained during each test.

#### 1.1 Scope of the Present Study

The aim of the present study is to provide a probabilistic approach to the safety prediction of earth retaining structures during earthquakes. It is considered that the main source of uncertainty is due to the randomness of (a) the strength parameters of the backfill and foundation materials, and (b) the friction coefficients between the two soil media and the wall. Safety predictions are made on the basis of the probability of failure of a retaining wall rather than the customary factor of safety.

Chapter 2 presents the findings of a detailed survey of field observations on the damage that has occurred to earth retaining structures during earthquakes together with a discussion of the main contributing factors. Theoretical models that have been proposed for damage assessment and prediction are presented in Chapter 3, while Chapter 4 provides the procedure required for the determination of the probability of failure

TABLE 1.1

## MODEL TEST RESULTS OF RIGID WALLS UNDER EARTHQUAKE-LIKE LOADS

INVESTIGATORS	TEST CONDITIONS	FINDINGS
Mononobe and Matsuo (1929)	<p>Models of Retaining Walls</p> <p>Apparatus: Metal lined box with a door hinged at base            Pressure gauge 4.5 ft. above base            Mounted on a shaking table</p> <p>Dimensions: 4 ft high, 9 to 12 ft long</p> <p>Material : Uniform clean dry sand</p> <p>Conditions: Horizontal acceleration, <math>0.0 \leq a_h \leq 0.4g</math></p>	<p>1. Dynamic force at  <math>h_d = H/3</math>            (<math>h_d</math> measured from            wall base)</p> <p>2. Worst Case:  <math>a_h</math> toward wall  <math>a_v</math> upward</p>
Matsuo and Ohara (1960)	<p>Models of Quay Walls</p> <p>Apparatus: Metal- or glass-lined box            Fixed or hinged at base            Pressure cells on wall centerline at 3            heights            Mounted on shaking table</p> <p>Dimensions: 0.4m high, 1.0m long</p> <p>Material : Uniform clean sand, dry and saturated</p> <p>Conditions: <math>0.2g \leq a_h \leq 0.4g</math></p>	<p>1. Dynamic force at  <math>h_d \approx 0.55H</math></p>

TABLE 1.1  
(continued)

INVESTIGATORS	TEST CONDITIONS	FINDINGS
Ishii, Arai, and Tsuchida (1960)	<p>Models of Retaining Walls            Apparatus: Three boxes of different dimensions, each with a door which could be fixed or hinged at bottom. Mounted on a shaking table            Dimensions: 30 cm high, 82 cm long                          50 cm high, 202 cm long                          70 cm high, 400 cm long            Material: Uniform clean dry sand            Conditions: horizontal oscillating acceleration, lasting for 2 min, starting at <math>a_h = 1 \text{ g}</math> and increased to a maximum <math>a_h = 1 \text{ g}</math></p>	<p>1. The pressure distribution after motion ends is greater than the initial static pressure            2. The dynamic pressure increment differs in phase from the table motion by as much as one half the period of motion</p>
Murphy (1960)	<p>Model of Quay Wall            Apparatus: Glass sided box built to 1:64 scale of the existing prototype. Mounted on a shaking table.            Material: Dry sand            Conditions: horizontal oscillating acceleration, <math>a_h = 2 \text{ g}</math></p>	<p>1. Inclination of the failure plane much flatter than for static loading.</p>
Ntwa (1960)	<p>Model of Quay Walls            Apparatus: A 3 meter high model wall, built in an excavated pit, and backfilled with sand. Excitation provided by eccentric weights driven by a motor, in a concrete lined excavation several meters behind the wall.            Dimensions: 3 m high, 5 m wide            Material: Dry sand            Conditions: horizontal oscillating acceleration of 2 g</p>	<p>1. Observed phase differences between wall motion and wall pressures</p>

TABLE 1.1  
(Continued)

INVESTIGATORS	TEST CONDITIONS	FINDINGS
Kurata, Arai, and Yokoi (1965)	<p>Models of Sheet Pile Walls            Apparatus: A box mounted on a shaking table            Dimensions: 1.5 m high, 2 m long            Material: Uniform dry sand            Conditions: Horizontal oscillating acceleration increased at approximately 3 g /sec to a maximum of 2 to 3 g depending on the test</p>	<p>1. Observed reduction in lateral subgrade modulus as wall rotation increased</p>
Ishihara et al (1977)	<p>Models of Quay Walls            Apparatus: A soil bin with a moveable wall and mounted on a shaking table            Dimensions: 75 cm high, 200 cm long            Material: Sand, dry and saturated            Conditions: horizontal oscillating acceleration of up to 6 g</p>	<p>1. Excess pore water pressures are involved by the inertia of the water mass and also by deformation of the sand.</p>
Sim and Berrill (1979)	<p>Model of Retaining Wall            Apparatus: A box mounted on a shaking table            Dimensions: 0.45 m high, 2.44 m long            Material: Dry Brighton Beach sand            Conditions: Horizontal oscillating acceleration and scaled El Centro time history  <math>.05g \leq a_h \leq 0.4 g</math></p>	<p>1. Total forces close to the Mononobe-Okabe equation's predictions            2. For pure translation, the wall slides with respect to the soil when the wall force exceeds the base resistance</p>
Lee (1981)	<p>Model of Retaining Wall            Apparatus: Plexiglass box with separate and instrumented aluminum wall. Mounted on a shaking table            Dimensions: 4 ft high, 8 ft long            Material: Ottawa sand, dry and saturated            Conditions: horizontal oscillating acceleration  <math>a_h &lt; 0.5 g</math> wall translation velocity held at a constant value</p>	<p>1. Wall movement required to develop the active state decreases with increasing soil strength.            2. Total static plus dynamic force at <math>h_d = .45H</math></p>

TABLE 1.1  
(continued)

INVESTIGATORS	TEST CONDITIONS	FINDINGS
Prakash et al. (1973)	<p>Models of Retaining Walls            Apparatus : Metal-lined wall inside a box                      8 pressure cells on wall face                      Shaking table struck by falling pendulum            Dimensions: 1 m. high, 5 m. long            Material : Uniform clean dry sand            Conditions: horizontal shock acceleration  <math>3.3g \leq a_h \leq 4.28</math></p>	<ol style="list-style-type: none"> <li>1. <math>0.36H \leq h_d \leq 0.444</math></li> <li>2. Dynamic pressure <math>\approx</math> parabolic</li> <li>3. Failure plane located at <math>\theta_{cr} &lt; 45^\circ + \phi/2</math>, slightly concave</li> </ol>
Nazarian et al. (1979)	<p>Reviewed previously done model tests, including those by Nandakumaran and Joshi</p>	<ol style="list-style-type: none"> <li>1. <math>h_d</math> increases parabolically as <math>\delta</math> decreases</li> <li>2. <math>h_d</math> decreases with <math>\beta</math></li> <li>3. <math>h_d</math> increases with surcharge</li> <li>4. <math>h_d</math> increases linearly with increasing <math>a_h</math></li> <li>5. <math>0.33H \leq h_d \leq 0.66H</math></li> </ol>

of retaining walls. A Bayesian approach for updating seismic safety predictions is given in Chapter 5. This takes into account the performance of retaining walls under static conditions, or the damage incurred during an earthquake, in order to provide improved estimates for the probability of failure. Chapter 6 presents an application of the theoretical developments to an actual case study. The information required for this purpose was obtained during detailed investigations on sites affected by the February and March, 1981, earthquakes in Greece. A list of references pertaining to the subject of this study is given in Chapter 7. Chapter 8 presents a discussion of the assumptions made in developing the present procedure, and of its applicability and limitations. Chapter 9 gives a summary of this study and together with some important conclusions.



CHAPTER 2  
FIELD OBSERVATIONS ON SEISMIC DAMAGE  
OF EARTH RETAINING STRUCTURES

This chapter presents the findings of a literature survey on the damage reported to have incurred to earth retaining structures during earthquakes. Because of differences in both design requirements and observed seismic behavior, six types of such structures may be distinguished, namely:

- (a) gravity retaining walls;
- (b) force-governed retaining walls;
- (c) bridge abutments;
- (d) wingwalls of bridge abutments;
- (e) quay walls: gravity type; and
- (f) quay walls: anchored bulkhead type.

The findings for each type of retaining structure are as follows:

2.1 Gravity Retaining Walls

Gravity retaining walls are generally located above the water table and are designed in a manner so that their weights can provide the resisting forces and moments required for their stability. Relatively few cases of damage caused by earthquakes to this type of retaining walls have been reported in the literature. This may be attributed to the fact that, traditionally, the primary concern of

engineers has been the safety of other types of structures, such as buildings, lifelines, etc. (e.g., Seed and Whitman, 1970). The few reports in the literature on damage or collapse of such walls do not necessarily indicate that they do not exhibit movements during earthquakes.

Nevertheless, some reports on damage incurred to gravity walls during earthquakes do exist in the literature. Seed and Whitman (1970) made reference to a gravity wall located at Frutillar, Chile, that was damaged during the 1960 Chile earthquake. The wall suffered severe damage along with a considerable relative displacement of the two edges of the crack. No signs of excessive tilting were observed.

Damage to gravity retaining walls also occurred during the San Fernando earthquake (Jennings, 1971). It was reported that, during this earthquake, one wall of the Balboa water treatment plant failed as a result of increased lateral earth pressures.

Finally, a number of reports exist about unreinforced rock walls that collapsed during the 1973 earthquake at Honomu, Hawaii (National Research Council, 1977) and the 1975 earthquake at Lima, Peru (Moran et al., 1975).

## 2.2 Force-Governed Retaining Walls

Force-governed retaining walls include sheetpile, cantilever, and braced walls. They are commonly placed above the water table and, in contrast to gravity walls, their weight alone cannot secure their stability. Thus, of necessity, this must be achieved

with the use of additional structural units which makes them more vulnerable to earthquake induced forces and displacements.

This type of earth retaining walls are more frequently used in geotechnical practice than the gravity type walls. As was the case with the latter, very few records have been made of damage incurred to force-governed walls during earthquakes.

Clough and Fragaszy (1977) investigated the performance of open channel floodway retaining structures during the 1971 San Fernando earthquake. The floodway system is located in the Greater Los Angeles area and consists of over 160 km of reinforced concrete U-shaped open channels and buried culverts. It was observed that the open channel section had suffered damage along a length of 1 km because of excessive tilting of the retaining walls.

The above walls were designed to resist only static loads. Although they were subjected to horizontal accelerations in the range of 0.2-0.65 g, the walls performed very well for values of the accelerations up to 0.45 g, where g is the acceleration of gravity. This may be attributed to the ample safety margin provided by the safety factors used in the conventional static design.

Damage caused by earthquakes to other reinforced concrete flood-control channels (such as the Wilson Canyon Channel) has also been reported in the literature (Wood, 1973; Nazarian and Hadjian, 1979).

### 2.3 Bridge Abutments

As the safety of bridge abutments is essential for the overall safety of the superstructure, a considerable attention has been paid

to the performance of the former under earthquake-induced loads.

Ross et al. (1969) conducted a thorough study on the damage induced to foundations of bridges during the 1964 Alaska earthquake. The structures examined were located within approximately 80 miles from the epicentral region.

The authors reported that, in some cases, abutment backwalls cracked and the abutments exhibited severe deformations or movements, such as rotations. A common characteristic in most of the cases was the fact that the approach fill to the abutments experienced settlement up to 2 ft relatively to the bridge deck. Moreover, the approach fill spread away from the abutment faces and sides, toward the channels over which the bridges extended. In a few cases, settlements in the abutments themselves were observed. The most usual type of damage, however, was caused by movements of the abutments toward the channels. The forces which induced these movements must have been a very high magnitude as, in many instances, compression and buckling of the superstructure had occurred.

The movement of the abutments toward the channel has been associated either with settlement of the backfills or with a general movement of the natural channel banks toward the river, or both. In the cases where liquefaction took place, it facilitated the movement and caused spreading and settlement of the backfills and severe differential settlement of the abutments. The overall abutment behavior followed the expected pattern i.e., one that involves tilting toward the channel

and broken abutment backwalls. The latter is commonly due to the restraints imposed by the superstructure.

Following the 1960 earthquake in Chile, a severe distortion was observed of the structure of the Isla Teja Bridge, located in Valdivia (Seed and Whitman, 1970). This was due to the movement of the abutment toward the channel that was caused by high lateral earth pressures induced by the earthquake.

The Inangahua, New Zealand earthquake of 1968 caused several levels of damage to bridge abutments. Evans (1971) reported that, from 39 bridge abutments located in an area within approximately 30 miles from the epicenter of the earthquake, 23 had moved considerably while 15 had been damaged. The overall behavior of these abutments involved movements toward the channel, rotation about their top (due to restraints imposed by the superstructure at that point), settlement of the approach fill by an amount of 10 to 15 percent of its thickness, and high residual lateral earth pressures (Richards and Elms, 1979).

The main cause of damage in the above case was considered the underestimation of the earth pressures acting upon the abutments during an earthquake. Back-calculations of lateral earth pressures (Richards and Elms, 1979) have shown that while the earth pressures due to the earthquake were  $3\frac{1}{2}$  to  $4\frac{1}{2}$  times greater than the static ones, the classical Mononobe-Okabe analysis provided earth pressures only  $2\frac{1}{2}$  times greater than their static values.

The damage caused to bridge abutments by the 1970 earthquake in Madang, New Guinea, was reported to Ellison (1971). The earthquake had a magnitude of 7.1 in Richter scale. The observed damage was similar to that caused by the Inangahua, New Zealand 1968 earthquake. Again, the

performance of the abutments followed the expected pattern of behavior. In total, 29 bridges were damaged and, in some of the cases, the abutments exhibited movements up to 20 in.

The damage incurred to highway bridges during the June, 1978, earthquake in Miyagiken-Okii, Japan, was reported by Kuribayashi et al. (1979). The earthquake magnitude was 7.4 in Richter scale. Many shear cracks were caused to abutment faces, particularly at locations where the cross-section of the abutment changed abruptly. The cracks were especially apparent in the cases of very rigid substructures. Settlements and displacements of the foundations were also observed as well as settlements of the abutment backfills.

Finally, damage or failures that occurred to bridge abutments during the 1960 Chile, 1964 Alaska, 1964 Niigata, 1968 Inangahua, 1970 Madang, 1971 San Fernanco, 1972 Managua, and 1974 Lima earthquakes were reported by Nazarian and Hadjian (1979). Common in all these cases was the settlement of the backfill and the movement of the abutments toward the channel. The latter generated forces of large magnitude in the longitudinal direction of the bridges which often caused buckling. This study concluded that earth pressures of great magnitude generated by the earthquakes were the major cause of damage to bridges.

#### 2.4 Wingwalls of Bridge Abutments

Field observations on damage caused by earthquakes to wingwalls of bridge abutments are very limited. Seed and Whitman (1970) reported the occurrence of an outward movement of the wingwalls of the Showa Bridge abutment during the 1964 earthquake in Niigata, Japan.

A similar movement occurred to a wingwall near the town of Plateas, Greece, during the February and March 1981 earthquakes. The wingwall had developed a crack under static conditions and before the occurrence of the earthquakes. This enabled the determination of the exact movement experienced by the wingwall during the ground shaking. Detailed information on the type and magnitude of damage caused to the Plateas wingwall is given below in the Case Study (Chapter 6).

### 2.5 Quay Walls of Gravity Type

Quay walls are water front structures that commonly extend below the water table and retain naturally or man-made backfill materials. Gravity type quay walls are those designed so that their weight can provide the resistance required for their stability.

Walls of this type are of great importance in harbor facilities. Consequently, a considerable amount of literature has accumulated on their performance during earthquakes.

Amano et al. (1956) reported the damage that incurred during several earthquakes to gravity type quay walls at harbors found in Japan. A summary of the observed damage is as follows:

(a) Gravity type quay walls in Kushiro Port were damaged during the 1952 Tokachioki earthquake that had an intensity equal to 5 on the Japanese Meteorological Agency scale. The damage included both settlement and sliding of the quay walls toward the sea.

(b) Gravity type quay walls in Uno-port were damaged by the 1946 Nakai earthquake. The incurred damage included base sliding of the walls and a slight settlement. Excessive settlement was prevented by the

piles used to support the wall.

The authors observed that the major cause of damage was sliding along the base of the walls over a maximum distance of 26 ft toward the sea.

Matsuo and Ohara (1960) reported that damage incurred to gravity type quay walls during four great earthquakes in Japan; namely, the 1923 Kanto, the 1935 Sizuoka, the 1946 Nankai, and the 1952 Tokachi earthquakes. The authors examined the performance of 23 damaged gravity type quay walls and found that 16 walls had experienced only sliding along their base while 7 had suffered both sliding and tilting. The greatest damage incurred to quay walls with saturated fills.

Severe damage also incurred to gravity type quay walls during the 1964 earthquake in Niigata, Japan. The length of these walls constituted 6 percent of the total length of the retaining structures in the Niigata harbor (Hayashi et al., 1966). Either extensive settlement or overturning or both were the major causes of damage.

The 1960 earthquake in Chile (of a magnitude 8.4 in Richter scale) also caused considerable damage to gravity type quay walls (Seed and Whitman, 1970). Such walls located in Puerto Mont consisted of reinforced concrete in their upper sections while their lower sections were made of caissons filled with soil. The earthquake caused a complete overturning of both sections along an approximate length of 900 ft; and a complete overturning of the upper sections and an outward tilting of the lower sections along an approximate length of 700 ft. The primary cause of damage was attributed to backfill liquefaction. This



was also the cause of failure of another wall of this type that was founded on medium density fine sand (Duke and Leeds, 1963; Emery and Thompson, 1976).

Extensive damage to gravity type quay walls also occurred during the 1964 earthquake in Alaska that had a magnitude equal to 8.3 in Richter scale (Arno and McKinney, 1973; Emery and Thompson, 1976). The major cause of damage was attributed to the effect of tsunamis and to liquefaction that resulted from the long duration of the shaking.

## 2.6 Quay Walls of Anchored Bulkhead Type

Quay walls of anchored bulkhead type serve the same purpose as the gravity quay walls and are designed so that anchors can provide the resistance required for their stability. Their performance during earthquakes has also received a considerable attention in the literature because of their importance in harbor facilities.

Amano et al. (1956) reported that anchored bulkhead type walls in Shimizu harbor were damaged during the 1930 Kitaizu, the 1935 Shizuoka, and the 1944 Tonankai earthquakes. In these cases, damage was due to settlement and sliding along the base of the wall. Sheetpile bulkheads were also damaged in Nagoya harbor during the 1944 Tonankai and the 1946 Nankai earthquakes that had an intensity of 5.6 in the Japanese Meteorological Agency scale. In this case, the major cause of damage was an outward movement of the bulkhead due to poor anchorage. Another anchored bulkhead quay wall, located in the harbour of Osaka, Japan, was also damaged during the 1946 Nankai earthquake. The damage was due to a shear movement

of the upper concrete blocks relative to the underlying sheetpile. Again, poor anchorage was responsible for the movement of the concrete blocks.

Hayashi et al. (1966) investigated the performance of anchored bulkhead type walls during the 1964 Niigata earthquake. In Niigata harbor, steel and concrete sheetpile anchored bulkheads constituted 7 and 8 percent, respectively, of the total existing length of retaining structures. The observed damage ranged from slight deformation toward the sea to complete collapse of these bulkheads and it was attributed to poor anchorage and backfill liquefaction. The latter caused a further increase in the lateral earth pressure of the backfill that resulted in additional lateral movements and subsequent damage to adjacent structures.

Damage also occurred to anchored bulkhead type quay walls during the 1960 earthquake in Chile. This involved outward movement (as much as 3 ft) along an approximate length of 1250 ft of the bulkheads that were located in Puerto Mont (Seed and Whitman, 1970). The outward movement caused settlement of the backfill and severe distortion of railway tracks adjacent to the wall.

## 2.7 Factors Contributing to Damage of Earth Retaining Structures

In order to better understand the factors that contribute to damage of earth retaining structures, the latter may be classified into two types: (a) those which are built over, and (b) those which extend below the water table or sea level. In the latter case, hydrodynamic effects have an important influence on the response of the structure to a seismic excitation.

In general, the seismic performance and possible damage of the first type of earth retaining structures is a function of the following factors (Amano et al., 1956; Emery and Thompson, 1976; Thompson and Emery, 1976; Nazarian and Hadjian, 1979):

- (a) the stratigraphy of the site where the retaining structure is built;
- (b) the properties and the stability of the soil on which the structure is founded;
- (c) the soil-structure interaction;
- (d) the type and the size of the structure;
- (e) the properties of the backfill material; and
- (f) insufficient (structural) response of the retaining structure.

Most of the damage that occurred to this type of retaining structure was due to increased lateral earth pressures and large additional inertia forces. Very often, a reduction in the strength of the foundation soil contributed to the damage. The above factors are by themselves, or in combination, the main cause that initiates overturning, bearing capacity failure, or sliding along the base of a retaining structure (Emery and Thompson, 1976; Nazarian and Hadjian, 1979). Overall sliding is usually due to the well known causes of slope instability.

In the second type of earth retaining structures, hydrodynamic effects are very significant to their stability. For example, possible reduction of water pressure may cause an increase in the applied loads well beyond those that the structure can carry safely (Seed and

Whitman, 1970). Very frequently, tsunamis generated by earthquakes may also result in severe damage.

A study on the performance of gravity type quay walls during earthquakes conducted by Emery and Thompson (1976) revealed that (a) such walls were damaged when the magnitude of the earthquake exceeded VII in the Modified Mercalli Intensity scale, and (b) their performance depended on the stability of submarine slopes on which they were founded. According to this study, overturning or sliding along the base of quay type structures are the most frequent modes of failure. Overall sliding also occurs, although somewhat less frequently.

Finally, Hayashi et al. (1966) have shown that severe damage to earth retaining structures may be caused by a combined action of two factors: (a) the use of small seismic coefficients in the design, and (b) a change of the initial characteristics of the structure due to repairs after its construction. The observed damage has been very slight in structures for which the design values for the seismic coefficient and the corresponding value of the factor of safety are relatively high.

## CHAPTER 3

### MODELS FOR DAMAGE ASSESSMENT AND PREDICTION:

#### A LITERATURE REVIEW

The ability to predict damage and economic losses expected to occur to geotechnical facilities during earthquakes is of paramount importance to their aseismic design. Several models of damage analysis and prediction have been reported in the literature. There are mainly concerned with structures, such as buildings and lifeline systems, and very little has been done about damage assessment of geotechnical type facilities.

Following Scholl and Kustu (1981), two types of models for damage analysis may be distinguished, namely; (a) empirical models, that correlate past records of earthquake-induced losses with either earthquake or structural characteristics or both; and (b) theoretical models, that incorporate engineering characteristics of both the structure and the earthquake.

The Spectral Matrix Method represents the first theoretical approach on the subject and was developed by Blume (1967, 1977). The method aims at the prediction of damage incurring to buildings by large underground nuclear explosions or natural hazards, such as earthquakes. According to this method, damage is determined with the aid of a damage factor, defined as the ratio of the cost of repair over that required for the replacement of the structure at the time of the damage. The statistical values of the damage factor are calculated on the basis of the

probability distributions of the capacity and the demand of the structure.

The need for earthquake insurance of wooden frame houses in California gave rise to an empirical method of damage prediction (Steinbrugge et al., 1969). This method is based on two relationships; one between the Modified Mercalli Intensity and the damage incurred to houses located within a certain area; and, another, between the damage that incurred during previous earthquakes and the estimated repair cost. In accordance with this procedure, damage is classified into four types, namely: slight; moderate; severe; and total loss.

The above empirical method was later extended in order to include other types of buildings (Algermissen et al., 1978a). Further development led to formulation of an easy-to-use general procedure for the estimation of earthquake-induced economic losses (Algermissen et al., 1978b).

Using a somewhat different procedure, Ross et al., (1969) examined the inter-dependence among factors which contributed to the damage that incurred to bridges and their foundations during the 1964 Alaska earthquake. In order to differentiate between bridge and foundation performance, two types of damage evaluation were used. The first referred to bridges and included five damage levels, namely, total collapse; severe deformation or partial collapse or both; moderate deformations of components; minor; and none. The second referred to foundations and included four levels, namely, severe; moderate; minor;

and nil. The limits of the damage levels are different in each type of damage evaluation.

As was the case with the Spectral Matrix Method, the Threshold Evaluation Method was initially developed by Blume (1969) for the theoretical prediction of damage incurred to buildings by large underground nuclear explosions (Scholl et al., 1981). Based on a dynamic analysis, the method predicts the earthquake-induced damage of buildings. The probability of exceedance of a certain damage level is determined by considering the relationship between the latter and the seismic response of the building under investigation. The acceptable probability of exceedance can be evaluated on the basis of the magnitude of the seismic excitation and the consequences of possible damage on the safety of the structure.

An additional study was conducted by Cornell (1970) in order to develop measures of earthquake-induced damage for structures. Two types of relationships between damage and peak ground acceleration were provided: a (usual) functional and a stochastic.

In the first case, the probability density function of the peak ground acceleration is obtained with the aid of a seismic hazard analysis of the site of the structure. This is used for the computation of the probability of exceedance of a certain level of damage. The levels of damage associated with each earthquake are assumed to be either independent, or dependent on the total accumulated damage. In the former approach, total damage is cumulative. In the latter approach, a Markov model is used for the prediction of damage.

In the second case, a random vibration analysis is used for the determination of the statistical values of the damage under a given peak ground acceleration. The probability of exceedance of a certain level of damage is computed with the aid of the probability density function of the peak ground acceleration obtained from a seismic hazard analysis. The total damage is the sum of the individual damages incurred to the structure over a certain period of time.

As was the case with the Spectral Matrix Method and the Threshold Evaluation Method, the Engineering Intensity Scale Method was originally developed by Blume (1970) for the prediction of damage incurred to buildings by underground nuclear explosions. The method estimates the area in which buildings will be damaged during an earthquake and evaluates possible levels of damage in terms of engineering intensities that characterize each level.

In order to predict the seismic damage to high-rise buildings, Czarnecki (1973) developed a theoretical method which uses a dynamic structural analysis for a given earthquake load and establishes the response pattern of the building. This pattern is then related to two types of damage: structural and non-structural. The former type refers to force bearing elements while the latter one refers to all other elements of the building.

Scholl and Farhoomand (1973) studied low-rise buildings and correlated their damage with ground motion data, as generated by an underground nuclear explosion. The developed procedure also applies



to the prediction of earthquake-induced damage, if it is coupled with seismic hazard analysis. Similar procedures have frequently appeared in the literature (Power, 1966; Blume, 1967; Blume, 1969, Nadolski, 1969; Blume, 1970). In the study by Scholl and Farhoomand (1973) the damage incurred to buildings was determined in terms of three factors: (a) the damage ratio, defined as the ratio of the number of damaged buildings over the total number of buildings; (b) the complaint ratio, defined as the ratio of the number of buildings from which complaints were received over the total number of buildings; and (c) the damage cost factor, defined as the ratio of the damage repair cost over the value of the buildings.

A different approach to the prediction of damage incurred to buildings by earthquakes is the one that makes use of damage probability matrices (Whitman et al., 1973; Whitman, 1975). These matrices provide the probability of occurrence of a certain level of damage, given that an earthquake of a certain Modified Mercalli Intensity has occurred.

The damage levels are defined in terms of both a single-word description and the central damage ratio. The latter is defined as the ratio of the repair cost over that required for the replacement of the structure. The mean damage ratio is then obtained as a weighted average of the various central damage ratios and the corresponding probabilities of occurrence for a certain Modified Mercalli Intensity.

Combining field data and theoretical methods, Culver, et al., (1975) developed a procedure for the prediction of damage of buildings due to natural hazards, such as hurricanes, tornadoes, and earthquakes. The procedure consists of three parts, namely, the field evaluation, the approximate analysis, and the detailed analysis.

The first part evaluates the damage level in qualitative terms on the basis of past records. The second part uses a dynamic structural analysis of the building for the loading conditions mentioned above. The response of the building is subsequently related to a certain damage level in a qualitative manner. The third part analyzes the response of the entire structure in order to estimate the expected damage level. Damage in this procedure is defined as a percentage of the cost of replacement of both structural and non-structural elements.

Using a procedure based on the structural response during earthquakes, Rosenblueth and Yao (1979) presented a model for the prediction of earthquake-induced damage to structures. The proposed model accounts for damage due to past earthquakes. In order to predict future damage, the model is coupled with seismic hazard analysis. Additional models of a similar type are discussed by Yao (1978; 1979).

In contrast to the methods reviewed above, Borg (1979) proposed a model in the form of damage contour charts. The model assumes that the damage of a structure is a function of the site acceleration and, in the provided charts, damage is directly related to the Modified Mercalli Intensity at the site.

In a more general approach, Kuribayashi et al. (1979) used the individual loss ratio for the quantitative description of damage incurred to various kinds of lifeline facilities during the 1978 Miyagiken-Oki earthquake in Japan. The loss ratio is defined as the ratio of the earthquake induced-losses over the existing public wealth in the damaged area, and it receives values that range between zero to one.

A procedure for the prediction of damage to individual building was developed by Kustu (1979). This utilizes either records on damage caused by past earthquakes or a dynamic response analysis of buildings based on the results of seismic hazard analysis of the particular site. Damage is classified according to the cause or type of building to which it refers and is measured in terms of the damage ratio (i.e., the ratio of the repair cost over that required for replacement at the time of damage).

A similar approach was developed by Del Tosto (1979) on the basis of records on damage incurred to buildings during past earthquakes. The approach consists of three stages. The first involves a correlation between the damage and the peak ground acceleration and velocity. The second involves the determination of the distributions for the peak ground acceleration and velocity with the aid of seismic hazard analysis. The third involves the determination of the distribution of the damage. In all three stages, damage is measured in terms

of the damage ratio.

Finally, in a somewhat different approach, Sauter (1979) developed a method to determine the expected annual losses for buildings of the same construction type. This method relates damage to the Modified Mercalli Intensity and determines the probability of exceedance of the latter using seismic hazard analysis. The peak ground acceleration may also be used in the place of the Modified Mercalli Intensity.

## CHAPTER 4

### FAILURE CRITERIA AND PROBABILITY OF FAILURE

#### 4.1 Modes of Failure and Failure Criteria

Gravity-type retaining structures may fail in four possible modes, as illustrated schematically in Fig. 4.1. These are: (a) rotation around any point on the wall plane (overturning); (b) sliding along the base of the wall; (c) failure in bearing capacity of the wall foundation; and (d) overall sliding, a slope-type failure that can take along the wall and its foundation.

Current design practice in geotechnical engineering requires a separate evaluation of the safety of a wall against each of the above four possible modes of failure. The safety measure employed is the factor of safety FS defined as the ratio of two point estimates: one, for the capacity C of the wall (i.e., its resistance against failure) and another, for its demand D (i.e., the forces or moments that tend to cause failure). That is,

$$FS = \frac{C}{D} \quad (4-1)$$

Conventionally, a retaining wall is considered to be safe in a certain mode when the resulting value of FS for this mode is greater than its allowable value  $FS_a$ . The numerical value of the latter is the result of the experience accumulated around the particular type of failure, and it depends on material conditions, applied loading, etc. Typical values of  $FS_a$  are 2 to 3 for the case of over-

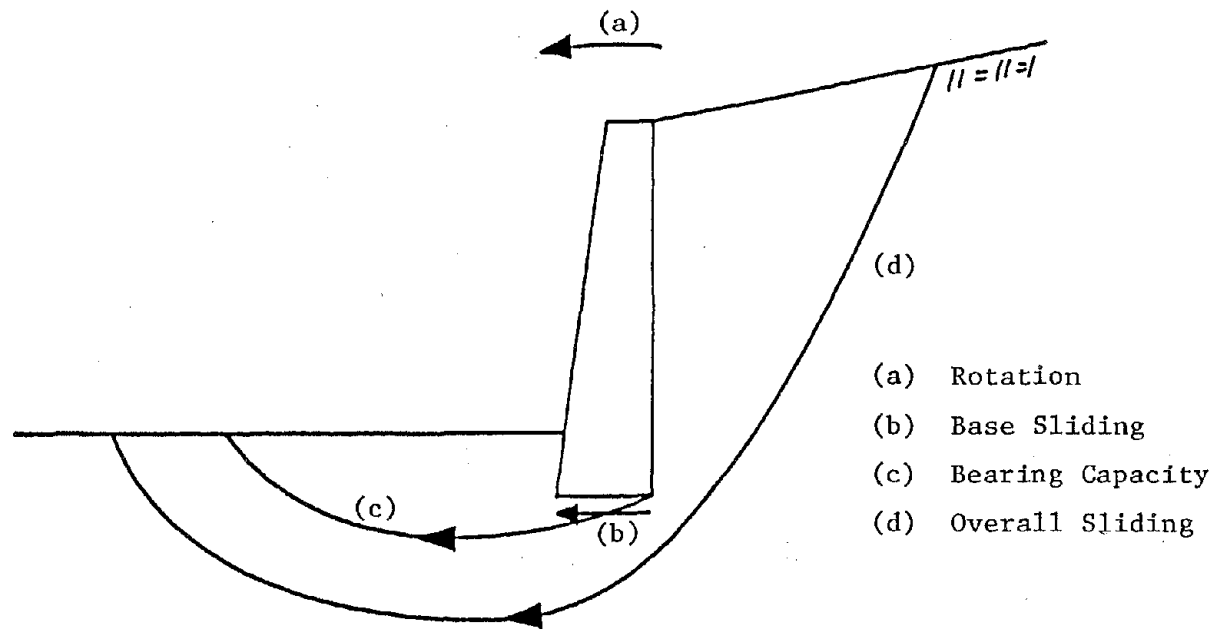


FIG. 4.1 THE POSSIBLE MODES OF FAILURE OF GRAVITY RETAINING WALLS

turning, 1.5 to 2 for base sliding, 3 to 4 for bearing capacity, and 1.2 or higher for slope-type failure.

In a probabilistic formulation of the safety analysis of a retaining wall, use is made of its safety margin  $SM_i$  in mode  $i$ . This is defined as the difference between the capacity  $C_i$  and demand  $D_i$  of the wall in mode  $i$ ; i.e.,

$$SM_i = C_i - D_i \quad (4-2)$$

A wall is considered to be safe in mode  $i$ , if the numerical value of the safety margin  $SM_i$  is positive (i.e.,  $SM_i > 0$ ); otherwise (i.e.,  $SM \leq 0$ ), the wall is considered to be unsafe.

An alternative criterion of safety of a retaining wall is the one that makes use of the concept of failure function (A-Grivas and Asaoka, 1982). This represents a more general formulation of safety as a failure function can be expressed either in terms of the factor of safety or the safety margin or any other convenient measure of safety such as the shear strength of soil, etc.

Thus, for example, if the failure function of a retaining wall in mode  $i$ , denoted as  $H_i$ , is defined on the  $c$ - $t$  plane ( $c$  = cohesion and  $t = \tan\phi$ , where  $\phi$  is soil's angle of internal friction), and  $G_o$  represents the specific conditions of the wall (i.e., geometry, material parameters, location of ground water table, etc.), limiting equilibrium in mode  $i$  may be expressed analytically as

$$H_i(c, t | G_o) = 0 \quad (4-3)$$

That is, for given geometry, loads, and other wall and soil parameters,  $H_i$  is a function of two random variables,  $c$  and  $t = \tan\phi$ .

This is shown schematically in Fig. 4.2. If the available values of  $c$  and  $t$  are such that the corresponding value of  $H_i$  is positive (i.e.,  $H_i > 0$ ), then the wall is considered to be safe under  $G_o$  conditions; otherwise (i.e.,  $H_i \leq 0$ ), the wall is considered to be unsafe. Therefore, failure in mode  $i$  is defined as

$$H_i(c, t | G_o) \leq 0 \quad (4-4)$$

If the failure function  $H_i$  is expressed in terms of the capacity  $C_i$  and demand  $D_i$  of the wall in mode  $i$ , i.e.,  $H_i = H_i(C_i, D_i)$ , then limiting equilibrium may be denoted as

$$H_i(C_i, D_i) = 0 \quad (4-5)$$

Similarly, safety corresponds to the event whereby  $H_i$  receives a positive value,  $H_i > 0$ , and failure to the event  $H_i \leq 0$ . In this case, the expression for the failure function becomes identical to that of the safety margin, i.e.,

$$H_i = SM_i = C_i - D_i \quad (4-6)$$

Finally, if the factor of safety  $FS_i$  in mode  $i$  is used as the criterion of limiting equilibrium, then the corresponding expression for the failure function becomes

$$H_i = FS_i - 1 = \frac{C_i}{D_i} - 1 \quad (4-7)$$



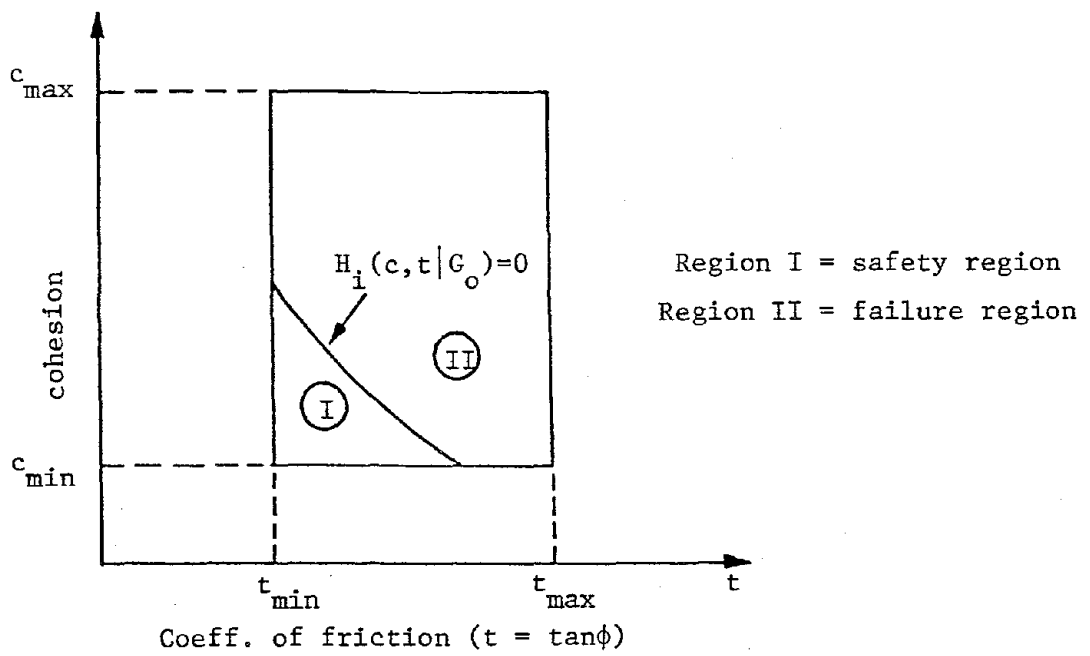


FIG. 4.2 DEFINITION OF FAILURE FUNCTION  
UNDER STATIC CONDITIONS  $G_o$

The analytical expressions for the capacity and demand of each of the four modes of failure of a retaining wall that are employed in this study are given below.

## 4.2 Expressions of Capacity and Demand

### 4.2.1 Overturning

In general, an earth retaining wall may rotate around any point on its plane. Experience, however, accumulated through observations on walls that have failed indicates that the most likely point of rotation is the front-end of its base. This is denoted as point O in Fig. 4.3 in which also shown are the forces that act on the wall under seismic conditions.

The capacity C of the wall is defined as the moment of forces resisting overturning around the center of rotation O (Fig. 4.3), and is expressed analytically as follows:

$$C = (1 + \alpha'_v)W_w \ell + P_A (B - h_A \tan\beta) \sin(\beta + \delta) \quad (4-8)$$

in which B, h,  $\beta$ ,  $h_A$ ,  $\ell$  are geometric quantities shown in Fig. 4.3,  $P_A$  = the total force acting on the wall,  $W_w$  = the weight of the wall,  $\delta$  = angle of friction between the wall and the backfill material, and  $\alpha'_h$ ,  $\alpha'_v$  = the horizontal and vertical accelerations experienced by the wall respectively. In this study,  $\alpha'_h$  and  $\alpha'_v$  are taken to be maximum horizontal and vertical ground accelerations.

In the above formulation, the vertical acceleration of the wall caused by a seismic event is taken to be directed downward as

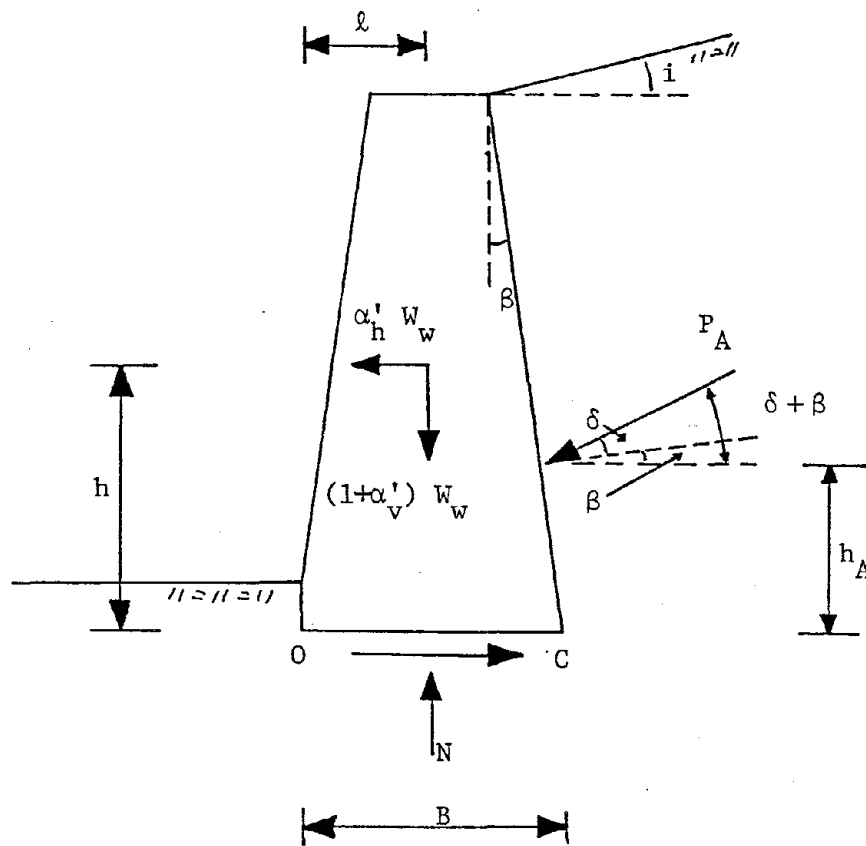


FIG. 4.3 SEISMIC LOADING ON RETAINING WALL FOR OVERTURNING AND BASE SLIDING

this represents the most critical loading condition.

The demand  $D$  on the wall is defined as the moment of the forces that tend to cause overturning around its center of rotation  $O$  (Fig. 4.3). The analytical expression of  $D$  is as follows:

$$D = \alpha'_h W_w h + P_A h_A \cos(\delta + \beta) \quad (4-9)$$

in which the various quantities are given in Eqn. (4-8) and are also shown in Fig. (4.3).

It should be noted that, in general, some additional resistance to overturning is developed in the embedded front side of the wall. However, this additional resistance is usually very small and can be considered negligible, an assumption that will produce somewhat conservative results.

#### 4.2.2 Base Sliding

The capacity  $C$  in base sliding is defined as the force that resists sliding along the wall base. This is equal to the product of the total vertical force at the wall base (force  $N$  in Fig. 4.3) times the coefficient of friction between the wall and the foundation material; i.e.,

$$C = [(1 + \alpha'_v) W_w + P_A \sin(\delta + \beta)] \tan \delta_f \quad (4-10)$$

in which  $\delta_f$  is the angle of friction between the wall base and the foundation soil, and all other quantities are shown in Fig. 4.3.

The demand  $D$  is defined as the force along the base of the

wall that tends to cause sliding. This is analytically expressed as (Fig. 4.3).

$$D = \alpha'_h W_w + P_A \cos(\delta + \beta) \quad (4-11)$$

#### 4.2.3 Bearing Capacity

Several analytical formulations are available in the literature that aim at the determination of the ultimate bearing capacity of a foundation medium. For example, following Meyerhof (1953), one has that for a footing with width  $B$  larger than the height  $D_f$  of the surcharge (i.e.,  $B > D_f$ ), the bearing capacity  $C$  of the foundation is equal to (Fig. 4.4)

$$C = \frac{A'}{2} \left(1 - \frac{2e}{B}\right) \left(1 - \frac{a}{\phi_o}\right)^2 \gamma_f B \lambda_{\gamma} d_{\gamma} N_{\gamma} + A' \left(1 - \frac{a}{90^\circ}\right)^2 \gamma_f D_f \lambda_q d_q N_q + A' \left(1 - \frac{a}{90^\circ}\right)^2 c_f \lambda_c d_c N_c \quad (4-12)$$

in which

$$N_{\phi} = \tan^2 \left(45 + \frac{\phi_o}{2}\right),$$

$$N_q = N_{\phi} e^{\pi \tan \phi_o},$$

$$N_{\gamma} = (N_q - 1) \tan(1.4 \phi_o),$$

$$N_c = (N_q - 1) \cot \phi_o$$

$$\lambda_c = 1 + 0.2 \frac{B}{L_w} N_{\phi},$$

$$\lambda_q = \lambda_{\gamma} = \begin{cases} 1 & , \text{ if } \phi_o = 0^\circ \\ 1 + 0.1 \frac{B}{L_w} N_{\phi} & , \text{ if } \phi_o > 0^\circ \end{cases}$$

$$d_c = 1 + 0.2 \frac{D_f}{B} \sqrt{N_\phi},$$

$$d_\gamma = d_q = \begin{cases} 1 & , \text{ if } \phi_o = 0^\circ \\ 1 + 0.1 \frac{D_f}{B} (N_\phi)^{1/2} & , \text{ if } \phi_o > 0^\circ \end{cases}$$

$$A' = (B - 2e) (L_w - 2e),$$

$\gamma_f$  = unit weight of the foundation material,

$\alpha$  = inclination with respect to the vertical of the force on the foundation,

$e$  = eccentricity of the force acting on the wall base,

$L_w$  = length of the footing,

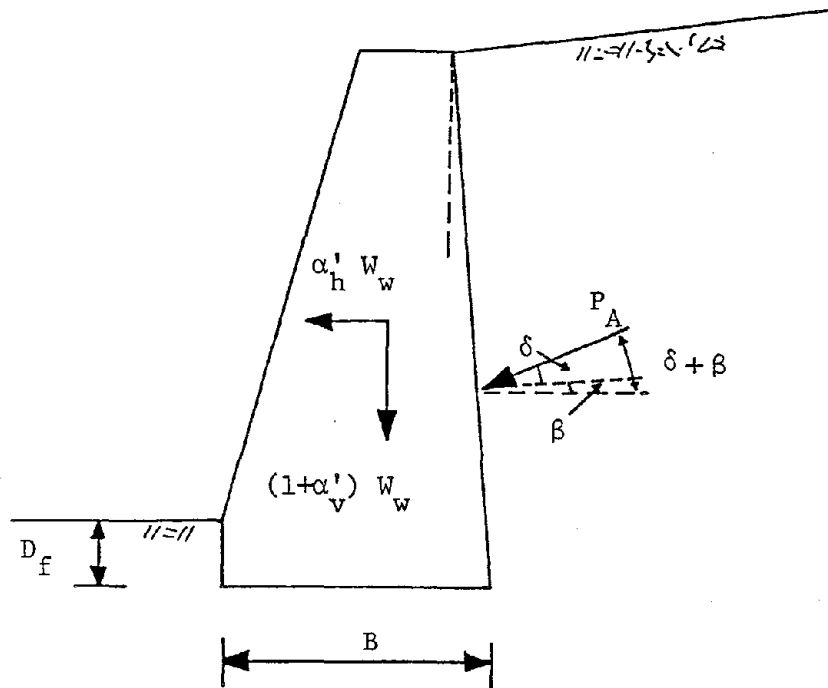
$c_f$  = cohesion of the foundation material,

$\phi_f$  = friction angle of the foundation material, and

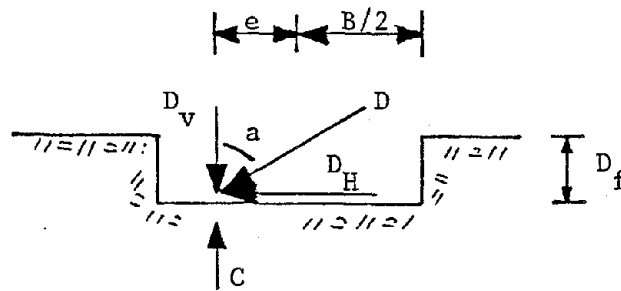
$$\phi_o = (1.1 - 0.1 \frac{B}{L_w}) \phi_f$$

The above expression for  $\phi_o$  may be used when  $\phi_f$  is determined from triaxial compression tests. If  $\phi_f$  is determined from direct-shear tests, then  $\phi_o$  should be taken to be equal to  $\phi_f$  (Meyerhof, 1953).

The demand  $D$  in bearing capacity is defined as the sum of the forces acting at the wall base, including the weight of the wall. Thus, from Fig. 4.4, one has that the expressions for the vertical and horizontal components of the demand,  $D_v$  and  $D_H$ , respectively, are equal to



(a) Force System on the Wall



(b) Force System on the Wall Foundation

FIG. 4.4 SEISMIC LOADING ON RETAINING WALL AND ITS FOUNDATION

$$D_v = (1 + \alpha'_v) W_w + P_A \sin(\delta + \beta) \quad (4-13)$$

$$D_H = \alpha'_h W_w + P_A \cos(\delta + \beta) \quad (4-14)$$

and the total demand D is

$$D = [D_v + D_H]^{1/2} \quad (4-15)$$

#### 4.2.4 Overall Sliding

This is a slope-type mode of failure in which the safety of an earth retaining wall is examined as part of a slope stability analysis that involves both the backfill and the foundation materials. Any procedure from those available for slope stability analysis may be used for this purpose, properly modified in order to account for the changes in inertia forces of the wall and soil medium caused by an earthquake.

In Fig. 4.5 is shown schematically the force system present in the overall sliding mode of failure. This corresponds to the simple method of slices, in which the seismic effect is taken into account by introducing additional horizontal and vertical forces at the centroid of each slice (Vlavianos, 1981). In this case, capacity C is defined as the moment of the resisting forces around the center of the (circular) failure surface and demand D as that of the driving forces around the same point. Their analytical expressions are as follows:

$$C = R \sum_{i=1}^{i=n} [c \Delta l_i + \{W_i (1 + \alpha'_v)\} \tan \phi \cos \theta_i] \quad (4-16)$$



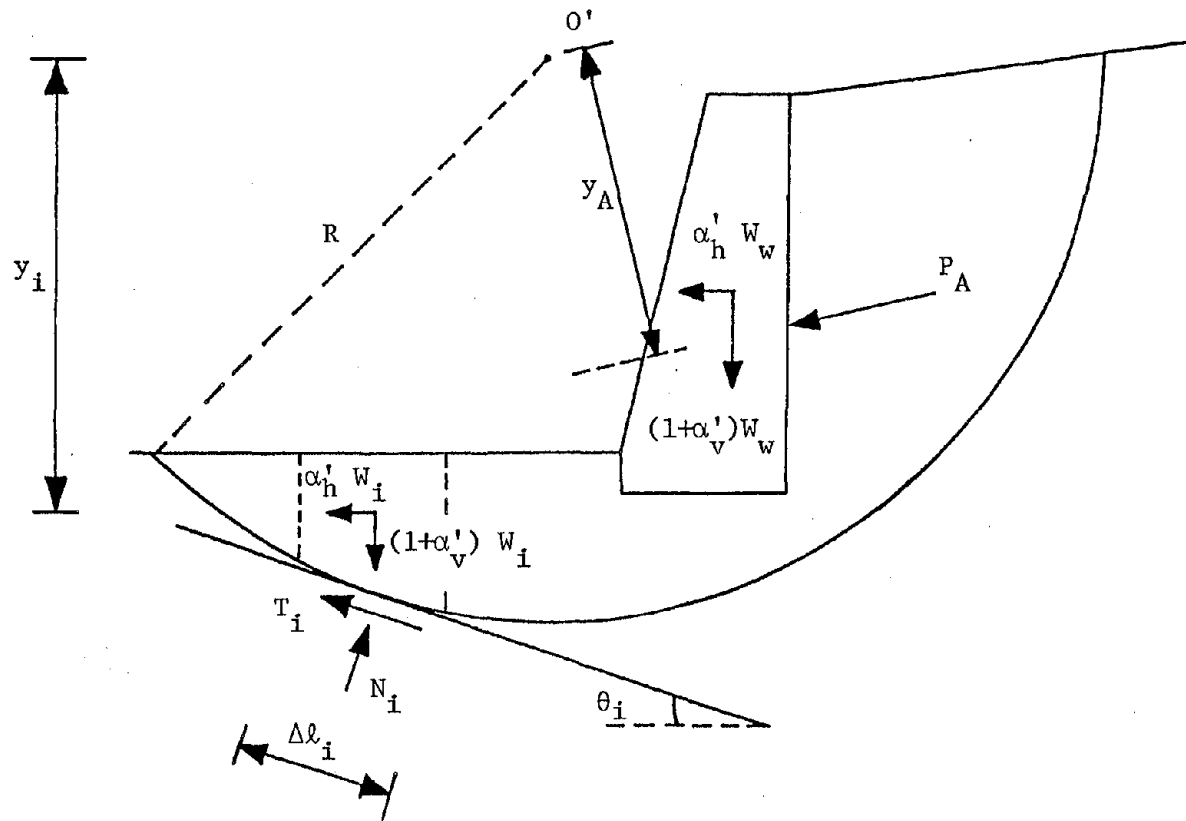


FIG. 4.5 SEISMIC LOADING ON RETAINING WALL FOR OVERALL SLIDING

$$D = R \sum_{i=1}^{i=n} W_i (1 + \alpha'_v) \sin \theta_i + \sum_{i=1}^{i=n} \alpha'_h W_i y_i + P_A y_A \quad (4-17)$$

in which  $n$  is the total number of slices and all other quantities are shown in Fig. 4.5.

### 4.3 Determination of the Probability of Failure

#### 4.3.1 Static Conditions

Using the definition of failure given in Eqn. (4-4), the probability of failure  $P_f$  of a retaining wall in mode  $i$  under static conditions ( $G_o$ ) may be determined as the probability with which the failure function receives values smaller than or equal to zero; i.e.,

$$P_{f_i} = P[H_i(c, \phi | G_o) \leq 0] \quad (4-18)$$

Furthermore, if  $\xi(c, t)$  represents the joint distribution of the two soil strength parameters  $c$  and  $t = \tan \phi$ , then for a given pair of values taken by  $c$  and  $t$ , one has

$$P[H_i(c, t | G_o) \leq 0 | c, t] = \begin{cases} 1 & , \text{ if } H_i(c, t | G_o) \leq 0 \\ 0 & , \text{ if } H_i(c, t | G_o) > 0 \end{cases} \quad (4-19)$$

The total probability of failure  $P_{f_i}(G_o)$  of a retaining wall in mode  $i$  under  $G_o$  conditions can be found with the aid of the total probability theorem (Harr, 1977) as follows:

$$P_{f_i}(G_o) = \iint P[H_i(c, t | G_o) \leq 0 | c, t] \xi(c, t) dc dt \quad (4-20)$$

in which the indicated integration is performed along the  $c$ - $t$  region

for which  $H_1(c, t|G_0) \leq 0$ , i.e., the failure region (Region I, Fig. 4.2).

Introducing Eqn. (4-19) into Eqn. (4-20), the following expression for  $P_{f_i}(G_0)$  is obtained:

$$P_{f_i}(G_0) = \iint \xi(c, t) dc dt \quad (4-21)$$

in which the integration domain is the same as in Eqn. (4-20).

In the special case of a cohesionless material (i.e.,  $c = 0$ ), Eqn. (4-21) is reduced to

$$P_{f_i}(G_0) = \int f_t(t) dt \quad (4-22)$$

in which  $f_t(t)$  is the probability density function of  $t$  and the integration is performed along the region of  $t$  for which  $H_1(t|G_0) \leq 0$ , i.e., the failure region (Region I, Fig. 4.6).

#### 4.3.2 Seismic Conditions

The effect of an earthquake on a retaining wall and the soil mass comprising its backfill and foundation materials is introduced as an increase in their inertia and is expressed in terms of the maximum acceleration expected to be experienced at the site of the wall.

Let  $\alpha$  denote the maximum ground acceleration and  $\Delta G$  the corresponding change in the wall's conditions because of the additional inertia, i.e.,  $\Delta G = \Delta G(\alpha)$ . The expression for the failure function for mode  $i$  in this case becomes

$$H_1(c, t|G + \Delta G) = 0 \quad (4-23)$$

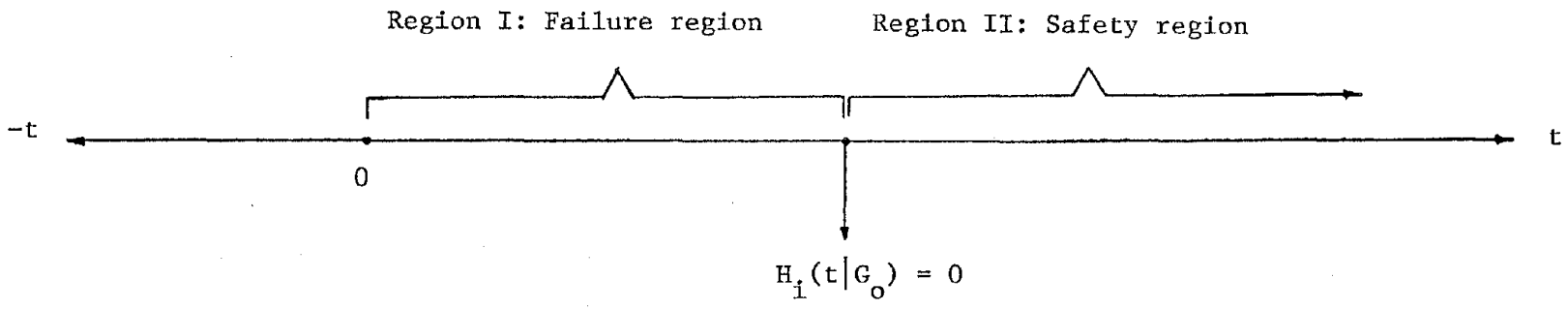


FIG. 4.6 DEFINITION OF FAILURE FUNCTION UNDER STATIC CONDITIONS

and the wall is considered to be safe, if  $H_i(c,t|G + \Delta G) > 0$ ; and unsafe, if  $H_i(c,t|G + \Delta G) \leq 0$ . This is shown schematically in Fig. 4.7, in which Region I corresponds to failure and Region II to safety.

The probability of failure  $P_{f_i}(G_o + \Delta G)$  of a retaining wall in mode  $i$  under seismic conditions ( $G_o + \Delta G$ ) can be determined in a manner similar to that described for static conditions, Eqn. (4-21). Its analytical expression is given as

$$P_{f_i}(G_o + \Delta G) = \iint \xi(c,t) dc dt \quad (4-24)$$

in which the indicated integration is performed along the  $c$ - $t$  region for which  $H_i(c,t|G_o + \Delta G) \leq 0$  (Region I, Fig. 4.7).

In the special case of a cohesionless material (i.e.,  $c = 0$ ), the expressions for  $P_{f_i}(G_o + \Delta G)$  is reduced to

$$P_{f_i}(G_o + \Delta G) = \int f_t(t) dt \quad (4-25)$$

in which  $f_t(t)$  is the probability density function of  $t$  and the indicated integration is performed along the region of  $t$  for which  $H_i(t|G_o + \Delta G) \leq 0$ , i.e., the failure region (Region I, Fig. 4.8).

#### 4.3.3 Total Probability of Failure

As a retaining wall may fail in four possible modes (Fig. 4.1), a system (or, combinatory) reliability analysis can be used to arrive at an expression for its total probability of failure (Harr, 1977; A-Grivas, 1979). Such an equivalent system representation is shown schematically in Fig. 4.9.

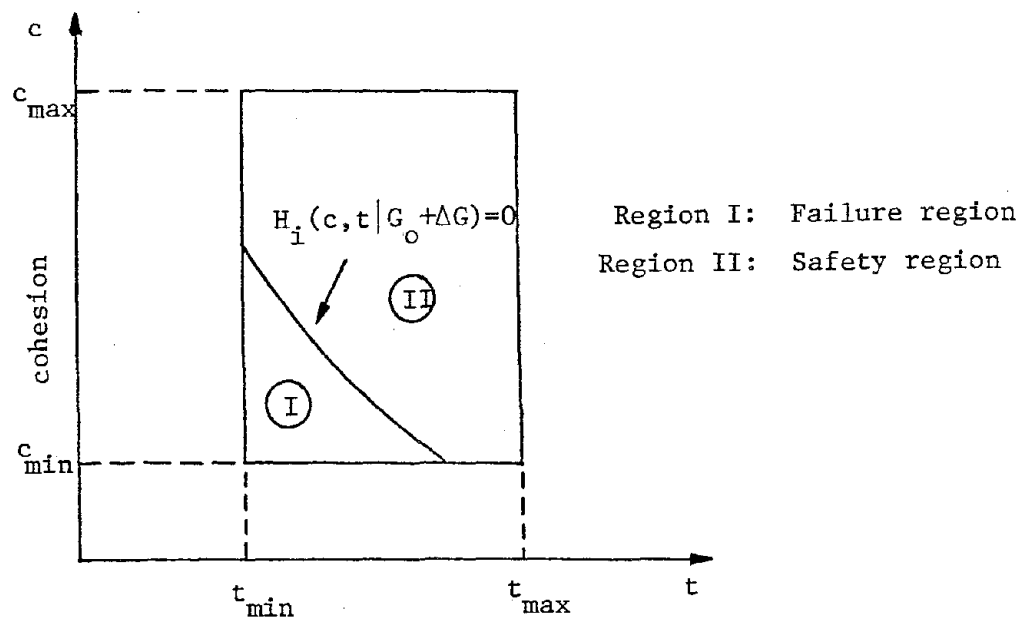


FIG. 4.7 DEFINITION OF FAILURE FUNCTION UNDER SEISMIC CONDITIONS

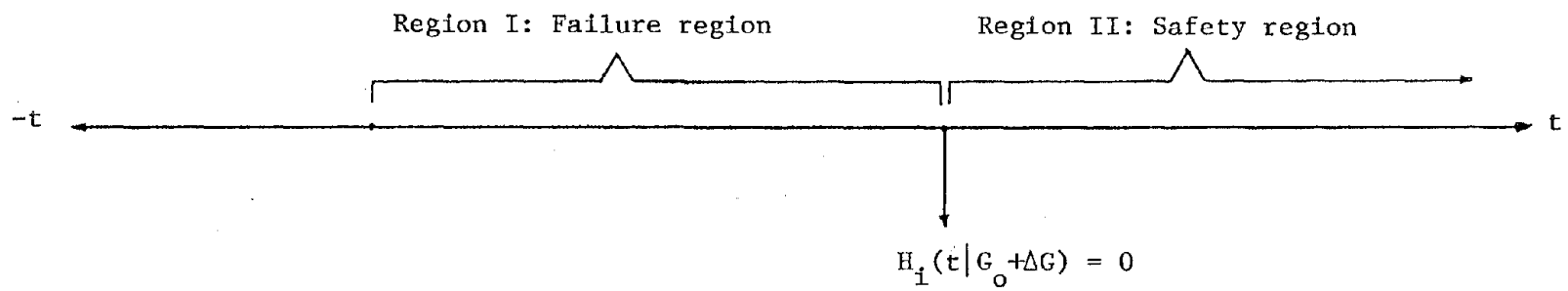


FIG. 4.8 DEFINITION OF FAILURE FUNCTION UNDER SEISMIC CONDITIONS

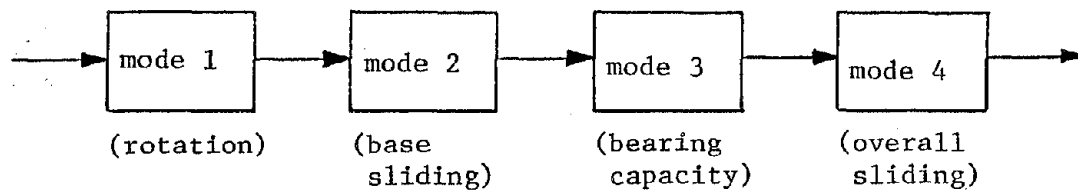


FIG. 4.9 EQUIVALENT SYSTEM REPRESENTATION OF A RETAINING WALL



If  $P_{f_i}$ ,  $i = 1, \dots, 4$ , denotes the probability of failure in the  $i$ -th mode (under static or seismic conditions), and if the four modes are assumed to be independent of one another, then the total probability of failure  $P_f$  of the wall is equal to

$$P_f = 1 - \prod_{i=1}^4 (1 - P_{f_i}) \quad (4-26)$$

in which  $\prod$  denotes multiplication of the quantities in parenthesis.

The complement of the probability of failure  $P_{f_i}$  is defined as the reliability  $r_i$  of the wall in mode  $i$ ; i.e.,

$$r_i = 1 - P_{f_i} \quad (4-27)$$

Combining Eqns. (4-26) and (4-27), one has that the total reliability  $r$  of the wall is equal to

$$r = 1 - P_f = \prod_{i=1}^4 r_i \quad (4-28)$$

## CHAPTER 5

### SEISMIC SAFETY PREDICTION

#### 5.1 Wall Performance under Static Conditions

Section 4.3 provided the expressions for the predicted values of the probability of failure of a retaining wall in any of the four possible modes of failure. These were given by Eqn. (4-21), for static conditions ( $G_o$ ), and Eqn. (4-24), for seismic conditions ( $G_o + \Delta G$ ). The latter provided the probability of failure during an earthquake without accounting for any information that might be available about its performance under static conditions (i.e., after the completion of the construction of the retaining wall but before the occurrence of an earthquake). In this sense,  $P_f(G_o + \Delta G)$  represents the predicted value of the probability of failure when the prediction is made during the design stage.

After the completion of the construction of the wall, however, and prior to the occurrence of an earthquake, observations made on the wall will provide additional information about its safety under static conditions ( $G_o$ ). This information may be expressed in the form of two alternatives, namely; (a) the wall has failed under static conditions, i.e.,  $P_f(G_o) = 1$ , in which case a prediction of the probability of failure under seismic loading is irrelevant; and (b) the wall is safe under static conditions, i.e.,  $P_f(G_o) = 0$ . As it will be seen below, this additional information obtained from

wall performance under static loading can be used to arrive at an improved prediction of its safety under seismic loading. The approach is general and therefore applicable to any of the four modes of failure.

## 5.2 Posterior Distribution of Soil Strength Parameters

Considering the definitions of failure function given in Section 4.1, the observation  $P_f(G_o) = 0$  may be interpreted to imply that the soil strength parameters  $c$  and  $t$  under static conditions ( $G_o$ ) produce a positive value for the failure function,  $H(c,t|G_o) > 0$ . That is,  $c$  and  $t$  lie within the safety region, Region I, as illustrated schematically in Fig. 4.2. This observation may be used to provide a modified expression for the joint distribution  $\xi(c,t)$  of  $c$  and  $t$ .

Let  $\xi'(c,t)$  denote the posterior (to the successful wall performance under static conditions) probability density function of  $c$  and  $t$ ; i.e.,

$$\xi'(c,t) = \xi[c,t|H(c,t|G_o) > 0] \quad (5-1)$$

A Bayesian analysis provides the following expression for  $\xi'(c,t)$ :

$$\xi'(c,t) = kL(c,t)\xi(c,t) \quad (5-2)$$

in which

$\xi(c,t)$  = the prior distribution of  $c$  and  $t$ ,

$L(c,t)$  = the likelihood function, and

$k$  = the normalizing constant.

The likelihood function  $L(c,t)$  provides the probability associated with the observation. In accordance with the interpretation of the observation given above, one has that  $L(c,t)$  is equal to

$$L(c,t) = P[H(c,t|G_0) > 0 | c,t] = \begin{cases} 1 & , \text{ if } H(c,t|G_0) > 0 \\ 0 & , \text{ if } H(c,t|G_0) \leq 0 \end{cases} \quad (5-3)$$

The normalizing constant  $k$  is needed so that  $\xi'(c,t)$  is a probability density function (i.e., its integral along the region of its variation is equal to unity). Its analytical expression is

$$k = 1 / \iint P[H(c,t|G_0) > 0 | c,t] \xi(c,t) dc dt \quad (5-4)$$

in which the indicated integration is performed over the region in which  $H(c,t|G_0) > 0$ , i.e., Region I in Fig. 4.2.

Combining Eqns. (5-2), (5-3) and (5-4), it is found that

$$\xi'(c,t) = \frac{\xi(c,t)}{\iint \xi(c,t) dc dt} \quad (5-5)$$

The denominator of Eqn. (5-5) is equal to  $1 - \iint \xi(c,t) dc dt$ , where the integration is performed along the domain wherein  $H(c,t|G_0) \leq 0$ , i.e., Region II in Fig. 4.2. Recalling that, in this case, the integral is equal to the probability of failure under  $G_0$  conditions, given in Eqn. (4-21), one has that Eqn. (5-5) can be written as

$$\xi'(c,t) = \frac{\xi(c,t)}{1 - P_f(G_0)} \quad (5-6)$$

That is, the posterior distribution of the strength parameters is equal to the ratio of their prior distribution over the complement of the probability of failure under static conditions.

### 5.3 Posterior Probability of Failure

The observation that a retaining wall is safe under static conditions can be used to provide an improved measure for the predicted probability of failure during an earthquake. In Bayesian parlance, this is called the "posterior" probability of failure and is denoted as  $P'_f(G_o + \Delta G)$ ; i.e.,

$$P'_f(G_o + \Delta G) = P_f(G_o + \Delta G | \text{safe under } G_o) \quad (5-7)$$

Using the posterior probability density function  $\xi'(c,t)$ , given in Eqn. (5-6), A-Grivas and Asaoka (1982) have shown that Eqn. (5-7) is reduced to the following expression:

$$P'_f(G_o + \Delta G) = \frac{P_f(G_o + \Delta G) - P_f(G_o)}{1 - P_f(G_o)} \quad (5-8)$$

The corresponding expression for the case of cohesionless soils is derived in Appendix A.

### 5.4 Seismic Capacity of a Retaining Wall

The posterior probability of failure  $P'_f(G_o + \Delta G)$  of a retaining wall is a function of the ground acceleration  $\alpha$ ; i.e.,

$$P'_f(G_o + \Delta G) = P'_f(\alpha) \quad (5-9)$$

Let  $R$  denote the maximum value of the acceleration that can be experienced by the retaining wall without failure. In this sense,

R represents the capacity of the retaining wall to undertake the additional seismic load expressed in the form of an acceleration. The probability density function  $f_R(R)$  of R has been shown to be equal to the derivative of  $P_f'(\alpha)$  in the respect to  $\alpha$ , in which  $\alpha$  is replaced by R (Matsuo and Asaoka, 1978; A-Grivas and Asaoka, 1982); i.e.,

$$f_R(R) = \left. \frac{dP_f'(\alpha)}{d\alpha} \right|_{\alpha = R} \quad (5-10)$$

The predicted probability of failure  $P_f$  during a future earthquake of maximum acceleration  $\alpha$  is computed as follows

$$P_f = \int f_R(R) dR \quad (5-11)$$

in which the integration domain is bounded by the lower limit of the range of R and the maximum acceleration  $\alpha$ .

### 5.5 Prediction of Wall Performance after the Occurrence of an Earthquake

After the occurrence of an earthquake the retaining wall has either performed successfully or has been damaged. Assuming that the shaking was of magnitude  $M = m_1$ , and occurred at a distance  $L = l_1$ , the realized maximum horizontal acceleration  $\alpha_1$  at the site of the wall is obtained from the following attenuation law provided by Seismic Hazard Analysis (A-Grivas, 1978)

$$\alpha_1 = b_1 e^{b_2 m_1 (\ell_1 + b_4)^{-b_3}} \varepsilon \quad (5-12)$$

or,

$$\alpha_1 = k_1 \varepsilon \quad (5-13)$$

where

$$k_1 = b_1 e^{b_2 m_1 (\ell_1 + b_4)^{-b_3}} \quad (5-14)$$

The parameter  $\varepsilon$  denotes the ratio of the observed to the computed values for the maximum horizontal acceleration and follows the lognormal distribution (Donovan, 1974). Since  $k_1$  is constant, the probability density function for  $\alpha_1$  can readily be determined as follows (Harr, 1977)

$$f_{\alpha_1}(\alpha_1) = \frac{f_{\varepsilon}[\varepsilon = \varepsilon(\alpha_1)]}{\left| \frac{d\alpha_1}{d\varepsilon} \right|} \quad (5-14)$$

Assuming that the seismic capacity  $R$  of the wall and the maximum horizontal acceleration  $\alpha_1$  are independent variables, leads to the following expression

$$f(R, \alpha_1) = f_R(R) f_{\alpha_1}(\alpha_1) \quad (5-15)$$

If the wall performed successfully during the earthquake, it is of interest to predict its behavior during a future earthquake.

The same reasoning as previously and incorporation of Eqn. (5-15) leads to the following prediction for the probability of failure  $P_f$  of a retaining wall during a future earthquake

$$P_f = \frac{E[(1-F_{\alpha}(R)) F_{\alpha_1}(R)]}{E[F_{\alpha_1}(R)]} \quad (5-16)$$

in which,  $F_{\alpha_1}(R)$  is the cumulative probability density function of  $\alpha_1$  and  $F_{\alpha}(R)$  is the cumulative probability density function of the maximum horizontal ground acceleration provided by Seismic Hazard Analysis.

If the wall has been damaged during the earthquake, its damage is quantified by the ratio of the cost of repairs over that required for the replacement of the wall at the time of damage

$$d_1 = D_r(\alpha_1, R) = \frac{\text{repair cost (R.C.)}}{\text{total replacement cost (T.R.C.)}} \quad (5-17)$$

Damage  $D_r$  is subsequently connected to both the realized maximum ground acceleration  $\alpha_1$  and the seismic resistance  $R$  of the wall, as follows

$$(D_r)^{\psi_d} = \frac{\alpha_1}{R} \quad (5-18)$$

where  $\psi_d$  is a coefficient to account for different design schemes. It is noted that damage  $D_r$ , as given by Eqn. (5-17) varies between 0 and 1. This means that the realized peak horizontal acceleration



$\alpha_1$  must have a value lower than the seismic capacity  $R$ . Had the opposite occurred, that is  $\alpha_1 > R$ , the wall would have failed.

Solving Eqn. (5-17) with respect to  $\alpha_1$  provides the following relationship

$$\alpha_1 = D_{\alpha_1}^{-1}(d_1, R) \quad (5-18)$$

Furthermore, the same reasoning and Eqn.(5-18) lead to the following prediction for the probability of failure  $P_f$  of a retaining wall during a future earthquake

$$P_f = \frac{E[(1-F_{\alpha}(R)) f_{\alpha_1}(D_{\alpha_1}^{-1}(d_1, R))]}{E[f_{\alpha_1}(D_{\alpha_1}^{-1}(d_1, R))]} \quad (5-19)$$

## CHAPTER 6

### CASE STUDY

#### 6.1 Description of the Facility

The developed probabilistic seismic safety analysis is applied to an actual case study, the required information for which was obtained during a site investigation into the February and March 1981 earthquakes in Greece. For the first time ever, detailed information is now available on the type and magnitude of the movement experienced by a retaining structure under earthquake loading.

The case study involves a concrete wingwall adjacent to a small, massive bridge that is located near the town of Plateas, Greece, just two miles from the main ground rupture that was caused by the earthquake. The wingwall provides support for the embankment of the main road that leads to the town. In Fig. 6.1 is shown a plan view of the wingwall, the adjacent bridge (associated with a torrent draining facility), the wall backfill and the supported embankment. A front view of the wingwall used in the case study and adjacent facilities is shown in Fig. 6.2. Characteristic cross-sections of the torrent draining facility (Fig. 6.1, Position A-A) and the wingwall (Fig. 6.1, Positions B-B and C-C) are shown in Figs. 6.3, 6.4 and 6.5.

The backfill and foundation media of the wingwall consist primarily of a coarse-grained material with an admixture of silt.

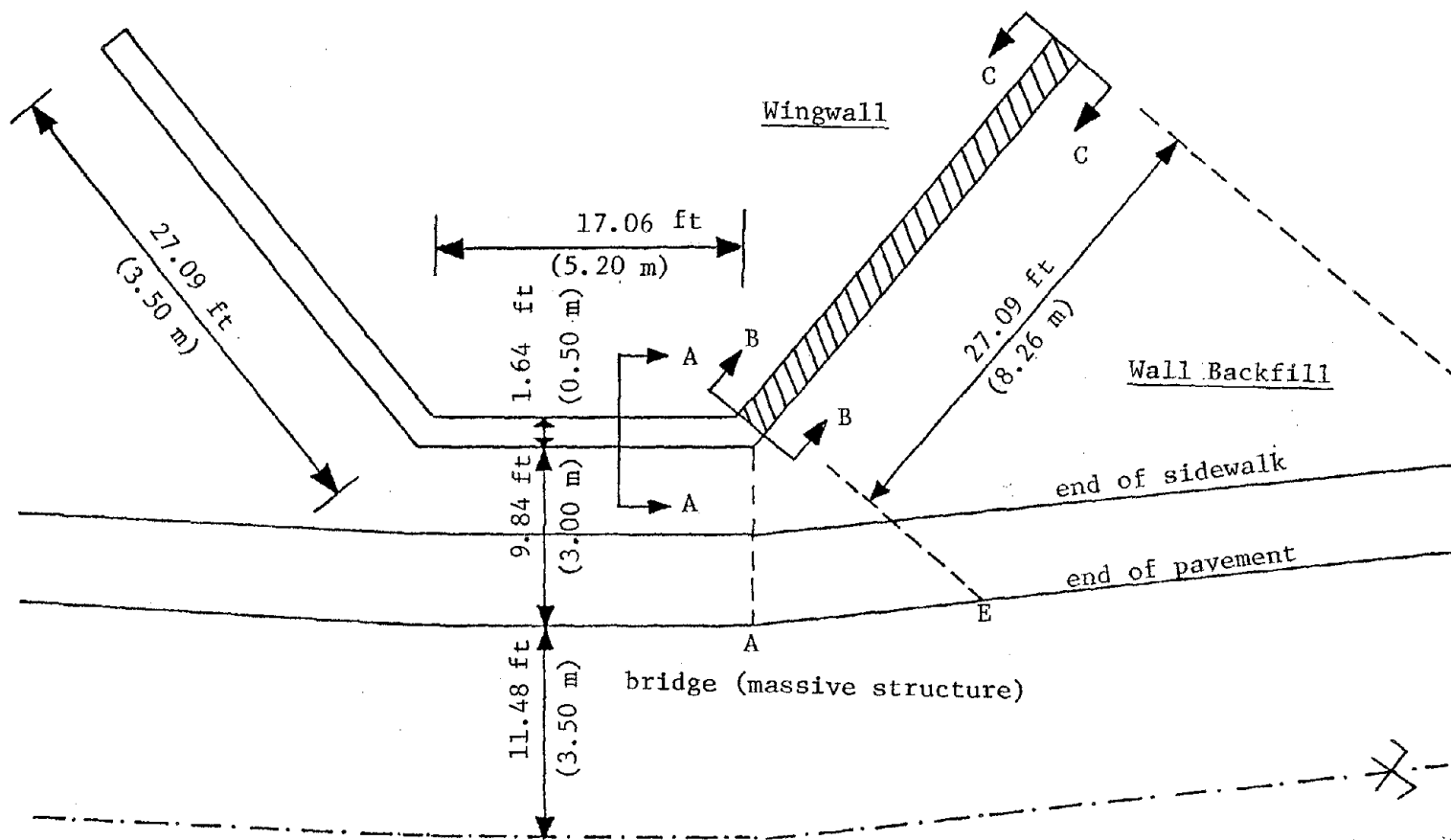


FIG. 6.1 PLAN VIEW OF THE WINGWALL AND ADJACENT STRUCTURES

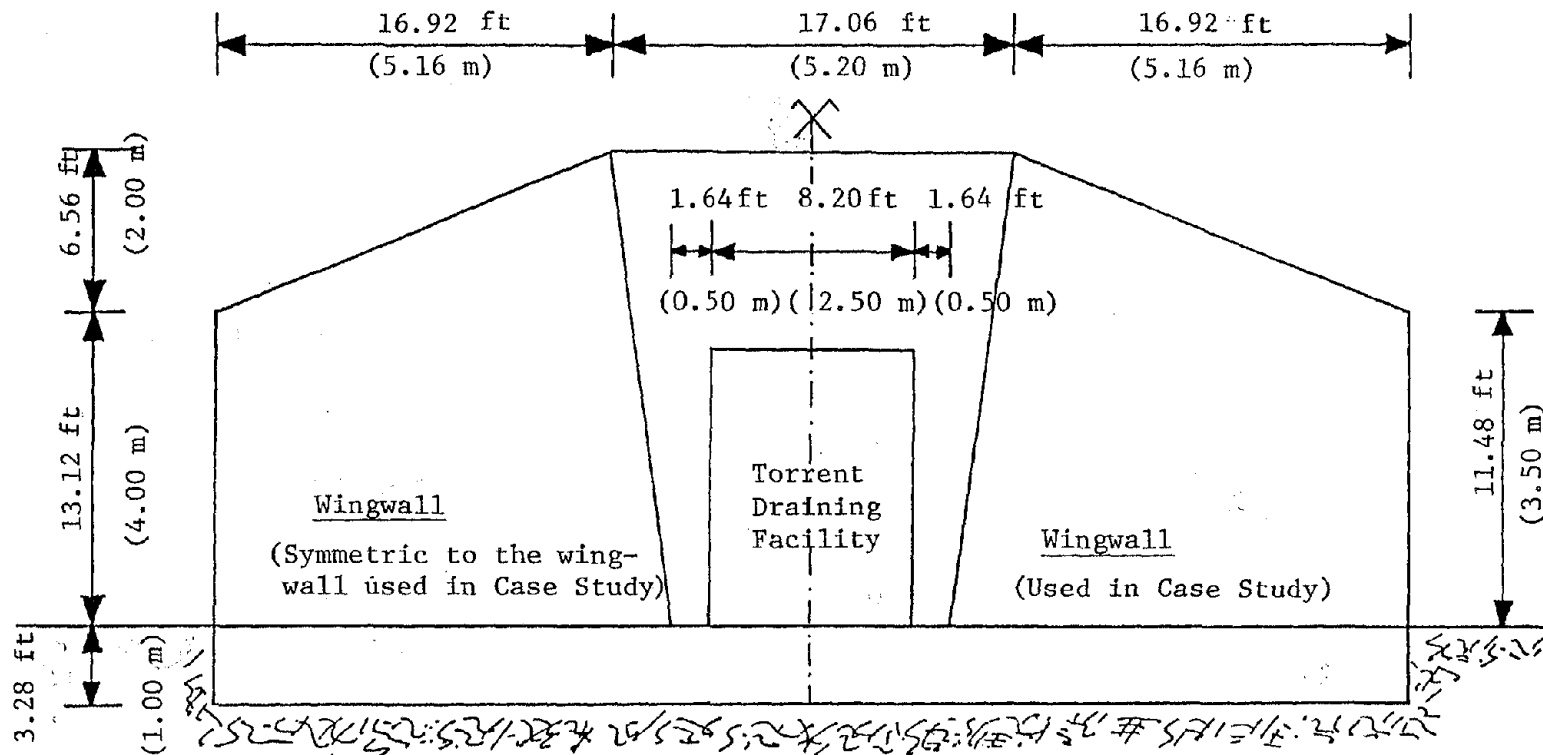


Fig. 6.2 FRONT VIEW OF THE WINGWALL USED IN CASE STUDY AND ADJACENT FACILITIES

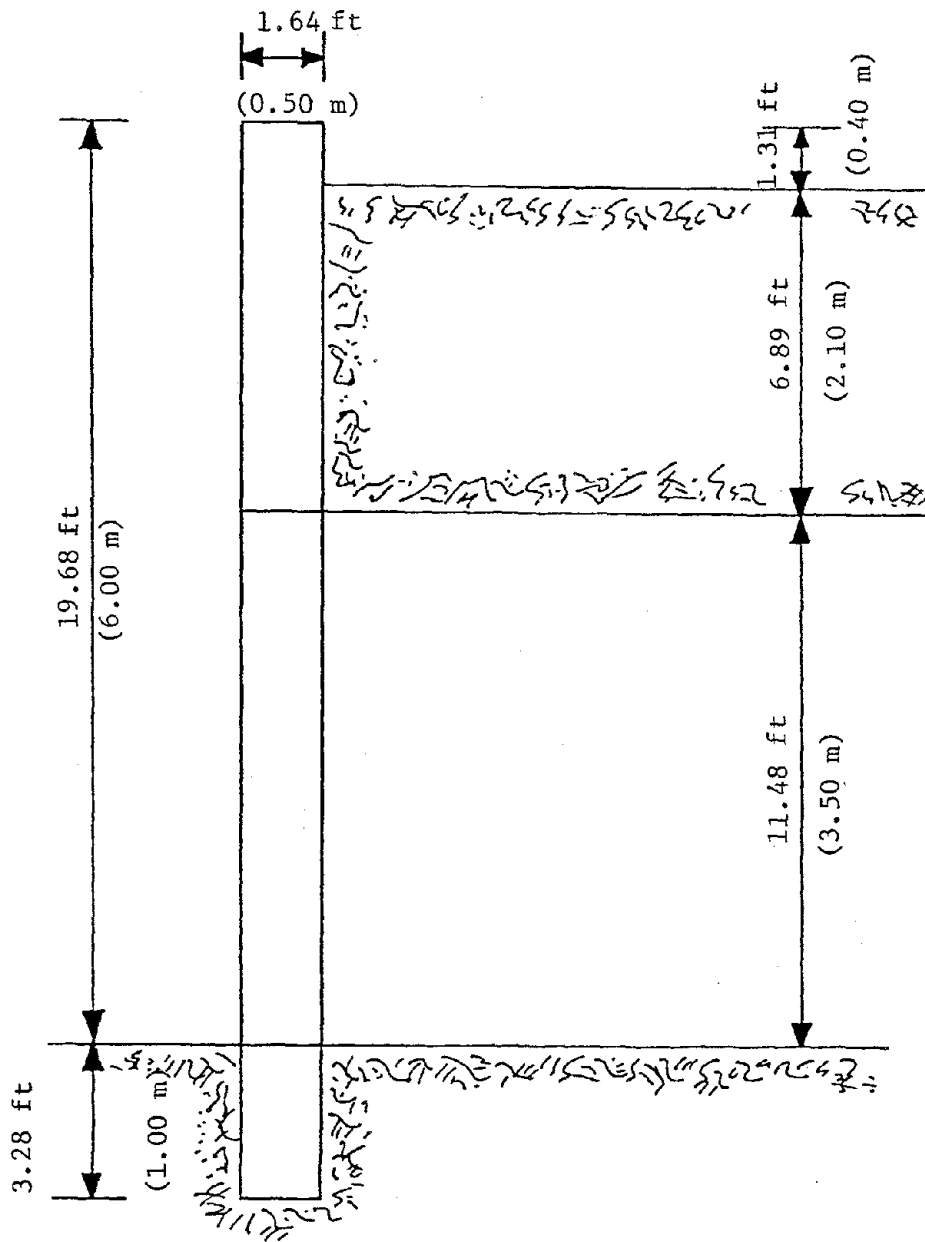


FIG. 6.3 CROSS-SECTION OF TORRENT DRAINING FACILITY  
AT LOCATION A-A (from Fig. 6.2)

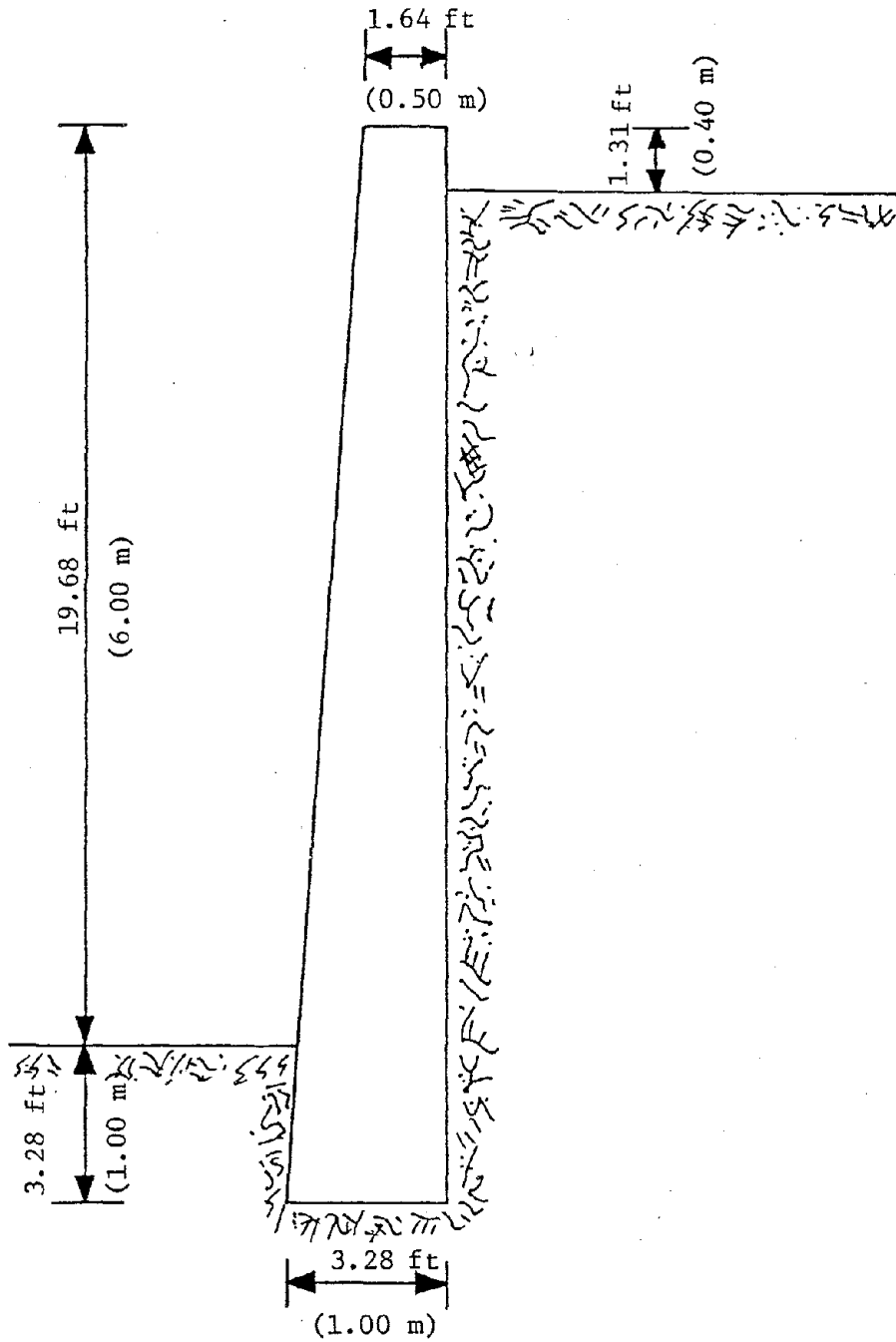


FIG. 6.4 CROSS-SECTION OF WINGWALL AT LOCATION B-B  
(from Fig. 6.2)

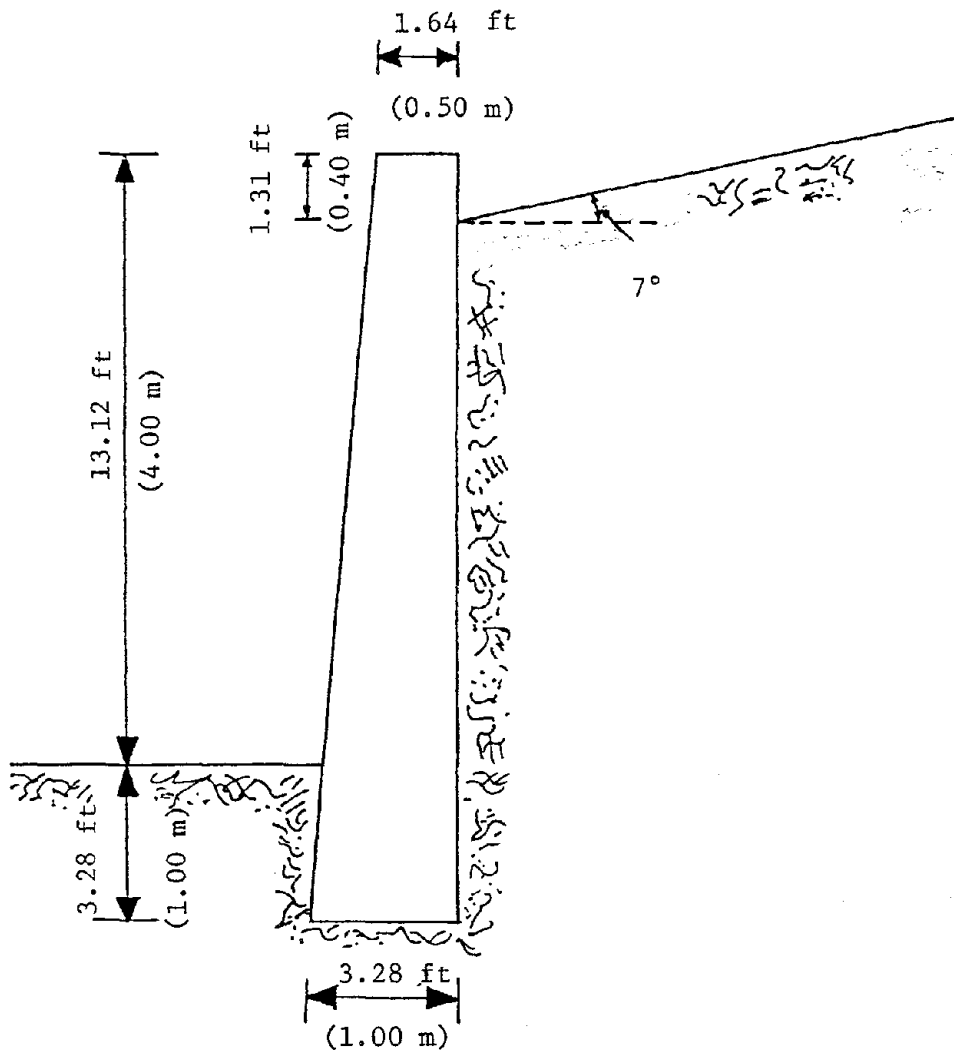


FIG. 6.5 CROSS-SECTION OF WINGWALL AT LOCATION C-C  
(from Fig. 6.2)

At the time of the site investigation (May 1981), the backfill was in a dry condition, an indication that the drainage system of the wingwall performed properly. From Figs. 6.4 and 6.5, it can be seen that the inclination of the backfill varies along the wingwall.

## 6.2 Ground Motion Parameters

In February and March, 1981, the site of the facility was subjected to three major earthquakes that caused severe damage to the town of Plateas and other towns in the vicinity of the facility. In Table 6.1 are listed the dates of the earthquakes, and the magnitudes of the local intensities, measured in accordance with the Modified Mercalli Intensity (MMI) scale. The latter were obtained during a damage assessment in the region affected by the seismic activities. In the same table are given the corresponding values of the maximum horizontal ground acceleration  $\alpha_h$  determined with the aid of the following expression (Gutenberg and Richter, 1954):

$$\log \alpha_h = \frac{I}{3} - 0.5 \quad (6-1)$$

in which I is the magnitude of the intensity (MMI) and  $\alpha_h$  is measured in  $\text{cm/sec}^2$  and g's.

## 6.3 Behavior of the Wingwall before the Seismic Activity

### 6.3.1 Description of Failure

During the compaction of the embankment and before the occurrence of the earthquakes, a vertical crack was developed in



TABLE 6.1

## CHARACTERISTICS OF THE SEISMIC ACTIVITY

DATE	LOCAL MMI	EPICENTRAL MAGNITUDE (in Richter's Scale)	$\alpha_h$ (cm/sec <sup>2</sup> )	$\alpha_h$ (in g's)
2/24/1981	7	6.6	68.13	0.07
2/25/1981	6	6.3	31.62	0.03
3/4/1981	8.5	6.2	215.44	0.22

the wingwall near its joint with the bridge. The two structures, though separated by the crack (the position of which is indicated as Point F in Fig. 6.6), remained in contact without any visible relative movement.

In Fig. 6.6 is shown schematically the distribution of the vertical settlement that took place in the backfill, at the position near the end of the pavement. The maximum value of the settlement was equal to 1.15 ft (0.35 m) and occurred at approximately the midpoint of segment AH (Fig. 6.6).

The cross-section of the wingwall at the position of the crack is shown in Fig. 6.7. The magnitude of the crack along the horizontal direction is 0.79 inches (2.01 cm), a value sufficiently large to render segment FG (Fig. 6.6) independent of the remaining of the facility. The separated segment of the wingwall was subsequently considered to behave as a retaining wall of gravity type in contact with a backfill material bounded by lines FE and GH, Fig. 6.6.

#### 6.3.2 Cause of Failure

In general, the stress system developed within wingwalls depends on their ability to act together with the more massive adjacent facility as a rigid structure. In accordance to current design practice, wingwalls are expected to behave as ordinary retaining structures and, therefore, are designed for the critical case of fully developed earth pressures within the backfill material (active conditions). The latter produce shear forces and bending moments

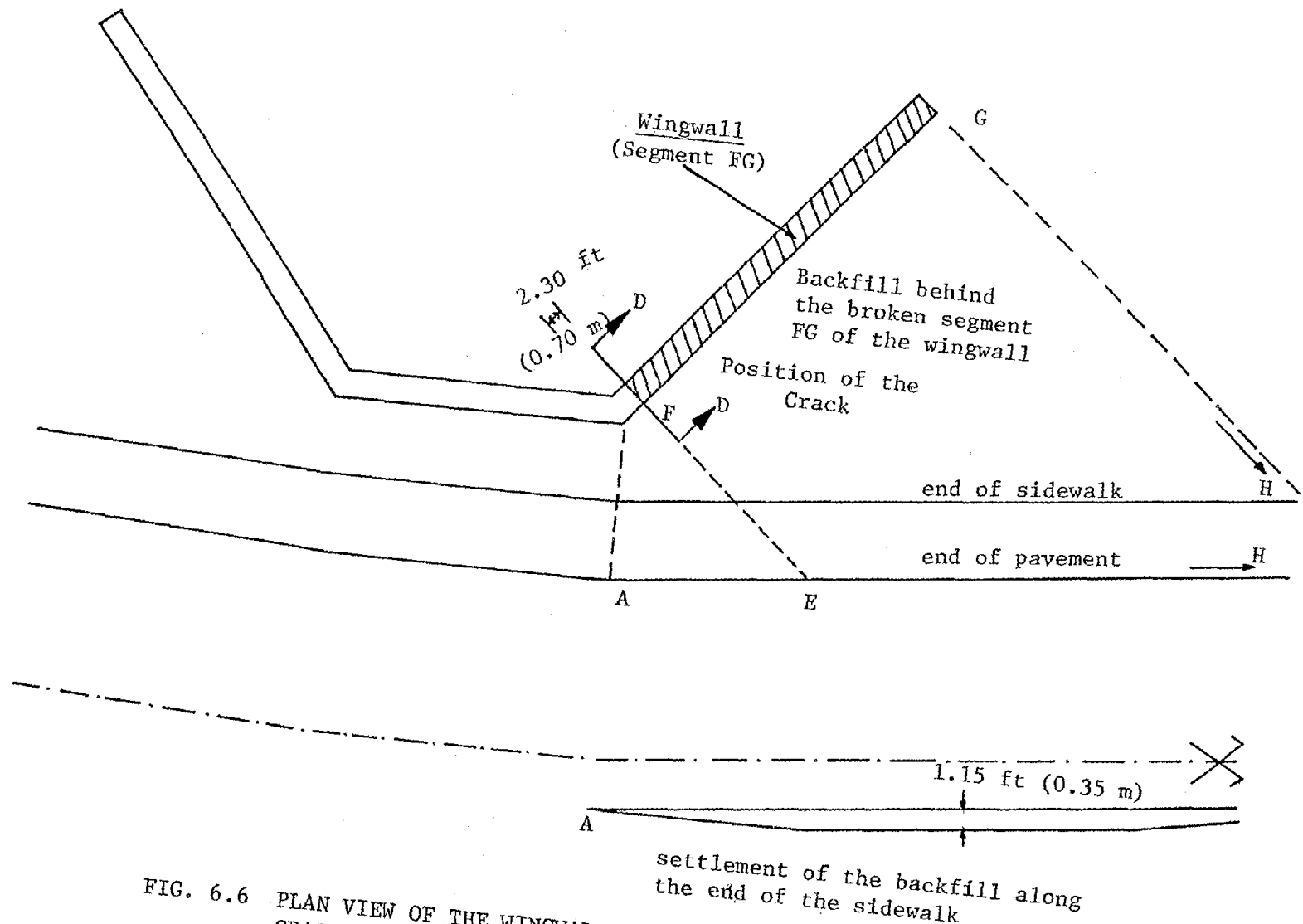


FIG. 6.6 PLAN VIEW OF THE WINGWALL ILLUSTRATING THE POSITION OF THE CRACK AND THE DISTRIBUTION OF THE SETTLEMENT OF THE BACKFILL

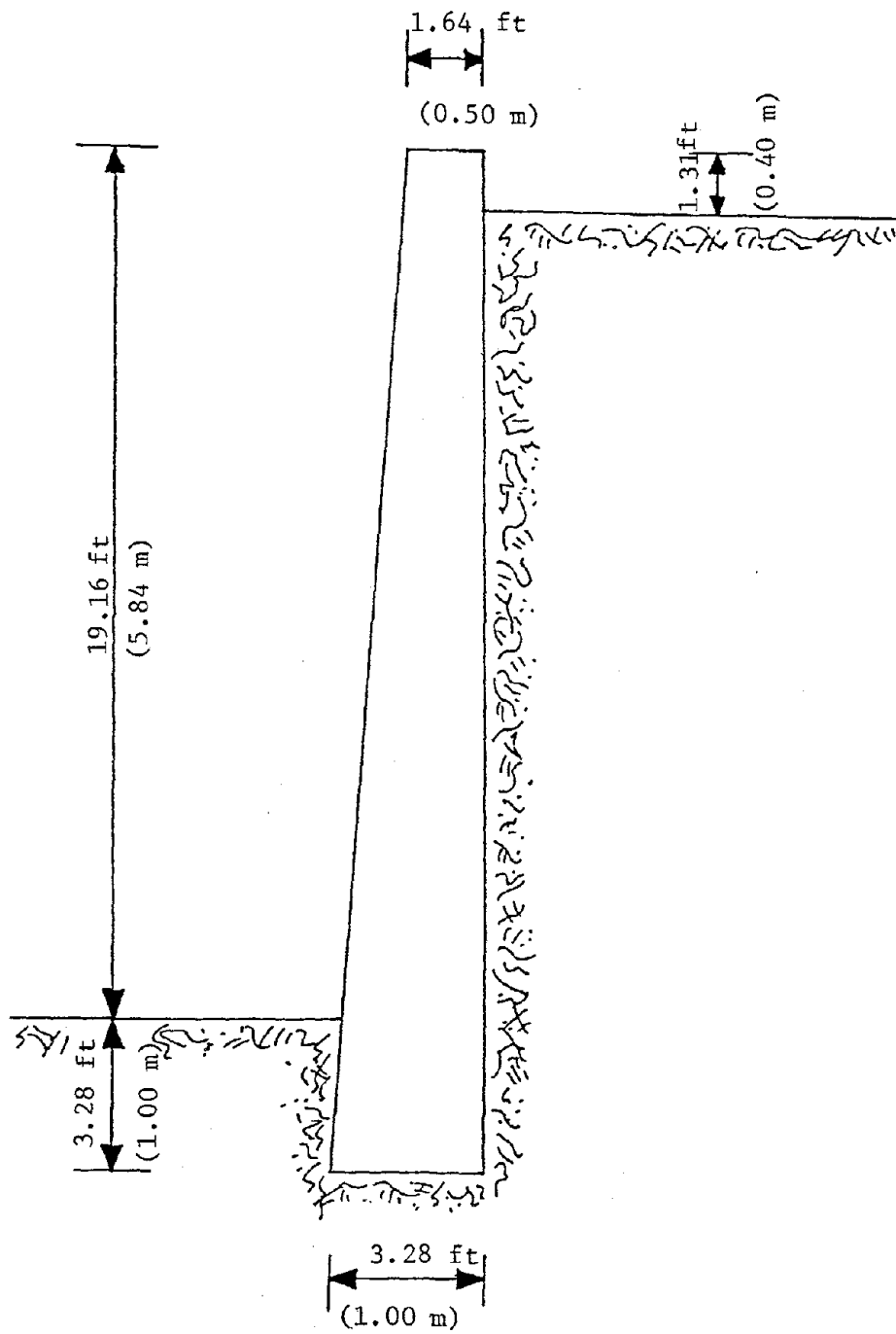


FIG. 6.7 CROSS-SECTION OF WINGWALL AT LOCATION D-D BEFORE THE EARTHQUAKE (from Fig. 6.2)

along the wingwall, the largest values of which are developed at the section where the wingwall is connected with the adjacent (usually more massive) facility. For the joint of the two structures to perform successfully, simple horizontal reinforcement is required in order to undertake the developed tensile stresses together with a possible increase of the wall thickness.

Observations on the behavior of such structures (e.g., Peck, 1974) have indicated that, when wingwalls are rigidly connected to massive facilities such as bridge abutments, most failures occur at or near their joints. This is due mainly to an inadequate structural design at this critical section. In addition, if the connection between the wingwall and the rest of the facility is rigid, the mobility of the former near the joint is very limited. As a result, active conditions at this location cannot be fully mobilized and, therefore, the force system along the wingwall is larger than the one an ordinary retaining wall can carry safely.

The above is considered to also be the cause of failure for the Plateas wingwall. The excessive settlement of the embankment overlying the backfill is an additional contributing factor. This was probably due to the inadequate compaction of the fill and produced a further increase in the load of the wall.

Nevertheless, the performed analysis has shown that, even if the excessive settlement of the backfill material had not taken place, the joint between the wingwall and the rest of the facility was not adequately designed and it would have failed even if active

conditions were only developed.

### 6.3.3 Representative Cross-Section and Material Parameters

Following the development of the crack, the reported section of the wingwall was free of any lateral restraints. Therefore, its subsequent behavior was assumed to be similar to that of a gravity type retaining wall with active pressures acting along its entire length.

In Fig. 6.8 is shown schematically a representative cross-section of the wall used in the stability analysis. As the height of the wall varies along its length (Fig. 6.2), the representative section has an average height of 20.29 ft (6.15 m) and is located at a distance equal to 11.78 ft (3.5 m) from the left end of the wall. Its center of gravity is determined in Table 6.2 while in Fig. 6.9 is shown a front view of the wingwall indicating the location of the representative cross-section.

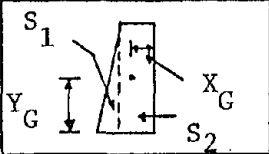
Both the backfill and foundation materials are assumed to be cohesionless ( $c = 0$ ). Their unit weight was estimated to be equal to 100 pcf ( $\gamma = \gamma_f = 100$  pcf) ( $15708.75 \text{ N/m}^3$ ) while the mean values of their angles of internal friction  $40^\circ$  ( $\phi = \phi_f = 40^\circ$ ). The unit weight of the wall concrete was equal to 144 pcf ( $22620.59 \text{ N/m}^3$ ).

The angle of friction  $\delta$  between the wall and the backfill material depends on the roughness of the back of the wall and the type of the soil. A typical value for  $\delta$  is equal to  $30^\circ$  (e.g., Lambe and Whitman, 1969) and this is the value assumed for the present study. For coarse



TABLE 6.2

DETERMINATION OF CENTER OF GRAVITY FOR  
THE REPRESENTATIVE SECTION OF THE WALL (from Fig. 6.8)

	AREA $A_i$	$Y_i$	$X_i$	$A_i Y_i$	$A_i X_i$
SECTION S1	16.56 ft <sup>2</sup> (1.54 m <sup>2</sup> )	2.19 ft (0.67 m)	6.73 ft (2.05 m)	36.27 ft <sup>3</sup> (1.03 m <sup>3</sup> )	111.45 ft <sup>3</sup> (3.16 m <sup>3</sup> )
SECTION S2	55.46 ft <sup>2</sup> (5.15 m <sup>2</sup> )	0.82 ft (0.25 m)	10.10 ft (3.08 m)	45.48 ft <sup>3</sup> (1.29 m <sup>3</sup> )	560.15 ft <sup>3</sup> (15.86 m <sup>3</sup> )
TOTAL SECTION	72.02 ft <sup>2</sup> (6.69 m <sup>2</sup> )	-	-	81.75 ft <sup>3</sup> (2.32 m <sup>3</sup> )	671.60 ft <sup>3</sup> (19.02 m <sup>3</sup> )

$$Y_G = \frac{\sum A_i Y_i}{\sum A_i} = \frac{81.75 \text{ ft}^3}{72.02 \text{ ft}^2} = 1.14 \text{ ft (0.35 m)}$$

$$X_G = \frac{\sum A_i X_i}{\sum A_i} = \frac{671.60 \text{ ft}^3}{72.02 \text{ ft}^2} = 9.33 \text{ ft (2.84 m)}$$



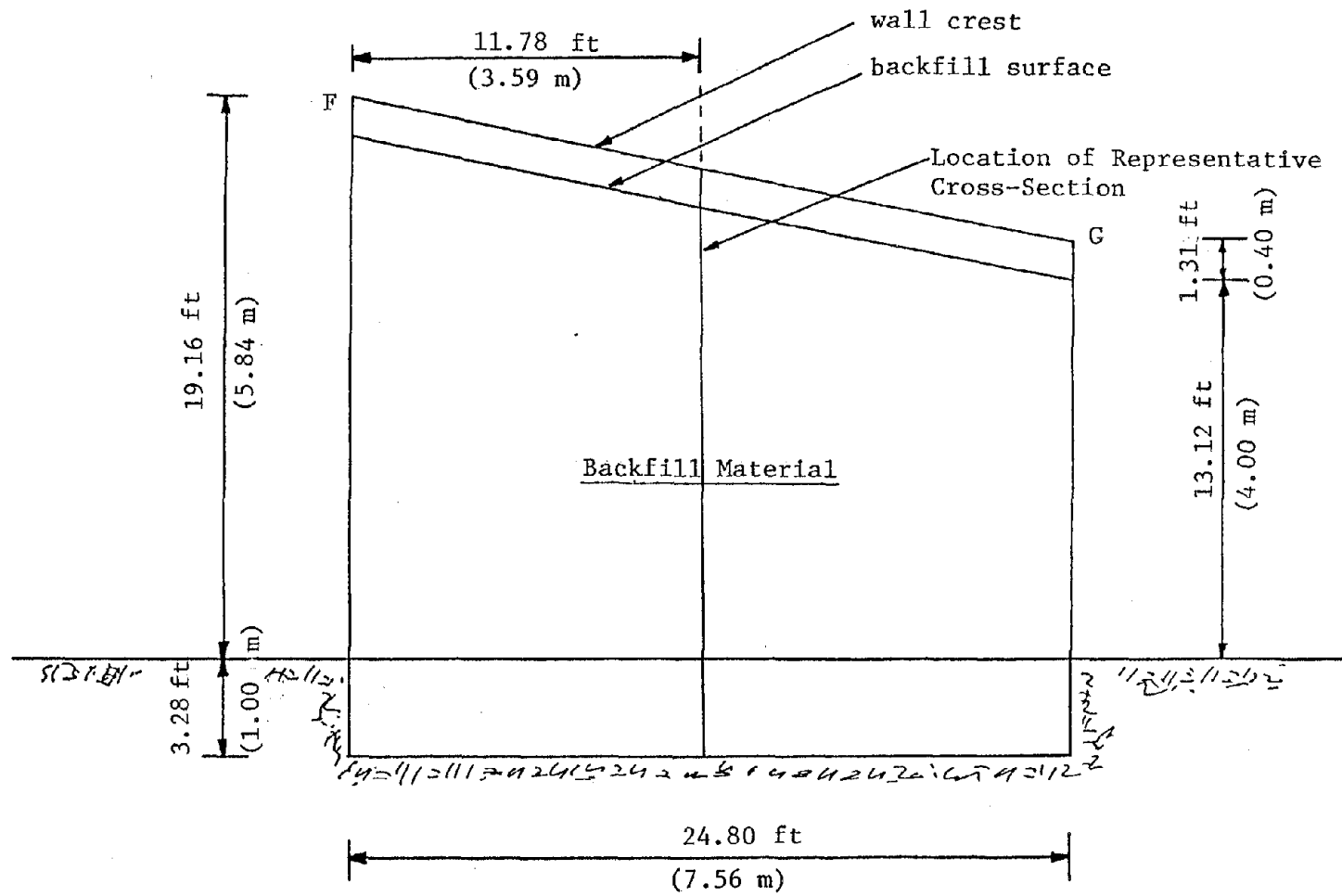


FIG. 6.9 FRONT VIEW OF THE WINGWALL SHOWING THE LOCATION OF THE REPRESENTATIVE CROSS-SECTION

grained soils with silt, a typical value for the coefficient of friction ( $\tan\delta_f$ ) between the wall base and the foundation material is 0.45 (e.g., Peck et al., 1974). Therefore, the value for the friction angle  $\delta_f$  employed in this study is  $24^\circ$  ( $\delta = 24^\circ$ ). A typical value equal to 10% (Harr, 1977) for the coefficient of variation of the friction angles of the backfill and foundation materials were assumed.

The statistical values of the material strength parameters are summarized in Table 6.3.

#### 6.3.4 Static Force System along the Wall

A description of the force system along the retaining wall under static conditions is made using the representative cross-section shown in Fig. 6.8. The total height of the wall is  $H = 20.19$  ft (6.15 m), the base width is  $B = 3.28$  ft (1.00 m), the width at the crest is  $c_r = 1.64$  ft (0.50 m), the depth of the foundation is  $D_f = 3.28$  ft (1.00 m) the inclination of the backfill material is  $i = 5^\circ$  and the distance between the backfill and the crest is 1.31 ft (0.40 m).

The distribution of the earth pressures  $p(z)$  along the depth of the wall under static conditions is determined using Dubrova's method (Harr, 1977; A-Grivas, 1979; Chang, 1981; Vlavianos, 1981). The analytical expression for  $p(z)$  is as follows:

TABLE 6.3  
STATISTICAL VALUES OF MATERIAL PROPERTIES

MATERIAL PROPERTY	MEAN VALUE	STANDARD DEVIATION	COEFFICIENT OF VARIATION
Backfill friction angles, $\phi$	40°	4°	10%
Backfill friction angle, $\delta$	30°	3°	10%
Foundation soil friction angle, $\phi_f$	40°	4°	10%
Wall-Foundation friction angle, $\delta_f$	24°	2.4°	10%

$$\begin{aligned}
p(z) = & \frac{\gamma z \cos(\psi - \beta)}{\cos^2 \beta \cos(\delta + \beta) (1 + \xi_k)^2} \left\{ \cos(\psi - \beta) - z \frac{d\psi}{dz} \left[ \sin(\psi - \beta) + \right. \right. \\
& + \frac{\cos(\psi - \beta)}{2(1 + \xi_k)} \left. \left. [(1 + m)\xi_k \cos(\psi + \delta) + \xi_k \cos(\psi - i) - \right. \right. \\
& \left. \left. - m \tan(\delta + \beta) \right] \right\} \quad (6-2)
\end{aligned}$$

in which  $\psi = \psi(z)$  is the mobilized shear strength along the depth  $z$  of the backfill,  $\gamma$  is the unit weight of the backfill, quantities  $\beta, \delta, i$  are shown in Fig. 4.3, and

$$\xi_k = \left[ \frac{\sin(|\psi + \delta|) \sin(|\psi - i|)}{\cos(i - \beta) \cos(\delta + \beta)} \right]^{1/2} \quad (6-3)$$

$$m = \frac{d\delta}{d\psi} = \frac{\delta}{\psi} \quad (6-4)$$

As active conditions are developed along the entire height of the wall, the mobilized strength  $\psi(z)$  is equal to the total strength available  $\phi$ ; i.e.,

$$\psi = \psi(z) = \phi \quad (6-5)$$

Introducing Eqn. (6-5) into Eqn. (6-2), the expression for the pressure distribution  $p(z)$  becomes

$$p(z) = \frac{\gamma z \cos^2(\phi - \beta)}{\cos^2 \beta \cos(\delta + \beta) (1 + \xi_k)^2} \quad (6-6)$$

in which

$$\xi_k = \left[ \frac{\sin(\phi+\delta)\sin(\phi-i)}{\cos(i-\beta)\cos(\delta+\beta)} \right]^{1/2} \quad (6-7)$$

i.e., the resulting distribution for  $p(z)$  is linear with depth  $z$ .

An integration of  $p(z)$  along the height  $H_b$  of the backfill provides the following expression for the total active force  $P_A$  on the wall:

$$P_A = \frac{1}{2} \gamma \lambda_A H_b^2 \quad (6-8)$$

in which  $\lambda_A$  is the coefficient of active earth pressure under static conditions and is equal to

$$\lambda_A = \frac{\cos^2(\phi-\beta)}{\cos^2\beta \cos(\delta+\beta) (1+\xi_k)^2} \quad (6-9)$$

and all other quantities are defined in Eqn. (6-6).

For the resulting hydrostatic pressure distribution, Eqn. (6-8), the point of application of the active thrust is at a depth equal to two thirds the height  $H_b$  of the backfill ( $2/3 H_b$ ). The horizontal and vertical components of  $P_A$ ,  $P_{A_h}$  and  $P_{A_v}$ , respectively, are equal to

$$P_{A_h} = P_A \cos(\beta+\delta) \quad (6-10)$$

$$P_{A_v} = P_A \sin(\beta+\delta)$$

## 6.4 Behavior of the Wingwall during the Seismic Activity

### 6.4.1 Observed Wall Movement and Design Specifications

The seismic activity caused the wall to move relatively to the much more massive adjacent structure. In Fig. 6.10 is shown schematically the cross-section of the wall at the position of the crack and the magnitude of the movement that occurred during the shaking. At the ground level, the wall moved outward a horizontal distance equal to 0.26 ft (0.08 m) while the outward movement at the top was 0.49 ft (0.15 m).

According to the Greek Aseismic Code, the seismicity of the wall site is characterized as Type II and the corresponding value of the equivalent horizontal seismic coefficient depends on the quality of the soil medium. Three types of soil qualities are distinguished, namely: quality a, for "soil with small seismic hazard"; quality b, for "soil with intermediate seismic hazard"; and quality c, for "soil with high seismic hazard". The suggested values for the horizontal seismic coefficient for these three types of soil are given in Table 6.4.

Because the design details of the facility are not available to the author at the present time, all three values of the horizontal seismic coefficient are considered in the back-calculation of the safety of the wall that is given below.

### 6.4.2 Back-Calculation of Wall Movement

The back-calculation of the permanent horizontal displacement of the wall is performed using a semi-empirical expression

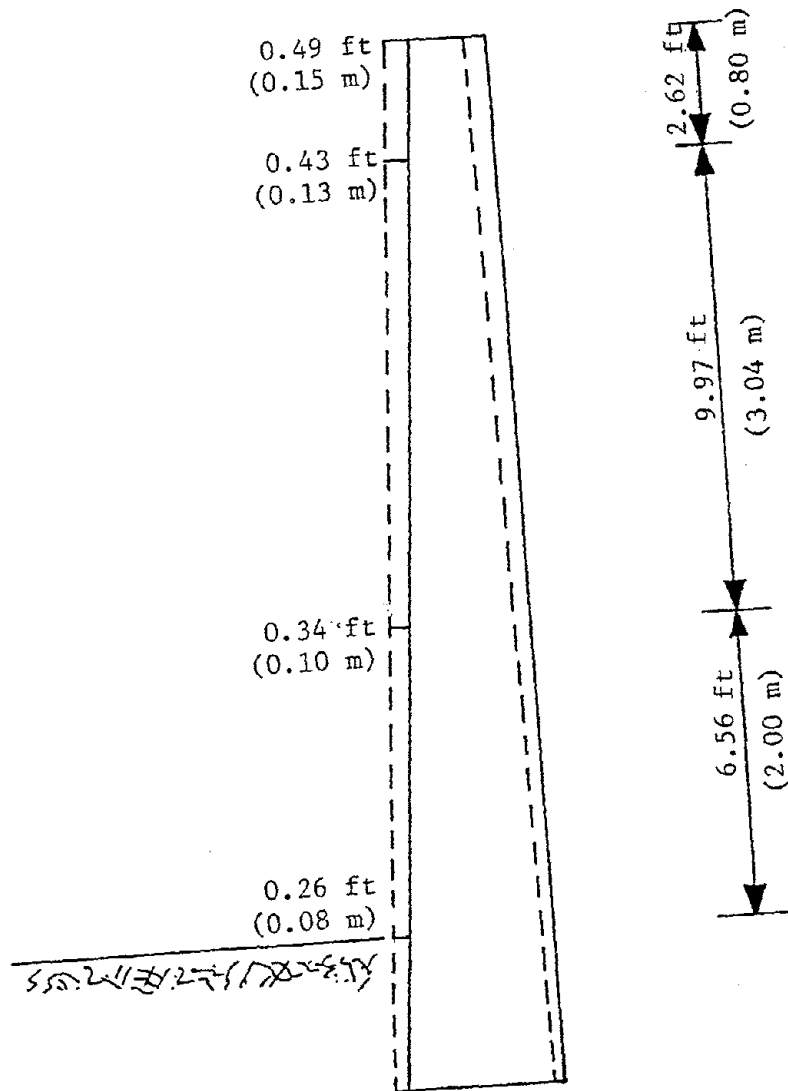


FIG. 6.10 CROSS-SECTION OF THE WINGWALL AT LOCATION D-D AND THE REALIZED MOVEMENT DUE TO THE EARTHQUAKE

TABLE 6.4

DESIGN SEISMIC COEFFICIENTS SUGGESTED BY  
THE GREEK ASEISMIC CODE (in g's)

	TYPE OF SOIL		
Seismicity of Wall Site	Small Seismic Hazard a	Intermediate Seismic Hazard b	High Seismic Hazard c
II	0.06	0.08	0.12



proposed by Richard and Elms (1979). This is equal to

$$d_p = 0.087 \frac{v^2}{A_h} \left( \frac{K_h}{\alpha_h} \right)^{-4} \quad (6-11)$$

in which  $d_p$  is the permanent displacement, in inches,  $A_h (= \alpha_h \cdot g)$  is the maximum horizontal ground acceleration due to an earthquake, in  $\text{in}/\text{sec}^2$ ,  $v$  is the corresponding maximum horizontal velocity, in  $\text{in}/\text{sec}$ , and  $K_h$  is the maximum horizontal ground acceleration the wall can experience without failure, in  $g$ 's (i.e.,  $K_h$  is the deterministic seismic capacity of the wall).

Acceleration  $A_h$  can be expressed as (Prakash, 1981)

$$A_h = \omega v \quad (6-12)$$

in which  $\omega$  is the circular frequency of the ground motion.

Solving Eqn. (6-12) with respect to  $v$ , one has

$$v = \frac{A_h}{\omega} = \frac{\alpha_h g T}{2\pi} \quad (6-13)$$

Introducing the above expression for  $v$  into Eqn. (6-11), the latter becomes

$$d_p = 0.087 \frac{\alpha_h g T^2}{4\pi^2} \left( \frac{K_h}{\alpha_h} \right)^{-4} \quad (6-14)$$

From the three earthquakes that took place at the vicinity of the facility in February and March, 1981 (Table 6.1), the first and third contributed to the movement of the wall while the second shaking had no effect on the facility. The estimated value for the

predominant period of the first influential earthquake is  $T_1 = 0.3$  sec while that of the second is  $T_2 = 0.55$  sec (Protonotarios, 1981).

The values of the horizontal permanent displacement of the wall that correspond to the two earthquakes are listed in Table 6.5 for each design value of the seismic coefficient appearing in the Greek Aseismic Code (Table 6.4). It may be noted that the total displacement predicted for the case of  $k_{h2} = 0.08 g$  is approximately equal to the observed value  $d_p = 0.26$  ft (0.08m), shown in Fig. 6.10.

#### 6.4.3 Seismic Force System along the Wall

The distribution of the earth pressures  $p(z)$  along the depth  $z$  of the wall under seismic conditions, found using Dubrova's method of "distribution of pressures" (A-Grivas, 1979; Chang, 1981; Vlavianos, 1981), is given as follows:

$$p(z) = \frac{\gamma z(1+\alpha_v) \cos(\psi-\beta-\theta)}{\cos\theta \cos^2\beta \cos(\delta+\beta+\theta) (1+\xi_k)^2} \left\{ \cos(\psi-\beta-\theta) - z \frac{d\psi}{dz} \sin(\psi-\beta-\theta) + \right. \\ \left. + \frac{\cos(\psi-\beta-\theta)}{2(1+\xi_k)} [(1+m)\xi_k \cos(\psi+\delta) + \xi_k \cos(\psi-i-\theta) - m \tan(\delta+\beta+\theta)] \right\} \quad (6-15)$$

in which  $\psi = \psi(z)$  is the mobilized shear strength along the depth  $z$  of the backfill,  $\gamma$  is the unit weight of the backfill, quantities  $\beta, \delta, i$  are shown in Fig. 4.3, and

$$\xi_k = \left[ \frac{\sin(|\psi+\delta|) \sin(|\psi-i-\theta|)}{\cos(i-\beta) \cos(\delta+\beta+\theta)} \right] \quad (6-16)$$

TABLE 6.5

## TOTAL HORIZONTAL PERMANENT DISPLACEMENT OF THE WALL

DESIGN SEISMIC COEFFICIENT IN GREEK ASEISMIC CODE	HORIZONTAL DISPLACEMENT		
	1st EARTHQUAKE ( $T_1=0.3$ sec, $\alpha_{h1}=0.07g$ )	2ND EARTHQUAKE ( $T_2=0.55$ sec, $\alpha_{h2}=0.22g$ )	TOTAL
$k_{h1} = 0.06$ g	0.0099 in $d_{11} = (2.51 \times 10^{-4} \text{ m})$	10.22 in $d_{12} = (0.2596 \text{ m})$	0.8525 ft $d_{p1} = (0.2598 \text{ m})$
$k_{h2} = 0.08$ g	0.0031 in $d_{21} = (7.87 \times 10^{-5} \text{ m})$	3.2337 in $d_{22} = (0.0821 \text{ m})$	0.2697 ft $d_{p2} = (0.0822 \text{ m})$
$k_{h3} = 0.12$ g	0.006 in $d_{31} = (1.52 \times 10^{-4} \text{ m})$	0.6388 in $d_{32} = (0.0162 \text{ m})$	0.0537 ft $d_{p3} = (0.0164 \text{ m})$

$$\theta = \tan^{-1} \left( \frac{\alpha_h}{1+\alpha_v} \right), \quad (6-17)$$

$$m = \frac{d\delta}{\psi} = \frac{\delta}{\psi}, \quad (6-18)$$

$\alpha_h$  = maximum horizontal acceleration  
(in g's), and

$\alpha_v$  = maximum vertical acceleration  
(in g's).

In Eqn. (6-17),  $\alpha_h$  is positive if it is directed toward the wall while  $\alpha_v$  is positive if it is directed downward. Critical loading conditions on the wall correspond to a positive value for  $\theta$  ( $\theta > 0$ ).

As active conditions are developed along the entire height of the wall, the mobilized strength  $\psi(z)$  is equal to the total strength available  $\phi$ ; i.e.,

$$\psi = \psi(z) = \phi \quad (6-19)$$

Introducing Eqn. (6-19) into Eqn. (6-15), the latter becomes

$$p(z) = \frac{\gamma z (1+\alpha_v) \cos^2(\phi-\beta-\theta)}{\cos\theta \cos^2\beta \cos(\delta+\beta+\theta) (1+\xi_k)^2} \quad (6-20)$$

in which

$$\xi_k = \left[ \frac{\sin(\phi+\delta) \sin(\phi-i-\theta)}{\cos(i-\beta) \cos(\delta+\beta+\theta)} \right]^{1/2} \quad (6-21)$$

i.e., the resulting distribution is linear with depth  $z$ .

An integration of  $p(z)$  along the height  $H_b$  of the backfill provides the following expression for the total active force

$P_A$  on the wall:

$$P_A = \frac{1}{2} \gamma (1 + \alpha_v) \lambda_A H_b^2 \quad (6-22)$$

in which  $\lambda_A$  is the coefficient of active earth pressure under seismic conditions and is equal to

$$\lambda_A = \frac{\cos^2(\phi - \beta - \theta)}{\cos \theta \cos^2 \beta \cos(\delta + \beta + \theta) (1 + \xi_k)^2} \quad (6-23)$$

The distribution along the wall under seismic conditions given in Eqn. (6-20) is hydrostatic and, therefore, the point of application of the total active thrust is at a depth equal to two thirds the backfill height  $H_b$  ( $2/3H_b$ ).

## 6.5 Failure Analysis

### 6.5.1 Statistical Values of Safety Margin

For the purposes of this case study, the failure function of the retaining wall for any mode of failure is taken to be equal to the safety margin SM. This is defined in Eqn. (4-2) as the difference between the capacity C and demand D of the wall, i.e.,

$$SM = C - D$$

In section 4.2 are provided the analytical expressions of C and D for each failure mode. It is seen that C and/or D, and therefore SM, are functions of one or more of the material parameters

that are introduced as random variables in this study, namely: the friction angles of the backfill and foundation material,  $\phi$  and  $\phi_f$ , respectively, the angle of friction  $\delta$  between the wall and the backfill, and the angle of friction  $\delta_f$  between the wall footing and the foundation material. For given statistical values of these random variables (obtained, say, through an analysis of laboratory test data), the corresponding statistical values of the safety margin may be determined with the aid of the point estimates method, proposed for the first time by Rosenblueth (1975). The method may be summarized as follows:

Let, in general,  $y$  represent a function of  $N$  random variables  $x_i$ ,  $i = 1, 2, \dots, N$ , i.e.,

$$y = y(x_1, x_2, \dots, x_i, \dots, x_N) \quad (6-24)$$

If  $\bar{x}_i$  and  $V_{x_i}$  denote the mean value and coefficient of variation of each  $x_i$ , respectively, and  $\bar{y}$  and  $V_y$  the corresponding statistical values of function  $y$ , then one has (Rosenblueth, 1975)

$$\frac{\bar{y}}{y_0} \approx \frac{\bar{x}_1}{y_0} \frac{\bar{x}_2}{y_0} \dots \frac{\bar{x}_i}{y_0} \dots \frac{\bar{x}_N}{y_0} \quad (6-25a)$$

$$1 + V_y^2 \approx (1 + V_{x_1}^2)(1 + V_{x_2}^2) \dots (1 + V_{x_i}^2) \dots (1 + V_{x_N}^2) \quad (6-25b)$$

in which

$$y_0 = y(\bar{x}_1, \bar{x}_2, \dots, \bar{x}_i, \dots, \bar{x}_N)$$

i.e.,  $y_0$  is equal to function  $y$  evaluated at the mean values of variables  $x_i$ . The latter are determined with the aid of two point estimates,  $x_{i-}$  and  $x_{i+}$ , respectively, depend on

$$\begin{aligned} x_{i-} &= \bar{x}_i - \sigma_{x_i} \\ x_{i+} &= \bar{x}_i + \sigma_{x_i} \end{aligned} \quad (6-26)$$

in which  $\sigma_{x_i}$  denotes the standard deviation of  $x_i$ . The expressions for the mean value, standard deviation and coefficient of variation of  $x_i$  in terms of the point estimates  $x_{i-}$  and  $x_{i+}$  are

$$\begin{aligned} \bar{x}_i &\approx \frac{x_{i-} + x_{i+}}{2} \\ \sigma_{x_i} &\approx \frac{|x_{i+} - x_{i-}|}{2} \end{aligned} \quad (6-27)$$

### 6.5.2 Determination of Probability of Failure

The probability of failure is determined as the probability with which the safety margin receives values smaller than or, at most, equal to zero, i.e.,

$$P_f = P[SM \leq 0] \quad (6-28)$$

It is assumed that SM follows a normal distribution expressed in the form

$$f(SM) = \frac{1}{\sigma_{SM}\sqrt{2\pi}} \exp\left[-\frac{(SM-\overline{SM})^2}{2\sigma_{SM}^2}\right]$$

in which  $\overline{SM}$  and  $\sigma_{SM}$  are the mean value and standard deviation of SM, respectively, which are found using Eqns. (6-25). If  $u$  denotes the standardized normal variate, i.e.,

$$u = \frac{SM - \overline{SM}}{\sigma_{SM}}$$

the numerical value of the probability of failure are obtained from Eqn. (6-28) as

$$P_f = P\left[u \leq -\frac{\overline{SM}}{\sigma_{SM}}\right] = \Phi\left(-\frac{\overline{SM}}{\sigma_{SM}}\right) \quad (6-29)$$

in which  $\Phi(\ )$  is the tabulated Gauss distribution (Harr, 1977) evaluated at the quantity shown in the parenthesis.

## 6.6 Results

Using the procedure described above, the safety of the wall shown in Fig. 6.8 is evaluated under both static and seismic conditions. Three modes of failure are examined, namely, rotation around the wall base (active case), base sliding and overall sliding. The safety of the bearing capacity of the wall used in this case study cannot be evaluated as there is no complete information concerning the details of its foundation (e.g., size of its footing, "smooth" or "rough" foundation conditions, etc.).



### 6.6.1 Static Conditions

In Table 6.6 are given the results found for the examined three modes of failure under static conditions. It can be seen that the obtained values of the central factor of safety CFS (defined as the ratio of the mean value  $\bar{C}$  of capacity over that of the demand  $\bar{D}$ , i.e.,  $CFS = \bar{C}/\bar{D}$ ) are 1.04, 1.24 and 2.31 for the cases of rotation, base sliding and overall sliding, respectively. The corresponding values of the probability of failure, determined with the aid of Eqn. (6-29) are 0.424, 0.130 and  $0.71 \times 10^{-3}$ , respectively. Listed in Table 6.6 are also the statistical values of the safety margin for each mode of failure considered.

### 6.6.2 Seismic Conditions

In Tables 6.7, 6.8, 6.9 and 6.10 are given the obtained results for the case where the wall is subjected to an earthquake with horizontal acceleration equal to 0.02g, 0.04g, 0.06g and 0.08g, respectively. For each loading condition, the values are listed of the central factor of safety, the mean, standard deviation and coefficient of variation of the safety margin, and the probability of failure of the wall in rotation, base sliding, and bearing capacity. In all cases, wall rotation has the highest value while overall sliding has the smallest value for the probability of failure. In Fig. 6.11 are shown schematically the details associated with the overall sliding mode of failure.

TABLE 6.6

DETERMINATION OF PROBABILITY OF FAILURE: STATIC CONDITIONS

FAILURE MODE	CENTRAL FACTOR OF SAFETY $CFS = \bar{C}/\bar{D}$	STATISTICAL VALUES OF SAFETY MARGIN			PROBABILITY OF FAILURE
		MEAN VALUE	STANDARD DEVIATION	COEFFICIENT OF VARIATION	
ROTATION	1.04	760 (lbft/ft)	3956 (lbft/ft)	521%	0.424
		3381 (nm/m)	17597 (nm/m)		
BASE SLIDING	1.24	776 (lb/ft)	690 (lb/ft)	89%	0.130
		11325 (N/m)	10070 (N/m)		
OVERALL SLIDING	2.31	$1.9 \times 10^6$ (lbft/ft)	$4.9 \times 10^5$ (lbft/ft)	26%	$0.71 \times 10^{-3}$
		$8.3 \times 10^6$ (Nm/m)	$2.2 \times 10^6$ (Nm/m)		

TABLE 6.7  
 DETERMINATION OF PROBABILITY OF FAILURE:  
 SEISMIC CONDITIONS ( $\alpha_h = 0.02g$ ,  $\alpha_v = 0$ )

FAILURE MODE	CENTRAL FACTOR OF SAFETY $\bar{C}/\bar{D}$	STATISTICAL VALUES OF SAFETY MARGIN			PROBABILITY OF FAILURE
		MEAN VALUE	STANDARD DEVIATION	COEFFICIENT OF VARIATION	
ROTATION	0.99	-29 (lbft/ft) -129 (Nm/m)	23107 (lbft/ft) 102785 (Nm/m)	788%	0.500
BASE SLIDING	1.19	645 (lb/ft) 9413 (N/m)	735 (lb/ft) 10727 (N/m)	114%	0.190
OVERALL SLIDING	2.18	$1.8 \times 10^6$ (lbft/ft) $7.9 \times 10^6$ (Nm/m)	$4.9 \times 10^5$ (lbft/ft) $2.2 \times 10^6$ (Nm/m)	28%	$0.14 \times 10^{-3}$

TABLE 6.8

DETERMINATION OF PROBABILITY OF FAILURE:  
SEISMIC CONDITIONS ( $\alpha_h = 0.04g$ ,  $\alpha_v = 0$ )

FAILURE MODE	CENTRAL FACTOR OF SAFETY	STATISTICAL VALUES OF SAFETY MARGIN			PROBABILITY OF FAILURE
		MEAN VALUE	STANDARD DEVIATION	COEFFICIENT OF VARIATION	
ROTATION	0.92	-838 (lbft/ft)	5348 (lbft/ft)	638%	0.562
		-3728 (Nm/m)	23789 (Nm/m)		
BASE SLIDING	1.14	507 (lb/ft)	811 (lb/ft)	160%	0.266
		7399 (N/m)	11836 (N/m)		
OVERALL SLIDING	2.07	$1.7 \times 10^6$ (lbft/ft)	$4.9 \times 10^5$ (lbft/ft)	29%	$0.28 \times 10^{-3}$
		$7.5 \times 10^6$ (lbft/ft)	$2.2 \times 10^6$ (Nm/m)		

TABLE 6.9

DETERMINATION OF PROBABILITY OF FAILURE:  
SEISMIC CONDITIONS ( $\alpha_h = 0.06g$ ,  $\alpha_v = 0$ )

FAILURE MODE	CENTRAL FACTOR OF SAFETY $\bar{C}/\bar{D}$	STATISTICAL VALUES OF SAFETY MARGIN			PROBABILITY OF FAILURE
		MEAN VALUE	STANDARD DEVIATION	COEFFICIENT OF VARIATION	
ROTATION	0.93	-1704 (lbft/ft)	3726 (lbft/ft)	219%	0.676
		-7580 (Nm/m)	16574 (Nm/m)		
BASE SLIDING	1.09	361 (lb/ft)	978 (lb/ft)	271%	0.356
		5268 (N/m)	14273 (N/m)		
OVERALL SLIDING	1.97	1606966(lbft/ft)	490805(lbft/ft)	31%	$0.53 \times 10^{-3}$
		7148138 (Nm/m)	2183209 (Nm/m)		

TABLE 6.10

DETERMINATION OF PROBABILITY OF FAILURE:  
SEISMIC CONDITIONS ( $\alpha_h = 0.08g$ ,  $\alpha_v = 0$ )

FAILURE MODE	CENTRAL FACTOR OF SAFETY $\bar{C}/\bar{D}$	STATISTICAL VALUES OF SAFETY MARGIN			PROBABILITY OF FAILURE
		MEAN VALUE	STANDARD DEVIATION	COEFFICIENT OF VARIATION	
ROTATION	0.90	-2614 (lbft/ft)	3478 (lbft/ft)	133%	0.744
		-11628(Nm/m)	15471 (Nm/m)		
BASE SLIDING	1.05	207 (lb/ft)	1571 (lb/ft)	758%	0.447
		3021 (N/m)	22927 (N/m)		
OVERALL SLIDING	1.87	152344 (lbft/ft)	491935(lbft/ft)	32%	$1.31 \times 10^{-3}$
		6775724(Nu/m)	2188235 (Nm/m)		

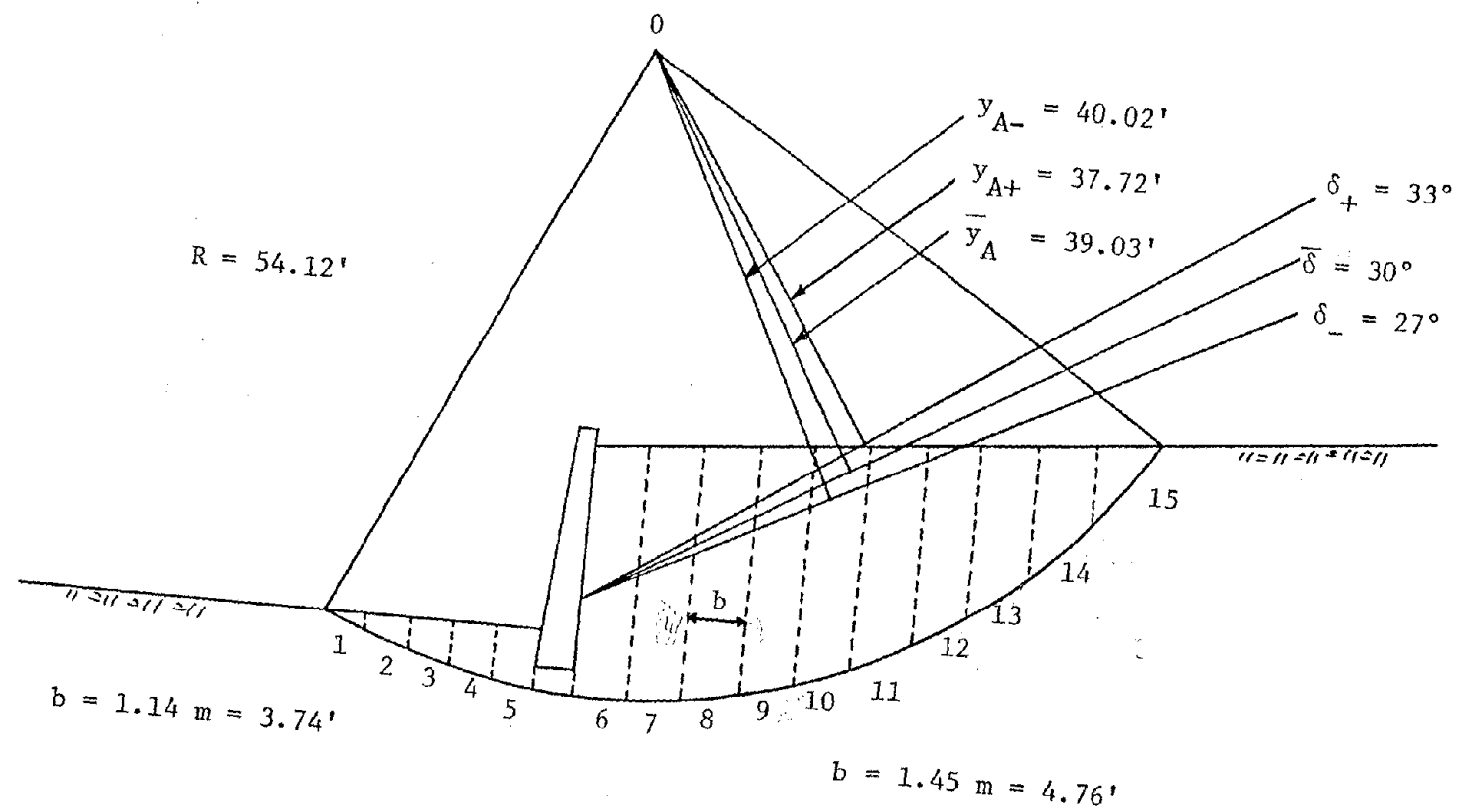


FIG. 6.11 SLICES USED IN THE OVERALL STABILITY ANALYSIS OF THE WINGWALL

The results of the Bayesian analysis are shown in Table 6.11. For each mode of failure considered, the values are listed of the predicted prior probability of failure (before the successful construction of the wall),  $P_f(G_o + \Delta G)$ , and of the predicted posterior probability of failure (after the successful construction of the wall),  $P'_f(G_o + \Delta G)$ . In all cases, the latter is smaller than the former, i.e.,  $P'_f(G_o + \Delta G) < P_f(G_o + \Delta G)$ .

The posterior probabilities of failure  $P'_f(G_o + \Delta G)$  are used for the determination of the statistical values (mean, standard deviation, and coefficient of variation) of the seismic capacity of the wall in each of the examined modes of failure. This is achieved with the aid of Fig. 6.12, involving a plot of the standardized normal variate  $u$  and its cumulative distribution  $\Phi(u)$ , and Fig. 6.13, that relates  $u$  to the seismic acceleration  $\alpha_h$ . The latter is determined by letting  $P'_f(G_o + \Delta G) = P'_f(\alpha_h)$  become equal to  $\Phi(u)$ , i.e.,  $P'_f(\alpha_h) = \Phi(u)$ , and performing a linear regression analysis between corresponding values of  $\alpha_h$  and  $u$ .

In Table 6.12 are listed the statistical values for the seismic capacity  $R$  of the wall in the rotation, base sliding and overall sliding for the cases where the distribution of  $R$  is approximated by the normal and lognormal models. Finally, the values of the predicted probability of failure as determined on the basis of the seismic capacity of the wall are listed in Table 6.13.



TABLE 6.11

## PRIOR AND POSTERIOR PROBABILITIES OF FAILURE

MODE OF FAILURE	PEAK HORIZONTAL GROUND ACCELERATION, $\alpha_h$ (in g's)								
	0	0.02		0.04		0.06		0.08	
	$P_f(G_o)$	$P_f(G_o + \Delta G)$	$P'_f(G_o + \Delta G)$	$P_f(G_o + \Delta G)$	$P'_f(G_o + \Delta G)$	$P_f(G_o + \Delta G)$	$P'_f(G_o + \Delta G)$	$P_f(G_o + \Delta G)$	$P'_f(G_o + \Delta G)$
Rotation	0.424	0.500	0.133	0.562	0.240	0.676	0.438	0.774	0.608
Base Sliding	0.130	0.190	0.069	0.266	0.156	0.356	0.260	0.448	0.365
Overall Sliding	$0.71 \times 10^{-4}$	$1.4 \times 10^{-4}$	$0.72 \times 10^{-4}$	$2.8 \times 10^{-4}$	$2.1 \times 10^{-4}$	$5.3 \times 10^{-4}$	$4.6 \times 10^{-4}$	$13 \times 10^{-4}$	$12.4 \times 10^{-4}$

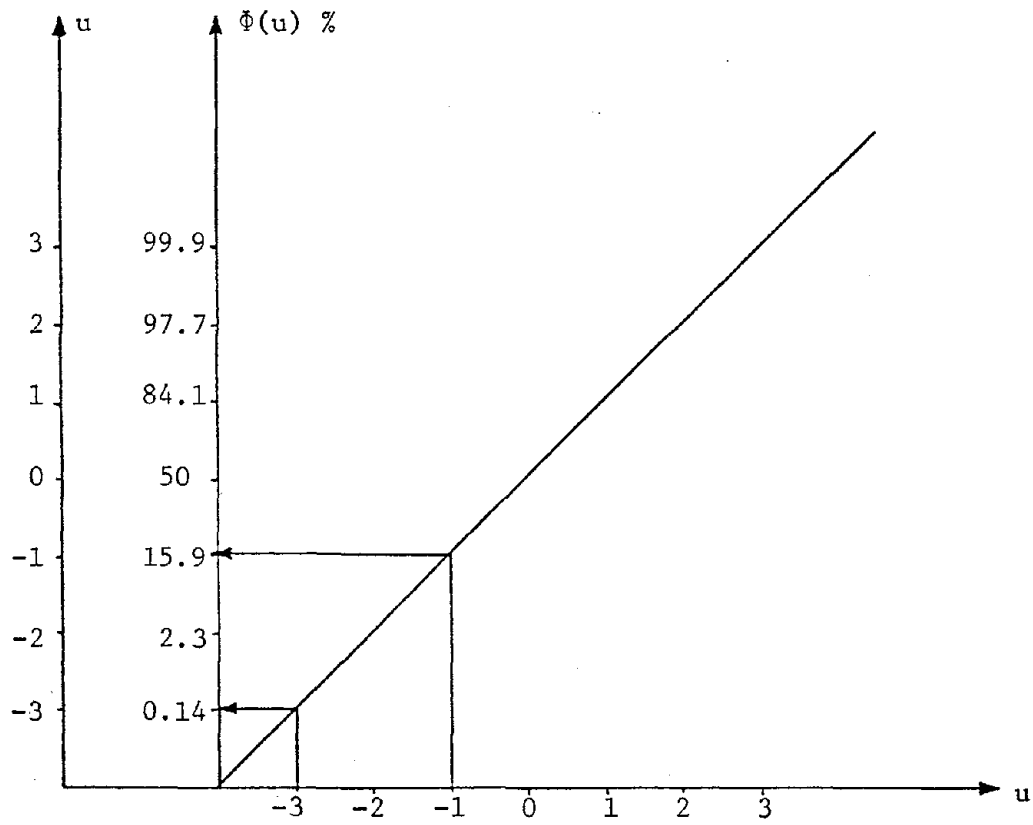


FIG. 6.12 THE STANDARDIZED NORMAL VARIATE  $u$   
AND ITS CUMULATIVE DENSITY FUNCTION  $\Phi(u)$

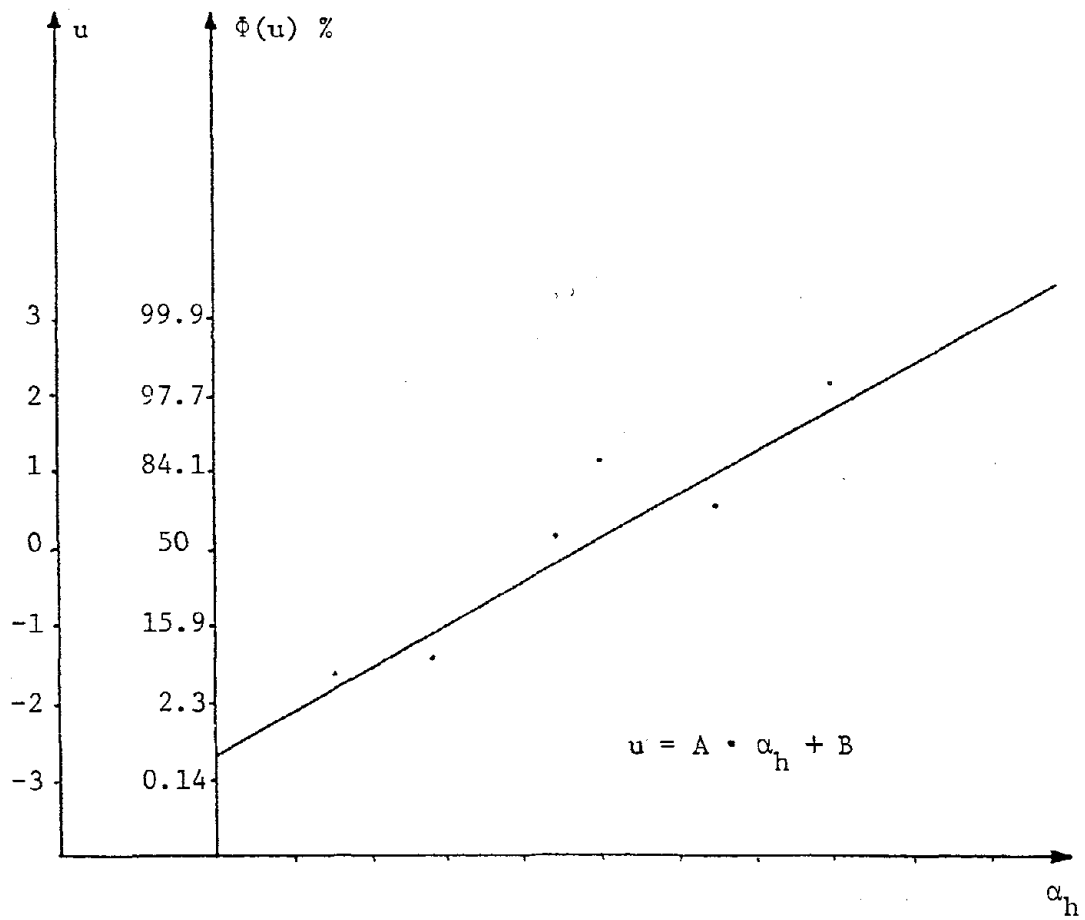


FIG. 6.13 DETERMINATION OF THE RELATIONSHIP BETWEEN  $u$  AND  $\alpha_h$  WITH THE AID OF LINEAR REGRESSION ANALYSIS

TABLE 6.12  
STATISTICAL VALUES OF THE SEISMIC CAPACITY

MODE OF FAILURE	NORMAL			LOGNORMAL		
	MEAN VALUE $\bar{R}$	STANDARD DEVIATION $S_R$	COEFFICIENT OF VARIATION $V_R$	MEAN VALUE $\bar{R}$	STANDARD DEVIATION $S_R$	COEFFICIENT OF VARIATION $V_R$
ROTATION	0.068	0.043	63%	0.114	0.153	134%
BASE SLIDING	0.096	0.053	55%	0.274	0.513	187%
OVERALL SLIDING	0.320	0.079	25%	156.442	895.465	572%

TABLE 6.13

PREDICTED PROBABILITY OF FAILURE ON THE  
BASIS OF THE SEISMIC CAPACITY OF THE WALL

MODE OF FAILURE	DISTRIBUTION OF CAPACITY	
	NORMAL	LOGNORMAL
ROTATION	0.999	0.875
BASE SLIDING	0.990	0.668
OVERALL SLIDING	0.103	0.005

## CHAPTER 7

### REFERENCES

- A-Grivas, D. (1976), "Reliability of Slopes of Particulate Materials", Ph.D. Dissertation, Civil Engineering Department, Purdue University, Indiana.
- A-Grivas, D. (1978), "Seismic Analysis of Slopes in the Northeast U.S.A.", Proceedings, VI Symposium on Earthquake Engineering, University of Roorkee, Vol. 1, October, pp. 157-161.
- A-Grivas, D. (1978), "Reliability of Retaining Structures during Earthquakes", VI Symposium on Earthquake Engineering, University of Roorkee, India, Vol. 1, pp. 265-269.
- A-Grivas, D. (1979), "Reliability Analysis of Retaining Structures", Proceedings of 3rd International Conference on Application of Statistics and Probability in Soil and Structural Engineering, Sydney, Australia, pp. 632-641.
- A-Grivas, D. and Harrop-Williams, K. (1979), "Joint Distribution of the Components of Soil Strength", Proceedings of the Third International Conference on Application of Statistics and Probability in Soil and Structural Engineering, Sydney, Australia, pp. 189-197.
- A-Grivas, D. and Asaoka, A. (1982), "Slope Safety Prediction under Static and Seismic Loads", Journal of Geotechnical Division, ASCE, Vol. 108, GT5.
- Algermissen, S.T., Steinbrugge, K.V. and Lagorio, H.L. (1978a), "Estimation of Earthquake Losses to Buildings (except single family dwellings)", Open File Report 78-441, U.S. Geological Survey.
- Algermissen, S.T., McGrath, M.B. and Hanson, S.L. (1978b), "Development of a Technique for the Rapid Estimation of Earthquake Losses", Open file report 78-440, U.S. Geological Survey.
- Amano, R., Azuma, H. and Ishii, Y. (1956), "Aseismic Design of Quay Walls in Japan", Proceedings, First World Conference on Earthquake Engineering, Berkeley, California, pp. 32-1 - 32-17.
- Arno, N.L. and McKinney, L.F. (1973), "Damage and Repair, Harbor and Waterfront. The Great Alaska Earthquake of 1964-Engineering", National Academy of Science, Washington, D.C., pp. 526-643.

- Benjamin, J.R. and Cornell, C.A. (1970), "Probability, Statistics and Decision for Civil Engineers", McGraw-Hill, New York.
- Blume, A.J. (1967), "Comments on Structural Response to Earthquake Motion as related to Damage Risk", Meeting on Seismology and Engineering Seismology, U.S. Department of Commerce, Rockville, Maryland.
- Blume, A.J. (1969), "A Threshold Evaluation Scale Procedure for Buildings subjected to Ground Motion", Letter report to E.M. Douthett, Director of Office of Effects Evaluation, U.S. Atomic Energy Commission, November 4.
- Blume, A.J. (1970), "An Engineering Intensity Scale for Earthquakes and other Ground Motion", Bulletin of the Seismological Society of America, Vol. 60, No. 1, pp. 217-229.
- Blume, A.J., Scholl, E.R. and Lum, K.P. (1977), "Damage Factors for predicting Earthquake Dollar Loss Probabilities", Final Technical Report, JABE/USGS-7642, Sponsored by U.S. Geological Survey, Contract No. 14-08-0001-15888, December.
- Borg, S.F. (1979), "Accelerogram, Intensity, Damage - A New Correlation for use in Earthquake Engineering Design", Technical Report ME/CE-791, Department of Mechanical Engineering (Civil Engineering), Stevens Institute of Technology.
- Chang, F.M. (1981), "Static and Seismic Lateral Earth Pressures on Rigid Retaining Structures", Ph.D. Dissertation, Civil Engineering Department, Purdue University, West Lafayette, Indiana, August.
- Chang, F.M. and Chen, F.W. (1981), "Lateral Earth Pressures on Rigid Retaining Walls subjected to Earthquake Forces", Report CE-STR-81-20, School of Civil Engineering, Purdue University, June.
- Clough, W. and Fragaszy, R. (1977), "A Study of Earth Loadings on Floodway Retaining Structures in the 1971 San Fernando Valley Earthquake", Proceedings, Sixth World Conference on Earthquake Engineering, New Delhi, India, pp. 2455-2460.
- Cornell, C.A. (1968), "Engineering Seismic Risk Analysis", Proceedings, Bulletin of the Seismological Society of America, Vol. 58, No. 5, pp. 1583-1606.
- Cornell, C.A. (1970), "Probabilistic Analysis of Damage to Structures under Seismic Loads", in "Dynamic Waves in Civil Engineering", Proceedings, Conference organized by the Society for Earthquake and Civil Engineering Dynamics held at University College of Swansea, 7-8, July, Editors Howells, D.A., Haigh, J.P., Taylor, C., Wiley Interscience, pp. 473-488.

- Culver, C.G., Lew, H.S., Hart, G.C. and Pinkham, C.W. (1975), "Natural Hazards Evaluation of Existing Buildings", Report BSS-G1, U.S. Department of Commerce National Bureau of Standards, Washington, D.C.
- Czarnecki, R.M. (1973), "Earthquake Damage to Tall Buildings", Research Report R73-8, ST No. 359, Department of Civil Engineering, MIT, Cambridge, Massachusetts.
- Del Tosto, R. (1979), "A Probabilistic Seismic Damage Model", Proceedings, 2nd National Conference on Earthquake Engineering, August 22-24, Stanford University, pp. 773-782.
- Donovan, C.N. (1971), "A Stochastic Approach to the Seismic Liquefaction Problem", Proceedings, First International Conference on Applications of Statistics and Probability to Soil and Structural Engineering, Hong Kong, September, pp. 513-535.
- Donovan, N.C. (1974), "A Stastical Evaluation of Strong Data including the February 9, 1971 San Fernando Earthquake", Proceedings, Fifth World Conference on Earthquake Engineering, Rome, pp. 1252-1261.
- Duke, C.M. and Leeds, J.D. (1963), "Response of Soils, Foundations and Earth Structures", Bulletin of the Seismological Society of America, Vol. 53, No. 2, pp. 309-357.
- Ellison, B.K. (1971), "Earthquake Damage to Roads and Bridges - Madang R.P.N.G. - November 1970", Bulletin of New Zeland Society of Earthquake Engineering, Vol. 4, No. 1, pp. 243-257.
- Emery, J.J. and Thompson, C.D. (1976), "Seismic Design Considerations for Gravity Retaining Structures", Can. J. Civ. Eng., Vol. 3, No. 2, June, pp. 248-264.
- Evans, G.L. (1971), "The Behavior of Bridges under Earthquake", Proceedings, New Zealand, Roading Symposium, Vol. 2, Victoria, University of Wellington, Wellington, New Zeland, pp. 664-684.
- Faccioli, E. (1973), "A Stochastic Model for Predicting Seismic Failure in a Soil Deposit", Proceedings, Earthquake Engineering and Structural Dynamics, Vol. 1, pp. 293-307.
- Freudenthal, A.M. (1947), "The Safety of Structures", Transactions, A.S.C.E, Vol. 112, pp. 1337-1375.
- Gutenberg, B. and Richter, C.F. (1956), "Earthquake Magnitude, Intensity, Energy and Acceleration", Bulletin of Seimsological Society of America, Vol. 46, No. 2, pp. 105-145.



- Harr, M.E. (1977), "Mechanics of Particulate Media - A Probabilistic Approach", McGraw Hill, New York.
- Harrop-Williams, K. (1980), "Reliability in Geotechnical Systems", Ph.D. Dissertation, Civil Engineering Department, Rensselaer Polytechnic Institute, August, Troy, New York.
- Hayashi, S., Kubo, K. and Nakose, A. (1966), "Damage to Harbor Structures in the Niigata Earthquake", Soils and Foundations, Vol. VI, No. 1, January, pp. 89-112.
- Höeg, K. and Murarka, R. (1974), "Probabilistic Analysis and Design of a Retaining Wall", Journal of Geotechnical Engineering Division, ASCE, GT3, March, pp. 349-366.
- Jennings, C.P. (1971), "Engineering Features of the San Fernando Earthquake, February 9, 1971", Report of Earthquake Engineering Research Laboratory, California Institute of Technology, Pasadena, California, June.
- Kuribayashi, E., Shioi, Y., Tazaki, T. and Kawashima, K. (1979), "Damage to Highway Bridges and other Lifeline Systems from the Miyagiken-Oki, Japan Earthquake of June 12, 1978", Proceedings, 2nd U.S. National Conference on Earthquake Engineering, August 22-24, Stanford University, pp. 353-362.
- Kustu, O. (1979), "A Practical Approach to Damage Mitigation in Existing Structures exposed to Earthquakes", Proceedings, 2nd U.S. National Conference on Earthquake Engineering, August 22-24, Stanford University, pp. 487-494.
- Lambe, T.W. and Whitman, V.R. (1969), "Soil Mechanics", John Wiley and Sons.
- Matsuo, H. and Ohara, S. (1960), "Lateral Earth Pressure and Stability of Quay Walls during Earthquakes", Proceedings, Second World Conference on Earthquake Engineering, Vol. 2, pp. 165-181.
- Matsuo, M. and Asaoka, A. (1978), "Dynamic Design Philosophy of Soils Based on the Bayesian Reliability of Soils Based on the Bayesian Reliability Prediction", Soils and Foundations, Vol. 18, No. 4, pp. 1-16.
- Meyerhof, G.G. (1953), "The Bearing Capacity of Foundation under Eccentric and Inclined Loads", Proceedings of 3rd International Conference on Soil Mechanics and Foundation Engineering, Zürich, Vol. 1, pp. 440-445.

- Moran, D., Ferver, G., Thiel, C., Stratta, J. Valera, J., Wyllie, L., Bolt, B. and Knudson, C. (1975), "Engineering Aspects of the Lima, Peru Earthquake of October 3, 1975", EERI Reconnaissance Team, Earthquake Engineering Research Institute, May.
- Mononobe, N. (1929), "Earthquake-proof Construction of Masonry Dams", Proceedings of World Engineering Conference, Vol. 9, pp. 275.
- Mononobe, N. and Matsuo, H. (1929), "On the Determination of Earth Pressures during Earthquakes", Proceedings, World Engineering Conference, Vol. 9, pp. 177.
- Nadolski, M.E. (1969), "Architectural Damage to Residential Structures from Disturbances", Bull. of the Seismological Society of America, Vol. 59, pp. 487-502.
- National Research Council (1977), "The Honomic, Hawaii Earthquake", Report of Inspection Committee on Natural Disasters Commission on Sociotechnical Systems, National Academy of Sciences, Washington, D.C.
- Nazarian, H. and Hadjian, A. (1979), "Earthquake Induced Lateral Soil Pressures on Structures", Journal of the Geotechnical Engineering Division, ASCE, GT9, September, pp. 1049-1066.
- Okabe, S. (1926), "General Theory of Earth Pressure", Journal of the Japan Society of Civil Engineers, Tokyo, Japan, Vol. 12, No. 1.
- Okamoto, S. (1956), "Bearing Capacity of Sandy Soil and Lateral Earth Pressure during Earthquakes", Proceedings, First World Conference on Earthquake Engineering, California, pp. 27-1 - 27-16.
- Peck, B.R., Hanson, E.W. and Thornburn, H.T. (1974), "Foundation Engineering", John Wiley and Sons, 2nd Edition.
- Power, D.V. (1966), "A Survey of Complaints of Seismic-Related Damage to Surface Structures following the Salmon Underground Nuclear Detonation", Bulletin of the Seismological Society of America, Vol. 56, pp. 1413-1428.
- Protonotarios, J. (1981), "General Subjects on Earthquakes and the Seismic Problem of Greece", Scientific Thought, No. 1, May - June, pp. 62-79.
- Richards, R. and Elms, D. (1979), "Seismic Behavior of Gravity Retaining Walls", Journal of the Geotechnical Engineering Division, ASCE, GT4, April, pp. 349-366.

- Rosenblueth, E. (1975), "Point Estimates for Probability Moments", Proceedings of National Academy of Science, USA, Vol. 72, No. 10, March, pp. 3812-3814.
- Rosenblueth, E. and Yao, T.P.J. (1979), "Appendix A, On Seismic Damage and Structural Reliability" included in Yao, T.P.J. (1979) "Reliability of Existing Buildings in Earthquake Zones - Final Report", Technical Report No. CE-STR-79-6, School of Civil Engineering, Purdue University.
- Ross, G., Seed, B. and Migliaccio, R. (1969), "Bridge Foundation Behavior in Alaska Earthquake", Journal of the Soil Mechanics and Foundations Division, ASCE, SM4, July, pp. 1007-1036.
- Sauter, F.F. (1979), "Damage Prediction for Earthquake Insurance", Proceedings, 2nd U.S. National Conference on Earthquake Engineering, August 22-24, Stanford University, pp. 99-108.
- Scholl, E.R. and Farhoomand, I. (1973), "Statistical Correlation of Observed Ground Motion with Low-Rise Building Damage", Bulletin of the Seismological Society of America, Vol. 63, pp. 1515-1537.
- Scholl, E.R. and Kustu, O. (1980), "Procedures and Data Bases for Earthquake Damage Prediction and Risk Assessment", Proceedings, XIII Conference on Evaluation of Regional Seismic Hazards and Risk, U.S. Geological Survey, August 25-27, 1980, Santa Fe, New Mexico, pp. 164-207.
- Seed, H.B. and Whitman, V.R. (1970), "Design of Earth Retaining Structures for Dynamic Loads", Proceedings of Specialty Conference on "Lateral Stressses in the Ground and Design of Earth Retaining Structures", ASCE, Cornell University, Ithaca, June 22-24, pp. 103-147.
- Sherif, A.M., Ishibashi, J. and Do Lee, C. (1982), "Static and Dynamic Earth Pressures against Rigid Retaining Walls", Journal of the Geotechnical Engineering Division, ASCE, (submitted for publication).
- Steinbrugge, K.V., McClure, F.E. and Snow, A.J. (1969), "Studies in Seismicity and Earthquake Damage Statistics; Appendix A", U.S. Department of Commerce Coast and Geodetic Survey, Washington, D.C.
- Thompson, C.D. and Emery, J.J. (1976), "Geotechnical Design Aspects for Large Gravity Retaining Structures under Seismic Loading", Can. Geotech. Journal, Vol. 13, pp. 231-242.

- Vlavianos, G. (1981), "Conventional and Probabilistic Evaluations of Seismic Safety of Rigid Retaining Walls", Master of Science Thesis, Civil Engineering Department, Rensselaer Polytechnic Institute, December, Troy, New York.
- Whitman, V.R., Reed, W.J. and Hong, T.S. (1973), "Earthquake Damage Probability Matrices", Proceedings, 5th World Conference on Earthquake Engineering, Rome, Italy, June, pp. 2531-2540.
- Whitman, V.R. (1975), "Costs and Benefits of Providing Increased Seismic Resistance", Proceedings, Earthquake Engineering Conference, College of Engineering, University of South Carolina, 23-24 January, pp. 149-185.
- Wood, J.H. (1973), "Earthquake Induced Soil Pressures on Structures", thesis presented to the California Institute of Technology at Pasadena, Calif., in partial fulfillment of the requirements for the Degree of Doctor of Philosophy.
- Yao, T.P.J. (1978), "Assessment of Seismic Damage in Existing Structures", Proceedings, U.S. - Southeast Asia Symposium on Engineering for Natural Hazards Protection, Manila, 1977, Edited by A.H-S. Ang, Department of Civil Engineering, College of Engineering, Univ. of Illinois at Urbana-Champaign, pp. 388-396.
- Yao, T.P.J. (1979), "Damage Assessment and Reliability Evaluation of Existing Structures", Eng. Struct., Vol. 1, October, pp. 245-251.
- Murphy, V.A. (1960), "The Effect of Ground Characteristics on the Aseismic Design of Structures", Proceedings of the 2nd World Conference on Earthquake Engineering, Japan, Vol. 1, pp. 231-248.
- Ishii, Y., Arai, H. and Tsuchida, H. (1960), "Lateral Earth Pressure in an Earthquake", Proceedings 2nd World Conference on Earthquake Engineering, Japan, Vol. 1, pp. 211-230.
- Sim, L.C. and Berril, J.B. (1979), "Shaking Table Tests on a Model Retaining Wall", Bulletin of the New Zealand National Society for Earthquake Engineering, Vol. 12, No. 3, June.
- Lee, C.D. (1981), "Dynamic Lateral Earth Pressures Against Retaining Structures", Ph.D. Dissertation, Dept. of Civil Engineering, University of Washington.
- Ishihara, M., Matsuzawa, H. and Kawamura, H. (1977), "Earthquake Resistant Design of Quay Walls", Proceedings of the 6th World Conference on Earthquake Engineering, New Delhi, India, Vol. 3, pp. 1969-1974.

- Kurata, S., Arai, H. and Yokoi, T. (1965), "On the Earthquake Resistance of Anchored Sheet-Pile Bulkheads", Proceedings of the 3rd World Conference on Earthquake Engineering, New Zealand, Vol. 3, Session 2, pp. 369-383.
- Niwa, S. (1960), "An Experimental Study of Oscillating Earth Pressures Acting on a Quay Wall", Proceedings of the 2nd World Conference on Earthquake Engineering, Japan, Vol. 1, pp. 281-297.
- Prakash, S. and Nandakumaran, P. (1973), "Dynamic Earth Pressure Distribution on Rigid Walls", Proceedings, Symposium on Earthquakes and Other Dynamic Loads, Roorkee, Vol. 1, pp. 11-16.
- Nandakumaran, P., and Joshi, V.H. (1973), "Static and Dynamic Active Earth Pressures behind Earth Retaining Walls", Paper No. 136, Bulletin I.S.E.T., Vol. 10, No. 3, pp. 113-123.
- Prakash, S. (1981), Soil Dynamics, McGraw Hill, New York.

## CHAPTER 8

### DISCUSSION

The procedure of safety prediction of retaining walls under seismic conditions presented in this study was based on three main assumptions, namely: (1) quasi-static loading conditions, in which the seismic effect is introduced through the maximum horizontal ground acceleration experienced at the site of the wall; (2) rigid-plastic behavior of the backfill and foundation materials (limiting equilibrium approach); and (3) the strength of the soil remains constant during the seismic loading.

The assumption of quasi-static conditions renders the developed analysis a simplified approach to the determination of the probability of failure of retaining walls under seismic conditions. This is considered to be sufficient for many encountered situations and, in particular, when not much information is available about the seismic environment of the site of the wall.

In Chapter 4, the state of limiting equilibrium (failure) was expressed in general as a function of the soil strength parameters  $c$  (cohesion) and  $t$  ( $t = \tan\phi$ ,  $\phi$  = angle of internal friction). In the case of a granular soil, the failure function depended only on the  $t$  ( $=\tan\phi$ ) parameter of strength. Both  $c$  and  $t$  are considered in this study as random variables, the statistical values of which are determined through an analysis of available data. The latter are usually given as the values of  $c$  and  $t$  obtained during commonly employed shear

tests (i.e., triaxial or simple shear).

The assumption of constant strength during the seismic loading is considered to be reasonable for a wide variety of soils. Both experience and experimental evidence indicate that, in all well compacted construction materials and in many natural soil strata, the dynamic shearing resistance is about the same as the static shearing resistance. This, however, is not the case for soils the resistance of which decreases drastically during the cyclic loading, e.g., the case of liquefaction of loose saturated sands or very sensitive clays.

In a Bayesian formulation of the safety of a retaining wall, the time at which the safety prediction is made is of importance. In this study, the first prediction was made during the design stage and before the construction of the facility. This provided two values for the predicted probability of failure: one, for static conditions ( $G_o$ ) and, another, for seismic conditions ( $G_o + \Delta G$ ), denoted as  $P_f(G_o)$  and  $P_f(G_o + \Delta G)$ , respectively. The second prediction was made at a time following the successful construction of the wall and before the occurrence of the earthquake. This provided the posterior (to the successful construction) probability of failure, denoted as  $P'_f(G_o + \Delta G)$ . Subsequent predictions can be made at times following the occurrence of each earthquake and can be accommodated for the damage incurred to the facility during each seismic activity.

The seismic capacity  $R$  of a retaining wall was defined as the maximum acceleration that could be experienced by the wall during

an earthquake without failure. As a retaining wall may fail in four different modes (e.g., overturning, base sliding, bearing capacity, and overall sliding), the employed Bayesian formulation enabled the derivation of four expressions for the probability density function  $f_R(R)$  of  $R$ , one for each mode.



## CHAPTER 9

### SUMMARY AND CONCLUSIONS

A procedure was presented for the determination of the probability of failure of earth retaining structures under static or seismic conditions. Four possible modes of failure were examined (i.e., overturning, base sliding, bearing capacity, and overall sliding) and their combined effect was evaluated with the aid of combinatorial analysis. Limit equilibrium was expressed as a function of the soil strength parameters (random variables) that are present in the development of the capacity (resistance) of the structure along a particular failure mode. The seismic load was introduced in terms of the maximum horizontal ground acceleration (random variable) expected to occur at the site of the facility. In a Bayesian formulation of the problem, it became possible to account for observations on the safety of the wall under static conditions (prior to the occurrence of an earthquake) in order to provide an improved measure for the predicted probability of failure under seismic loading. This formulation provided an expression for the seismic capacity of the wall, defined as the maximum horizontal ground acceleration that could be experienced by the wall without failure. Introducing the concept of damage factor into the Bayesian safety analysis, the posterior (to the occurrence of an earthquake) probability of failure for a wall was determined.

The developed procedure was applied to an actual case study involving the safety of a wingwall. The information required for this purpose was obtained during investigations on sites affected by the February and March, 1981, earthquakes in Greece. A detailed description was provided of the behavior of the wingwall before and during the seismic activity and predictions were made for its probability of failure.

On the basis of the analysis and the results obtained in this study, the following conclusions are drawn:

(1) The probability of failure is a more adequate measure of safety than the customary factor of safety. As earth retaining structures may fail in four distinct modes, a system (or, combinatory) analysis can provide a single estimate for the probability of failure of such facilities.

(2) A Bayesian formulation of the safety of retaining walls provides an improved measure for the predicted probability of failure under seismic loading.

(3) When the safety prediction is made before construction (at the design stage), the probability of failure under seismic conditions is always greater than that predicted under static conditions. When the safety prediction is made after the successful construction of the retaining wall, the new predicted probability of failure under seismic loading (posterior) is always smaller than that predicted before construction (prior).

(4) The seismic capacity  $R$  of a retaining wall in any failure mode against a future earthquake is equal to the derivative of the posterior probability of failure of the wall in this mode with respect to the acceleration  $\alpha$ , in which  $\alpha$  is replaced by  $R$ .

(5) The presented Bayesian analysis can account for the damage incurred to a retaining wall during an earthquake in order to provide an improved estimate for its probability of failure during future seismic events.

APPENDICES

APPENDIX A

POSTERIOR PROBABILITY OF FAILURE FOR  
THE CASE OF COHESIONLESS SOILS

In this case, soil strength is expressed in terms of only a parameter,  $t = \tan\phi$ . The observation that a retaining wall is safe under static conditions provides the following expression for the probability associated with the failure function H:

$$P[H(t|G_o) > 0|t] = \begin{cases} 1 & , \text{ if } H(t|G_o) > 0 \\ 0 & , \text{ if } H(t|G_o) \leq 0 \end{cases} \quad (A-1)$$

Using Bayes theorem, the posterior probability density function of  $t$ , becomes equal to  $f'_t(t) = f_t[t|H(t|G_o) > 0]$ .

$$f'_t(t) = \frac{P[H(t|G_o) > 0|t] f_t(t)}{\int P[H(t|G_o) > 0|t] f_t(t) dt} \quad (A-2)$$

in which  $f_t(t)$  is the prior probability density function of  $t$ , and the integration indicated in the denominator is performed along the region for which  $H(t|G_o) > 0$ .

Introducing Eqn. (A-1) into Eqn. (A-2), it is found that

$$f'_t(t) = \frac{f_t(t)}{\int f_t(t) dt}$$

or,

$$f'_t(t) = \frac{f_t(t)}{1 - \int f_t(t) dt} \quad (A-3)$$

in which the integration is performed along the region where  $H(t|G_0) \leq 0$ . From Eqn. (4-22), one has that the integral appearing in the denominator of Eqn. (A-3) is equal to the probability of failure under  $G_0$  condition,  $P_f(G_0)$ . Therefore, Eqn. (A-3) may be written as

$$f'_t(t) = \frac{f_t(t)}{1 - P_f(G_0)} \quad (A-4)$$

The predicted probability of failure of a retaining wall under seismic conditions ( $G_0 + \Delta G$ ), given that the wall was safe under static conditions ( $G_0$ ), is equal to the probability with which the failure function  $H(t|G_0 + \Delta G)$  becomes negative. This is denoted as

$$P'_f(G_0 + \Delta G) = P[H(t|G_0 + \Delta G) \leq 0 | H(t|G_0) > 0] \quad (A-5)$$

A prediction on the safety of the wall under seismic conditions provides the following expression:

$$P[H(t|G_0 + \Delta G) \leq 0 | H(t|G_0) > 0; t] = \begin{cases} 1, & \text{if } H(t|G_0 + \Delta G) \leq 0 \\ 0, & \text{if } H(t|G_0 + \Delta G) > 0 \end{cases} \quad (A-6)$$

Combining Eqns. (A-5) and (A-6),

$$P'_f[G_0 + \Delta G] = \int P[H(t|G_0 + \Delta G) \leq 0 | H(t|G_0) > 0; t] f'_t(t) dt \quad (A-7)$$

in which the integration is performed along the region of  $t$  that is equal to the difference between the two regions that correspond to

$G_o + \Delta G$  and  $G_o$  conditions.

Introducing Eqn. (A-6) into Eqn. (A-7), it is found that

$$P'_f(G_o + \Delta G) = \int f_t [t | H(t | G_o) > 0] dt \quad (A-8)$$

Finally, combining Eqns. (A-4) and (A-8), the expression for

$P'_f(G_o + \Delta G)$  is found as

$$P'_f(G_o + \Delta G) = \int \frac{f_t(t)}{1 - P_f(G_o)} dt$$

or,

$$P'_f(G_o + \Delta G) = \frac{P_f(G_o + \Delta G) - P_f(G_o)}{1 - P_f(G_o)} \quad (A-9)$$

since,

$$P_f(G_o + \Delta G) = \int f_t(t) dt \quad (A-10)$$

The left hand side of Eqn. (A-9) provides the prior, to a seismic event  $\Delta G$ , probability of failure.

## APPENDIX B

### COMPUTER PROGRAMS

Two computer programs were developed in the course of this study. They are written in BASIC language for the Radio Shack TRS-80 Microcomputer. A short description precedes each program and an illustrative example shows the necessary input and the display.

The programs achieve the following two objectives:

- (a) design of a gravity earth retaining wall under static and seismic conditions, and
- (b) evaluation of the mean value and the standard deviation of a function of random variables with the aid of Rosenblueth's method.

#### B.1 Design of Gravity Retaining Walls

In this program, the earth pressures against a rigid retaining wall are computed on the basis of the assumption that the wall moves sufficiently for active conditions to develop. Three modes of failure are addressed, that is, overturning, sliding and bearing capacity. For each mode the program calculates both the safety factor and the safety margin. In addition, the program is capable of doing both static and pseudo-static seismic analysis and it can take into consideration inertia effects on the retaining wall.

The present program is based on Sections 4.2.1, 4.2.2, and 4.2.3 and refers to the Fig. 4.3 and 4.4. The equations used in the



program are summarized below.

(a) Computation of Lateral Earth Pressures:

$$P_A = \frac{1}{2} \gamma H_b^2 (1 + \alpha_v) \lambda_A \quad (B-1)$$

$$\lambda_A = \frac{\cos^2(\phi - \theta - \beta)}{\cos \theta \cos^2 \beta \cos(\delta + \beta + \theta) \left[ 1 + \sqrt{\frac{\sin(\phi + \delta) \sin(\phi - \theta - i)}{\cos(\delta + \beta + \theta) \cos(i - \beta)}} \right]^2} \quad (B-2)$$

$$\theta = \tan^{-1} \left( \frac{\alpha_h}{1 + \alpha_v} \right) \quad (B-3)$$

$$P_{AH} = P_A \cos(\beta + \delta) \quad (B-4)$$

$$P_{AV} = P_A \sin(\beta + \delta) \quad (B-5)$$

(b) Analysis of Overturning:

$$W_w = \frac{1}{2} (B + c_r) H \gamma_b \quad (B-6)$$

$$C_1 = (1 + \alpha'_v) W_w \ell + P_{AV} (B - h_A \tan \beta) \quad (B-7)$$

$$D_1 = \alpha'_h W_w h + P_{AH} h_A \quad (B-8)$$

$$SMR_1 = C_1 - D_1 \quad (B-9)$$

$$FSR_1 = \frac{C_1}{D_1} \quad (B-10)$$

$$C_2 = (1 + \alpha'_v) W_w \ell \quad (B-11)$$

$$D_2 = \alpha'_h W_w h + P_{AH} h_A - P_{AV} (B - h_A \tan \beta) \quad (B-12)$$

$$SMR_2 = C_2 - D_2 \quad (B-13)$$

$$FSR_2 = \frac{C_2}{D_2} \quad (B-14)$$

(c) Analysis of Sliding:

$$C = [(1 + \alpha'_v) W_w + P_{AV}] \tan \delta_f \quad (B-15)$$

$$D = \alpha'_h W_w + P_{AH} \quad (B-16)$$

$$SMS = C - D \quad (B-17)$$

$$FSS = \frac{C}{D} \quad (B-18)$$

(d) Analysis of Bearing Capacity:

$$q = \frac{C}{A'} = \frac{1}{2} \left(1 - \frac{2e}{B}\right) \left(1 - \frac{a}{\phi_o}\right)^2 \gamma_f B \lambda_{\gamma} d_{\gamma} N_{\gamma} + \left(1 - \frac{a}{90}\right)^2 \gamma_f D_d \lambda_{q_d} d_{q_d} N_{q_d} + \left(1 - \frac{a}{90}\right)^2 c_f \lambda_c d_c N_c \quad (B-19)$$

$$N_{\phi} = \tan^2 \left(45 + \frac{\phi_o}{2}\right) \quad (B-20)$$

$$N_q = N_{\phi} e^{\pi \tan \phi_o} \quad (B-21)$$

$$N_{\gamma} = (N_q - 1) \tan(1.4 \phi_o) \quad (B-22)$$

$$\lambda_c = 1 + 0.2 \frac{B}{L_w} N_{\phi} \quad (B-23)$$

$$\lambda_q = \lambda_{\gamma} = 1 \quad \text{if } \phi_o = 0 \quad (B-24)$$

$$\lambda_d = d_Y = 1 + 0.1 \frac{B}{L_w} N_\phi \quad \text{if } \phi_o > 10^\circ \quad (\text{B-25})$$

$$d_c = 1 + 0.2 \frac{D_f}{B} \sqrt{N_\phi} \quad (\text{B-26})$$

$$d_q = d_Y = 1 \quad \text{if } \phi_o = 0 \quad (\text{B-27})$$

$$d_q = d_Y = 1 + 0.1 \frac{D_f}{B} \sqrt{N_\phi} \quad \text{if } \phi_o > 10^\circ \quad (\text{B-28})$$

$$A' = (B-2e)(L_w-2e) \quad \text{if } L_w < E99 \quad (\text{B-29})$$

$$A' = B - 2e \quad \text{if } L_w = E99 \quad (\text{B-30})$$

$$C = qA' \quad (\text{B-31})$$

$$e = \frac{(1+\alpha'_v)W_w(B-l) + \alpha'_h W_h h + P_{AH} h_A + P_{AV} h_A \tan \beta}{(1+\alpha'_v)W_w + P_{AV}} - \frac{B}{2} \quad (\text{B-32})$$

$$a = \tan^{-1} \left[ \frac{\alpha'_h W_h + P_{AH}}{(1+\alpha'_v)W_w + P_{AV}} \right] \quad (\text{B-33})$$

$$D = (1+\alpha'_v)W_w + P_{AV} \quad (\text{B-34})$$

$$BC - SM = C - D \quad (\text{B-35})$$

$$BC - FS = \frac{C}{D} \quad (\text{B-36})$$

In the case that  $0 < \phi_o \leq 10^\circ$ , linear interpolation provides the values for  $\lambda_q, \lambda_Y, d_q$  and  $d_Y$ .

(e) Program Variables:

Execution of the program requires that the values of certain variables be given as data. These variables are shown in Table B-1 in the order they appear in the sequence of data together with their name in the program and a short description of them.

(f) Analysis Program:

The statements of the program are presented along with a description of the memory contents in the following table under the title "Retaining Wall".

(g) Illustrative Example:

In order to illustrate how the program works, the following data has been considered:  $\beta = 0^\circ$ ,  $H = 20$  ft (6.10 m),  $h = 7.619$  ft (2.32 m),  $B = 6$  ft (1.83 m),  $\lambda = 3.9524$  ft (1.20 m),  $h_A = 8$  ft (2.44 m),  $\alpha'_h = 0$ ,  $\alpha'_v = 0$ ,  $\delta_f = 30^\circ$ ,  $c_r = 1$  ft (0.30 m),  $\gamma_b = 150$  pcf (23563.01 N/m<sup>3</sup>),  $\phi = 35^\circ$ ,  $\gamma = 110$  pcf (17279.54 N/m<sup>3</sup>),  $\delta = 29^\circ$ ,  $\alpha_h = 0.07$ ,  $\alpha_v = 0$ ,  $i = 0$ ,  $H_b = 20$  ft (6.10 m),  $\phi_f = 37^\circ$ ,  $D_f = 3$  ft (0.91 m),  $\gamma_f = 110$  pcf (17279.54 N/m<sup>3</sup>),  $c_f = 0$  and  $L_w = E99$ . Corresponding results are as follows:  $\lambda_A = 0.289$ ,  $P_A = 6361.09$  lb/ft (92832.68 N/m),  $P_{AH} = 5563.5337$  lb/ft (81193.28 N/m),  $P_{AV} = 3083.9171$  lb/ft (45006.17 N/m),  $SMR - 1 = 15495.462$  lb.ft/ft (68926.91 Nm/m),  $FSR - 1 = 1.348$ ,  $SMR - 2 = 15495.462$  lb.ft/ft (68926.91 Nm/m),  $FSR - 2 = 1.596$ ,  $SMS = 2279.149$  lb/ft (33261.52 N/m),  $FSS = 1.410$ ,  $BC - SM = 9208.746$  lb/ft (134390.89 N/m), and  $BC - FS = 1.68$ .

In detail, data is provided to the computer and results are obtained as presented in Table B-2.

TABLE B-1

## NAME AND DESCRIPTION OF PROGRAM VARIABLES

VARIABLE	NAME	DESCRIPTION
$\beta$	WI	wall back inclination
H	WH	wall height
h	COGH	wall center of gravity height from foundation level
B	WB	wall base
$\ell$	DL	distance of wall center of gravity from the front point of wall base
$h_A$	APOPA	application point of $P_A$
$\alpha'_h$	A!HSC	inertia effect $\alpha'_h$
$\alpha'_v$	A!VSC	inertia effect $\alpha'_v$
$\delta_f$	WBSFA	base-foundation function angle
$c_r$	WC	wall crest
$\gamma_b$	WUW	wall unit weight
$\phi$	BFA	backfill friction angle
$\gamma$	BUW	backfill unit weight

TABLE B-1 (contd)

## NAME AND DESCRIPTION OF PROGRAM VARIABLES

VARIABLE	NAME	DESCRIPTION
$\delta$	WBCFA	wall-backfill friction angle
$\alpha_h$	AHSC	seismic coefficient $\alpha_h$
$\alpha_v$	AVSC	seismic coefficient $\alpha_v$
$i$	BI	backfill inclination
$H-h_b$	WBS	wall-backfill step
$\phi_f$	FSAIF	foundation soil angle of internal friction
$D_f$	DF	depth of foundation level
$\gamma_f$	GF	foundation soil unit weight
$c_f$	CF	foundation soil cohesion
$L_w$	LW	wall length

Title				RETAINING WALL	
Memory content			Line number	Statements	
A	1	$\beta$ $N_\phi$	10	INPUT "WI = "; A, "WH = ";	
B	2	H $\phi_f$		B, "COGH = "; C, "WB = "; D,	
C	3	h $N_q$		"DL = "; E, "APOPA = "; F, "A!H	
D	4	B		SC = "; G, "A!VSC = "; H	
E	5	$\lambda$ $N_\gamma$	20	INPUT "WBSFA = "; I, "WC = ";	
F	6	$h_A$ $N_c$		J, "WUW = "; K, "BFA = "; L, "BUW	
G	7	$\alpha'_h$ $\lambda_c$		= "; M, "WBCFA = "; N, "AHSC = ";	
H	8	$\alpha'_v$ $\lambda_q = \lambda_\gamma$		O	
I	9	$\delta_f$ $D_f$	30	INPUT "AVSC = "; P, "BI = ";	
J	10	$c_r$ $\gamma_f$		Q, "WALL-BACKFILL-STEP = "; U	
K	11	$\gamma_b$ $c_f$	40	R = ATN (O/(1 + P))	
L	12	$\phi$ e	50	S = .5 *K*B*(D + J)	
M	13	$\gamma$ a	60	J = $\sqrt{((\sin(L + N)*\sin(L -$	
N	14	$\delta$ $d_c$		R - Q)) / (COS(N + A + R) * COS(	
O	15	$\alpha'_h$ $d_q = d_\gamma$		Q - A))	
P	16	$\alpha'_v$ q	70	K = (1 + J) $\wedge$ 2	
Q	17	i	80	J = COS(R) *COS(A) * COS(A)	
R	18	$\theta, K_A$ $A'$		*COS(N + A + R)	
S	19	$W_w$	90	O = COS(L - R - A) *COS(L - R - A)	
T	20	$P_A$ $L_w$	100	R = O/(J*K)	
U	21	$P_{AH}$	110	PRINT "KA = "; R	
V	22	$P_{AV}$	120	T = .5 *M*(B-U)*(B-U)*	
W	23	C		(1 + P) * R	
X	24	D	130	PRINT "PA = "; T	
Y	25	SM	140	LET B = U	
Z	26	FS	150	U = T * COS(A+N)	
			160	PRINT "PAH = "; U	
			170	V = T * SIN(A + N)	
			180	PRINT "PAV = "; V	
			190	W = (1 + H) *S*E + V* (D - F*	
				TAN(A))	
			200	X = G*S*C + U*F	
			210	Y + W - X	

Title		RETAINING WALL		
Memory content		Line number	Statements	
A	1	220	PRINT "SMR - 1 = "; Y	
B	2	230	Z = W/X	
C	3	240	PRINT "FSR - 1 = "; Z	
D	4	250	W = (1 + H) *S*E	
E	5	260	X = G*S*C+U*F-V*(D -	
F	6		F*TAN(A))	
G	7	270	Y = W - X	
H	8	280	PRINT "SMR - 2 = "; Y	
I	9	290	Z = W/X	
J	10	300	PRINT "FSR - 2 = "; Z	
K	11	310	W = ((1 + H) *S+V) *TAN(I)	
L	12	320	X = G*S + U	
M	13	330	Y = W - X	
N	14	340	PRINT "SMS = "; Y	
O	15	350	Z = W/X	
P	16	360	PRINT "FSS = "; Z	
Q	17	370	INPUT "FSAIF = "; B, "DF =	
R	18		"; I, "GF = "; J, "CF = "; K,	
S	19		"LW = "; T	
T	20	380	M = (1 + H) *S* (D - E) + G*S*C	
U	21		+ U*F+V*F*TAN(A)	
V	22	390	N = (1 + H) *S + V	
W	23	400	L = (M/N) - (D/2)	
X	24	410	M = ATN((G*S + U)/((1	
Y	25		+ H) *S + V))	
Z	26	420	X = (1 + H) * S + V	
		430	A = (TAN(45 + B/2))/^2	
		440	C = A * EXP( $\pi$ *TAN(B))	
		450	E = (C-1)*TAN(1.4*B)	
		460	F = (C-1)/TAN(B)	
		470	G = 1 + (.2*D*A)/T	
		480	IF B = 0 LET H = 1	
		490	IF B < 10 LET H = 1 + (.0142	





TABLE B-2  
DATA INPUT AND DISPLAY OUTPUT

DATA		DISPLAY
	RUN	WI =
0	ENTER	WH =
20 ft	ENTER	COGH =
7.619 ft	ENTER	WB =
6 ft	ENTER	DL =
3.9524 ft	ENTER	APOPA =
8 ft	ENTER	A!HSC =
0	ENTER	A!VSC =
0	ENTER	WBSFA =
30°	ENTER	WC =
1 ft	ENTER	WUW =
150 pcf	ENTER	BFA =
35°	ENTER	BUW =

TABLE B-2 (contd)  
DATA INPUT AND DISPLAY OUTPUT

DATA		DISPLAY
110 pcf	ENTER	WBCFA =
29°	ENTER	AHSC =
0.07	ENTER	AVSC =
0	ENTER	BI =
0	ENTER	WALL-BACKFILL-STEP =
0	ENTER	$\lambda_A = 0.289$
	ENTER	$P_A = 6361.09 \text{ lb/ft}$
	ENTER	$P_{AH} = 5563.5337 \text{ lb/ft}$
	ENTER	$P_{AV} = 3083.9171 \text{ lb/ft}$
	ENTER	SMR - 1 = 15495.462 lb.ft/ft
	ENTER	FSR - 1 = 1.348
	ENTER	SMR - 2 = 15495.462 lb.ft/ft
	ENTER	FSR - 2 = 1.596

TABLE B-2 (contd)  
 DATA INPUT AND DISPLAY OUTPUT

DATA		DISPLAY
	ENTER	SMS = 2279.15 lb/ft
	ENTER	FSS = 1.410
	ENTER	FSAIF =
37°	ENTER	DF =
3 ft	ENTER	GF =
110 pcf	ENTER	CF =
0	ENTER	LW =
E 99	ENTER	BC - SM = 9208.75 lb/ft
	ENTER	BC - FS = 1.678

## B.2 COMPUTATION OF STATISTICAL VALUES

This program computes the mean value, the standard deviation and the coefficient of variation of a function of random variables on the basis of the assumption that the latter are mutually independent. The program is based on Rosenblueth's method (Rosenblueth, 1975) which is described in Section 6.7. For clarification purposes, equations that are used by the program are repeated here.

### (a) Computation of Statistical Values

$$x = g(x_1, x_2, \dots, x_N) \quad (\text{B-37})$$

$$\frac{\bar{x}}{x_0} = \frac{\bar{x}'_1}{x_0} \frac{\bar{x}'_2}{x_0} \dots \frac{\bar{x}'_N}{x_0} \quad (\text{B-38})$$

$$1 + V_x^2 = (1 + V_{x_1}^2)(1 + V_{x_2}^2) \dots (1 + V_{x_N}^2) \quad (\text{B-39})$$

$$x_0 = g(\bar{x}_1, \bar{x}_2, \dots, \bar{x}_N) \quad (\text{B-40})$$

$$V_x = \frac{S_x}{\bar{x}} \quad (\text{B-41})$$

$$V_{x'_i} = \frac{S_{x'_i}}{\bar{x}'_i} \quad (\text{B-42})$$

$$x_{i+} = \bar{x}_i + S_{xi} \quad (\text{B-43})$$

$$x_{i-} = \bar{x}_i - S_{xi} \quad (\text{B-44})$$

$$x'_{i+} = g(\bar{x}_1, \bar{x}_2, \dots, x_{i+}, \dots, \bar{x}_N) \quad (\text{B-45})$$

$$x'_{i-} = g(\bar{x}_1, \bar{x}_2, \dots, x_{i-}, \dots, \bar{x}_N) \quad (\text{B-46})$$

$$\bar{x}'_i = \frac{x'_{i+} + x'_{i-}}{2} \quad (\text{B-47})$$

$$S_{x'_i} = \frac{|x'_{i+} - x'_{i-}|}{2} \quad (\text{B-48})$$

$$V_{x'_i} = \left| \frac{x'_{i+} - x'_{i-}}{x'_{i+} + x'_{i-}} \right| \quad (\text{B-49})$$

### (b) Analysis Program

The statements of the program are presented together with a description of the memory contents in the following table under the title "Statistical Values".

### (c) Illustrative Example

In order to illustrate the use of the program, the following data has been selected:  $N = 2$ ,  $x_0 = 1.5959$ ,  $\bar{x}_1 = 1.6014$ ,  $S_{x_1} = 0.1183$ ,  $V_{x_1} = 0.0739$ ,  $\bar{x}_2 = 1.6049$ ,  $S_{x_2} = 0.1548$ , and  $V_{x_2} = 0.0964$ . The corresponding results are:  $\bar{x} = 1.6104$ ,  $S_x = 0.1960$ , and  $V_x = 0.1217$ .

The data is provided to the computer and the results are obtained as presented in Table B-3.

Title		STATISTICAL VALUES		
Memory content		Line number	Statements	
A	1	N	10	INPUT "NO-OF-VARIABLES-
B	2	$x_0 = g(\bar{x}_1, \bar{x}_2, \dots, \bar{x}_N)$		-N = "; A
C	3	$x_{i+}' = g(x_1, x_2, x_{i+}, x_N)$	20	INPUT "XO=G(MEAN-XI) + ";
D	4	$x_{i-}' = g(x_1, x_2, x_{i-}, x_N)$		B
E	5	$\bar{x}_i'$	30	LET N = 1
F	6	$S_{x_i}'$	40	FOR K = 1 TO (A - 1)
G	7	$V_{x_i}'$	50	N = N*B
H	8	$\bar{x}$	60	NEXT K
I	9	$S_x$	70	H = 1/N
J	10	$V_x$	80	LET M = 1
K	11	COUNTER	90	FOR K = 1 to A
L	12	$x_0^{N-1}$	100	PAUSE "X(I)+, XI(I)+, I =
M	13			"; K
N	14		110	INPUT "X(I)+ = "; C
O	15		120	PAUSE "X(I)-, XI(I)-, I =
P	16			"; K
Q	17		130	INPUT "X(I)-- = "; D
R	18		140	E = (C + D)/2
S	19		150	Z = (C - D)/2
T	20		160	F = ABS(Z)
U	21		170	Z = F/E
V	22		180	G = ABS(Z)
W	23		190	H = H*E
X	24		200	M = M* (1+G*G)
Y	25		210	NEXT K
Z	26		220	PRINT "AVE - X = "; H
			230	J = $\sqrt{M - 1}$
			240	I = J*H
			250	PRINT "S - X = "; I
			260	PRINT "V - X = "; J
			270	END

TABLE B-3  
DATA INPUT AND DISPLAY OUTPUT

DATA		DISPLAY
	RUN	NO-OF-VARIABLES-N =
2	ENTER	XO = G(MEAN - XI) =
1.5959	ENTER	X(I)+ =
1.6014+0.1183	ENTER	X(I)- =
1.6014-0.1183	ENTER	X(I)+ =
1.6049+0.1548	ENTER	X(I)- =
1.6049-0.1548	ENTER	AVE-X = 1.6104
	ENTER	S - X = 0.1960
	ENTER	Y - X = 0.1217